

THESIS FOR THE DEGREE OF DOCTOR OF PHILOSOPHY

**Design, Synthesis and Modelling of Conjugated  
Polymers for Organic Photovoltaics**

WENLIU ZHUANG



Polymer Technology

Department of Chemical and Biological Engineering

CHALMERS UNIVERSITY OF TECHNOLOGY

Göteborg, Sweden 2013

# **Design, Synthesis and Modelling of Conjugated Polymers for Organic Photovoltaics**

WENLIU ZHUANG

© WENLIU ZHUANG, 2013.  
ISBN 978-91-7385-952-3

Doktorsavhandlingar vid Chalmers tekniska högskola  
Ny serie nr 3634  
ISSN 0346-718X

Polymer Technology  
Department of Chemical and Biological Engineering  
Chalmers University of Technology  
SE-412 96 Gothenburg  
Sweden  
Telephone +46 (0) 31-772 10 00

Cover: Illustration of photoinduced electron transfer from the HOMO of donor polymer PBDTA-MIM to the LUMO of PCBM acceptor.

Chalmers Reproservice  
Gothenburg, Sweden 2013

# Design, Synthesis and Modelling of Conjugated Polymers for Organic Photovoltaics

WENLIU ZHUANG

*Department of Chemical and Biological Engineering*  
Chalmers University of Technology  
Gothenburg, Sweden

## ABSTRACT

---

Secure, clean and renewable energy sources are believed to be the eventual solution for sustainable energy, especially by the direct utilization of solar energy. Organic photovoltaics offer such an option to convert solar energy into electricity based on solution-processed, lightweight, large-area, and potentially flexible devices. The current challenges for organic photovoltaics remain to further improve efficiency as well as durability and cost-effectiveness, to compete with traditional silicon-based solar cells.

Material design through band gap and energy level tuning has been playing a key role in developing new donor materials for efficient polymer solar cells. Computationally driven material design can accelerate the search for optimal conjugated polymers, and the exploration of chemical methodologies is highly desirable in pushing the efficiency further toward the theoretical limit.

This thesis deals with the design, synthesis, characterization, and computational modelling of  $\pi$ -conjugated polymers for bulk heterojunction organic solar cells. It focuses on material design of conjugated donor polymers through band gap and energy level engineering via structural modifications such as backbone manipulations, side-chain engineering, as well as incorporation of newly developed building blocks. This also establishes structure–property relationships of the polymer systems here studied, and explores potential chemical methodologies for future judicious material design.

*Keywords: conjugated polymers, organic photovoltaics, material design, band gap, energy level, computational modelling, structure–property relationships*



*To my family*

# List of Publications

This thesis is partially based on the work contained in the following scientific papers, referred to by their Roman numerals in the text. The papers are appended at the end of the thesis.

**I Molecular Orbital Energy Level Modulation through Incorporation of Selenium and Fluorine into Conjugated Polymers for Organic Photovoltaic Cells**

Wenliu Zhuang,\* Hongyu Zhen, Renee Kroon, Zheng Tang, Stefan Hellström, Lintao Hou, Ergang Wang, Desta Gedefaw, Olle Inganäs, Fengling Zhang, Mats R. Andersson\*

*Journal of Materials Chemistry A* **2013**, *1* (43), 13422–13425.

**II Computational Modelling of Donor–Acceptor Conjugated Polymers through Engineered Backbone Manipulations Based on a Thiophene–Quinoxaline Alternating Copolymer**

Wenliu Zhuang,\* Angelica Lundin, Mats R. Andersson\*

*Journal of Materials Chemistry A*, Accepted, DOI: 10.1039/C3TA14456A.

**III Influence of Incorporating Different Electron-Rich Thiophene-Based Units on the Photovoltaic Properties of Isoindigo-Based Conjugated Polymers: An Experimental and DFT Study**

Wenliu Zhuang,\* Margherita Bolognesi, Mirko Seri, Patrik Henriksson, Desta Gedefaw, Renee Kroon, Markus Jarvid, Angelica Lundin, Ergang Wang, Michele Muccini, Mats R. Andersson\*

*Macromolecules* **2013**, *46* (21), 8488–8499.

**IV Conjugated Polymers Based on Benzodithiophene and Fluorinated Quinoxaline for Bulk Heterojunction Solar Cells: Thiophene versus Thieno[3,2-*b*]thiophene as  $\pi$ -Conjugated Spacers**

Desta Gedefaw,<sup>‡</sup> Marta Tessarolo,<sup>‡</sup> Wenliu Zhuang,<sup>‡</sup> Renee Kroon, Ergang Wang, Margherita Bolognesi, Mirko Seri,\* Michele Muccini, Mats R. Andersson\*

*Polymer Chemistry*, Accepted, DOI: 10.1039/C3PY01519J. (<sup>‡</sup>Co-first author)

**V Side-Chain Architectures of 2,7-Carbazole and Quinoxaline-Based Polymers for Efficient Polymer Solar Cells**

Ergang Wang,\* Lintao Hou, Zhongqiang Wang, Zaifei Ma, Stefan Hellström, Wenliu Zhuang, Fengling Zhang, Olle Inganäs, Mats R. Andersson\*

*Macromolecules* **2011**, *44* (7), 2067–2073.

## **Contribution Report**

- I** Main author. Significant contributions in the interpretation of the results with input from the co-authors. Active in planning the study. Performed all of the modelling work and most of the experimental work. Prepared the manuscript.
- II** Main author. Significant contributions in the interpretation of the results together with co-authors. Active in planning the study. Performed all of the modelling work. Prepared the manuscript.
- III** Main author. Significant contributions in the interpretation of the results with input from the co-authors. Active in planning the study. Performed all of the modelling work and most of the experimental work. Prepared the manuscript.
- IV** Co-first author. Significant contributions in the interpretation of the results in conjunction with other co-authors. Performed all of the modelling work and responsible for part of the synthesis. Some writing.
- V** Co-author. Active in planning the study. Responsible for part of the experimental work and design of the polymers.

## Related Publications Not Included in the Thesis

### VI 2D $\pi$ -Conjugated Benzo[1,2-*b*:4,5-*b'*]dithiophene- and Quinoxaline-Based Copolymers for Photovoltaic Applications

Margherita Bolognesi, Desta Gedefaw, Dongfeng Dang, Patrik Henriksson, **Wenliu Zhuang**, Marta Tessarolo, Ergang Wang, Michele Muccini, Mirko Seri and Mats Andersson

*RSC Advances* **2013**, 3 (46), 24543–24552.

### VII Synthesis and Photovoltaic Properties of Conjugated Polymers Incorporating a Fused Lactam Unit

**Wenliu Zhuang**,<sup>‡</sup> Renee Kroon,<sup>‡</sup> Armantas Melianas, Timothy T. Steckler, Desta Gedefaw, Olle Inganäs and Mats R. Andersson\*

*Manuscript*

## List of Symbols and Abbreviations

AM1.5G	Air Mass 1.5 Global
BHJ	bulk heterojunction
OPV	organic photovoltaic
PSC	polymer solar cell
PCE	power conversion efficiency
$J-V$	current density–voltage
$J_{SC}$	short-circuit current density
$V_{OC}$	open-circuit voltage
FF	fill factor
$P_{in}$	power density of the incident light irradiation
EQE	external quantum efficiency
D/A	donor/acceptor
$\bar{M}_n$	number-average molar mass
$\bar{M}_w$	mass-average molar mass
$\mathcal{D}_M$	molar-mass dispersity
$\bar{X}_n$	number-average degree of polymerization
HOMO	highest occupied molecular orbital
LUMO	lowest unoccupied molecular orbital
$E_g$	band gap, or energy gap
$E_g^{opt}$	optical gap
$E_g^{ec}$	electrochemical band gap
$E_{CT}$	energy of charge-transfer state
DFT	density functional theory
TD-DFT	time-dependent density functional theory

AFM	atomic force microscopy
DSC	differential scanning calorimetry
TGA	thermogravimetric analysis
GPC	gel permeation chromatography
SEC	size exclusion chromatography
MALDI	matrix-assisted laser desorption/ionization
NMR	nuclear magnetic resonance
SWV	square-wave voltammetry
UV-vis	ultraviolet-visible
RMS	root mean square
FWHM	full width at half-maximum
BDT	benzo[1,2- <i>b</i> :4,5- <i>b'</i> ]dithiophene
CF	chloroform
DCB	<i>o</i> -dichlorobenzene
DIO	1,8-diiodooctane
DMF	<i>N,N</i> -dimethylformamide
Fc	ferrocene
ITO	indium tin oxide
THF	tetrahydrofuran
NBS	<i>N</i> -bromosuccinimide
<i>n</i> -BuLi	<i>n</i> -butyllithium
PC <sub>61</sub> BM	[6,6]-phenyl-C <sub>61</sub> -butyric acid methyl ester
PC <sub>71</sub> BM	[6,6]-phenyl-C <sub>71</sub> -butyric acid methyl ester
Pd <sub>2</sub> (dba) <sub>3</sub>	tris(dibenzylideneacetone)dipalladium(0)
P( <i>o</i> -tol) <sub>3</sub>	tri( <i>o</i> -tolyl)phosphine
Ni(dppp)Cl <sub>2</sub>	[1,3-bis(diphenylphosphino)propane]dichloronickel(II)

# Table of Contents

<b>ABSTRACT .....</b>	<b>III</b>
<b>List of Publications .....</b>	<b>VI</b>
<b>List of Symbols and Abbreviations .....</b>	<b>IX</b>
<b>1 Introduction.....</b>	<b>1</b>
1.1 Energy .....	1
1.2 Organic Photovoltaics .....	1
1.3 Aim and Outline of the Thesis .....	2
<b>2 Organic Photovoltaics.....</b>	<b>3</b>
2.1 Background .....	3
2.1.1 Solar Energy .....	3
2.1.2 A Brief History of Solar Cells .....	3
2.2 Photovoltaic Device Operation .....	4
2.2.1 Organic Heterojunction .....	4
2.2.2 Operation Principle .....	6
2.2.3 Photovoltaic Characteristics .....	8
2.3 Band Gap and Energy Level Modulation .....	10
2.3.1 Band Gap and Optical Gap .....	10
2.3.2 Band Gap and Energy Level Modulation .....	12
<b>3 Conjugated Polymers for Organic Solar Cells .....</b>	<b>14</b>
3.1 Polymers and Dispersity.....	14
3.2 Conjugated Polymers .....	14
3.3 Required Properties of Donor Materials.....	15
3.4 Material Design and Donor–Acceptor Strategy .....	15
3.4.1 Donor Polymer Design .....	15

3.4.2	<i>Aromatic and Quinoid Resonance</i> .....	16
3.4.3	<i>Donor–Acceptor Motif</i> .....	17
3.4.4	<i>Building Blocks</i> .....	19
3.5	Synthesis of Conjugated Polymers.....	20
3.5.1	<i>Suzuki Polycondensation</i> .....	21
3.5.2	<i>Stille Polycondensation</i> .....	22
3.5.3	<i>Degree of Polymerization Control for Synthesis of Conjugated Polymers</i> ...	23
3.6	Polymer Characterization.....	24
3.6.1	<i>Gel Permeation Chromatography</i> .....	24
3.6.2	<i>UV–Vis Spectroscopy</i> .....	24
3.6.3	<i>Cyclic Voltammetry</i> .....	25
3.6.4	<i>Square-Wave Voltammetry</i> .....	26
3.7	Computational Modelling .....	26
3.7.1	<i>Computationally Driven Material Design</i> .....	26
3.7.2	<i>Density Functional Theory</i> .....	27
3.7.3	<i>General Computation Considerations</i> .....	27
<b>4</b>	<b>Energy Level Modulation</b> .....	<b>29</b>
4.1	Introduction.....	29
4.2	Energy Level Modulation by Synergistically Combining Fluorine Substitution and Selenium Substitution.....	30
4.2.1	<i>Fluorine Substitution</i> .....	31
4.2.2	<i>Selenium Substitution</i> .....	32
4.2.3	<i>Synergistic Effect of Fluorine and Selenium Substitutions</i> .....	33
4.3	Computational Modelling Tool in Search for Chemical Methodologies .....	35
4.3.1	<i>Electronic Effect of Incorporating Fluorine and Nitrogen Atoms into the Acceptor Units</i> .....	36

4.3.2	<i>Heteroatom Effect of Chalcogen Substitutions into the Donor Units</i> .....	39
4.3.3	<i>Effect of Extended Conjugation and Fused Units in the Donor Moiety</i> .....	39
4.3.4	<i>Implications and Guidance for Material Design</i> .....	40
<b>5</b>	<b>Engineering Donor Units in Isoindigo-Based Conjugated Polymers</b> .....	<b>43</b>
5.1	Material Design, Synthesis and Structural Characterization .....	44
5.2	Electronic Structures and Optoelectronic Properties .....	47
5.3	Photovoltaic Performance .....	49
<b>6</b>	<b>Engineering <math>\pi</math>-Bridges in Quinoxaline-Based Polymers</b> .....	<b>50</b>
6.1	Highlights.....	50
6.2	Chain Conformations and Optoelectronic Properties .....	53
<b>7</b>	<b>Side-Chain Engineering in 2,7-Carbazole- and Quinoxaline-Based Polymers</b> ...	<b>57</b>
7.1	Introduction.....	57
7.2	Material Synthesis and Characterization .....	57
7.3	Optical and Electrochemical Properties .....	58
7.4	Photovoltaic Properties .....	60
<b>8</b>	<b>Concluding Remarks</b> .....	<b>61</b>
	<b>Acknowledgments</b> .....	<b>63</b>
	<b>References</b> .....	<b>65</b>
	<b>Publications</b> .....	<b>79</b>



# 1 Introduction

## 1.1 Energy

Energy remains a critical issue for the survival and prosperity of human civilization. The use of energy is projected to increase with population and economic growth in the world.<sup>1</sup> Currently, the energy consumption mainly originates from fossil resources (e.g., petroleum, coal and natural gas). In addition to the environmental and climate impacts (e.g., environmental pollutions and global warming) caused by the production and combustion of fossil fuels, these non-renewable resources are also becoming increasingly shorter in supply. Secure, clean and renewable energy sources are believed to be the eventual solution for sustainable energy, to avoid an energy crisis, especially by the direct utilization of solar energy that can be affordable, inexhaustible and clean. Among the options for sustainable energy, photovoltaic technologies offer a way to harness an unlimited energy resource (i.e., solar energy) to generate electricity with minimum environment impacts, compared to other alternatives such as water, wind and nuclear energy resources.<sup>2</sup>

## 1.2 Organic Photovoltaics

Organic photovoltaics are a promising technology for solar energy conversion based on solution-processed, lightweight, large-area, and potentially flexible devices. In particular, during the past five years we have witnessed a rapid progress of bulk heterojunction organic photovoltaics boosted by (i) design and synthesis of novel conjugated donor materials, (ii) control and optimization of device fabrication, and (iii) the development of new device architectures such as tandem and ternary solar cells. The current challenges for OPVs remain to further improve photovoltaic efficiency as well as durability and cost-effectiveness, to compete with silicon-based solar cells.<sup>3</sup> Material design through band gap and energy level tuning has been playing a key role in developing new donor materials for efficient organic solar cells. Computationally driven material design has received increasing interest to accelerate the search for optimal conjugated photovoltaic materials, and the exploration of chemical methodologies is highly desirable in pushing the efficiency further toward the theoretical limit.

### **1.3 Aim and Outline of the Thesis**

The goal with this project is to synthesize polymers for efficient solar cells. The work described in this thesis deals with the design, synthesis, characterization, and computational modelling of  $\pi$ -conjugated polymers for bulk heterojunction organic photovoltaic solar cells. It focuses on material design of conjugated donor polymers through band gap engineering via structural modifications such as backbone manipulations, side-chain engineering, as well as incorporation of newly developed building blocks. This also establishes structure–property relationships of the polymer systems here studied, and explores potential chemical methodologies for future judicious material design.

The thesis includes an introduction to organic photovoltaics (Chapter 2) and conjugated polymers (Chapter 3). Chapter 4 describes energy level modulation with chemical strategies described in further detail in Paper I and II. In Chapter 5 the influence of different donor units in the donor–acceptor polymers will be discussed, which is based on Paper III. Chapter 6 discusses the influence of conjugated bridges in the donor polymer design featured in Paper IV. Chapter 7 features a discussion on the effect of side-chain engineering on photovoltaic performance that originates from work presented in Paper V. Some concluding remarks are provided in Chapter 8 to sum up the thesis.

The synthesis, characterization, and computational modelling has been done at Chalmers University of Technology, Göteborg, Sweden, through a Ph.D. studentship funded by the Swedish Energy Agency, the European Commission FP7 collaborative project SUNFLOWER and the Swedish Research Council, while device characterization has been mainly conducted at Linköping University, Linköping, Sweden, within the framework of Center of Organic Electronics (COE), and Consiglio Nazionale delle Ricerche (CNR), Bologna, Italy, within the European Commission FP7 collaborative project SUNFLOWER.

## 2 Organic Photovoltaics

### 2.1 Background

#### 2.1.1 Solar Energy

The solar radiation that hits the earth consists of a distribution of photons with varying energy. Shown in **Figure 2.1** is the spectral distribution of photon flux at  $\sim 48^\circ$  relative to the Earth's normal, based on the standardized AM1.5G solar radiation spectrum, as is used to test the photovoltaic performance of the solar cells. Ideally a photovoltaic material should absorb as many of the available photons as possible and convert them to electricity. Also included are the Shockley–Queisser efficiency limit<sup>4</sup> of a  $p$ – $n$  junction solar cell and the maximum theoretical current density under AM1.5G illumination.<sup>5</sup>

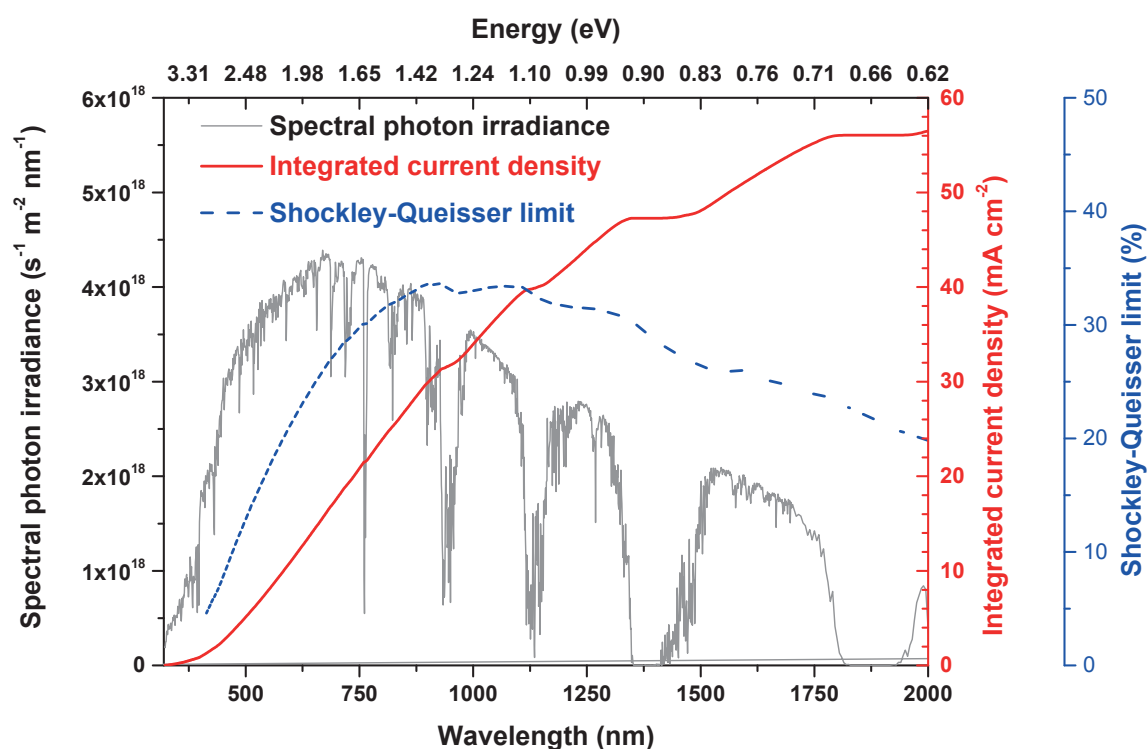


**Figure 2.1** AM1.5G solar radiation spectrum and Shockley–Queisser limit.

#### 2.1.2 A Brief History of Solar Cells

Solar cells harness solar energy, which is an abundant and renewable energy resource, and convert it directly into electrical energy by the photovoltaic effect. The photovoltaic effect was discovered in 1839 by French physicist Edmund Becquerel,<sup>6</sup> but the first working

solar cell was created in 1883 by American inventor Charles Fritts, who achieved around 1% efficiency, based on the junctions from the semiconductor selenium coated with an extremely thin layer of gold.<sup>7</sup> In 1946 Bell Laboratories patented the modern junction semiconductor solar cell,<sup>8</sup> and in 1954 the first practical photovoltaic cell was developed using a diffused silicon *p-n* junction that reached 6% efficiency.<sup>9</sup> The best efficiency of silicon solar cells to date is around 25%.<sup>10</sup> Even though silicon solar cells can be efficient and reliable, they are still too expensive to compete with fossil fuels, due to the need of the photoactive materials of high purity,<sup>10c</sup> apart from the serious environmental impact of the silicon industry.<sup>3b</sup>

During the past half century, organic solar cells have been attracting interest in both academia and industry. By the use of organic photoactive materials (e.g. semiconductive polymers) and low-temperature solution processing techniques, they show great potential for low-cost, lightweight, large-area and flexible devices.<sup>11</sup> The first organic solar cell was made in 1959 by Kallmann et al. based on a single crystal of anthracene. It was not until 1986 that an organic solar cell reached about 1% efficiency, based on a thin-film bilayer heterojunction from copper phthalocyanine and a perylene tetracarboxylic derivative, pioneered by Physical Chemist Ching Wan Tang.<sup>12</sup> The success of the electron donor/acceptor heterojunction concept largely stimulated the research in the organic photovoltaics field. The current state-of-the-art device structures are based on the concept of bulk heterojunction (BHJ),<sup>13</sup> and organic solar cells have achieved rapid progress especially during the past few years,<sup>10a,14</sup> with power conversion efficiency (PCE) as high as 8.6%<sup>15</sup> and 9.35%<sup>16</sup> respectively reported for conventional and inverted single-junction solar cells. The development of new device architectures including tandem<sup>17</sup> and ternary<sup>18</sup> solar cells has now enabled OPVs to break through the benchmarking efficiency of 10%.<sup>10a,17c,d</sup> In June 2012, Mitsubishi Chemical announced a world record efficiency of ~11% for organic thin-film photovoltaic cells.<sup>10a</sup> The current challenges for OPVs are to further improve photovoltaic efficiency as well as durability and cost-effectiveness, to compete with silicon-based solar cells.<sup>3</sup>

## **2.2 Photovoltaic Device Operation**

### **2.2.1 Organic Heterojunction**

The success of the donor/acceptor heterojunction concept in a thin-film bilayer device

architecture<sup>12</sup> in 1980s greatly vitalized the research in the organic photovoltaics field.<sup>19</sup> The discovery of fullerenes in an earlier year, for which the Nobel Prize in Chemistry in 1996 was awarded jointly to Robert F. Curl, Harold W. Kroto and Richard E. Smalley,<sup>20</sup> also enlivened the organic photovoltaics field, due to the synthesis of new fullerene derivatives and their applications as the electron acceptor in the heterojunction structure.<sup>21</sup> The problem with the bilayer heterojunction device architecture is that the exciton diffusion lengths in these organic materials are typically ~10 nm,<sup>19,22</sup> much shorter than the active layer thickness (~100 nm) commonly required to ensure sufficient light absorption. Consequently, many of the generated excitons may not be able to reach the interface to dissociate into free carriers. To overcome this issue, the two materials, acting as an electron donor and an electron acceptor respectively, can be deposited as a finely intermixed blend film, forming a so-called bulk heterojunction (BHJ).<sup>13</sup> Ideally, a bicontinuous interpenetrating blend is formed as the BHJ, with domain sizes of approximately twice the exciton diffusion length that potentially allows efficient charge separation and transport. The BHJ structure can provide a much larger interfacial area due to the interpenetrating network formed, as compared to the bilayer device architecture.

It should be pointed out that the interplay of these two components in the heterojunction is among the most important aspects determining the properties of the solar cell. A small change in the chemical structure of one material could alter its molar mass, solubility, band gap, mobility, stability, and interplay with the other component. Therefore, understanding how the chemical structure influences the polymer properties is of crucial importance in the solar energy material design. One should also bear in mind that in BHJ organic photovoltaics, control of the active layer morphology can be of critical importance, apart from altering the chemical structure of the materials. Insufficiently exploring processing parameters may cause a potentially good candidate of photovoltaic material to drop significantly in photovoltaic performance. It has been shown that the choice of proper solvents for the materials,<sup>23</sup> control of spin-speed during spin-coating to change the drying time and thickness of films,<sup>24</sup> the use of processing additives,<sup>25</sup> or thermal annealing<sup>26</sup> can alter the morphology and the performance.

In this thesis, unless otherwise specified, OPV devices are fabricated in a conventional device architecture based on polymer:fullerene bulk heterojunctions as the active layer, as

schematically shown in **Figure 2.2**.<sup>27</sup>

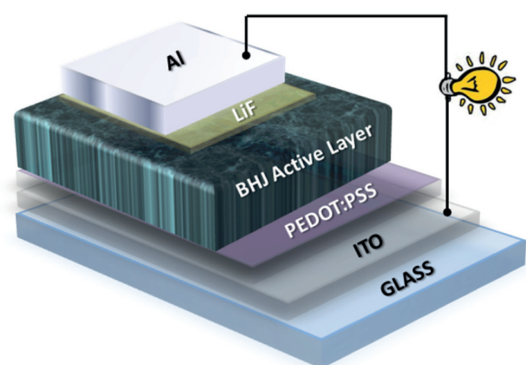
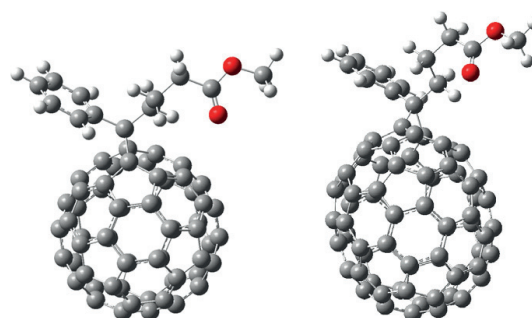


**Figure 2.2** Schematic device structure of an organic photovoltaic cell.



PC<sub>61</sub>BM

PC<sub>71</sub>BM

**Figure 2.3** Molecular structures of PC<sub>61</sub>BM and PC<sub>71</sub>BM.

In bulk heterojunction<sup>13</sup> polymer:fullerene solar cells, [6,6]-phenyl-C<sub>61</sub>-butyric acid methyl ester (PC<sub>61</sub>BM) or [6,6]-phenyl-C<sub>71</sub>-butyric acid methyl ester (PC<sub>71</sub>BM) (**Figure 2.3**) are among the most widely used as the electron acceptor in the active layer. The intermixed blend film is sandwiched between two electrodes, typically a transparent conducting anode (e.g., indium tin oxide (ITO)) and a metal cathode in a conventional device configuration (**Figure 2.2**). Additionally, a thin layer of poly(3,4-ethylenedioxythiophene) poly(styrenesulfonate) (PEDOT:PSS) is generally applied in between the ITO and the active layer to improve their electrical contact and to adjust energy levels as well as to smoothen the ITO surface.<sup>28</sup> More recently, the incorporation of a cathode interlayer, such as lithium fluoride (LiF), or poly[9,9-bis(3'-(*N,N*-dimethylamino)propyl)fluorene-2,7-diyl)-*alt*-(9,9-dioctylfluorene-2,7-diyl)] (PFN), has also been shown to greatly enhance the device performance.<sup>15d</sup>

Worth mentioning is the fast development of inverted solar cells and other new device architectures including tandem<sup>17</sup> and ternary<sup>18</sup> solar cells, which has now enabled OPVs to break through the benchmarking efficiency of 10%.<sup>10a,17c,d</sup> Photovoltaic data included in this thesis work only resulted from single-heterojunction devices, but the material design concept for tandem and ternary solar cells may also be touched.

## 2.2.2 Operation Principle

The design and synthesis of new conjugated donor materials with desirable chemical and physical properties has played a key role in realizing highly efficient OPVs, along with an

improved understanding and control behind the photovoltaic device operation in terms of absorption of light and photogeneration of excitons,<sup>29</sup> exciton diffusion and dissociation,<sup>22b,e,30</sup> charge transport,<sup>31</sup> and charge extraction.<sup>19</sup>

The operation of an organic photovoltaic cell is illustrated in **Figure 2.4**, in a simplified manner. (a) A photon is absorbed and an exciton is created. (b) The exciton diffuses toward the heterojunction interface and (c) forms an intermediate state by performing a charge transfer. (d) The exciton is then dissociated into free charge carriers, (e) which are transported to their respective electrodes and collected. It is worth emphasizing that upon charge transfer between the donor and the acceptor, electrons and holes are still Coulombically bound though spatially separated across the interface, forming a new state which is referred to as the charge-transfer (CT) state. After the interfacial CT state is formed, the first and desired possibility is for the excitons in the CT state to dissociate into free charge carriers that can be transported to their respective electrodes and collected there. However, it may decay radiatively (luminescence) or nonradiatively (by the release of heat), which results in a loss of photocurrent.<sup>32</sup> It has been found that the photovoltage that can be obtained for the photovoltaic cell is directly related to the energy of the CT state.<sup>33</sup>

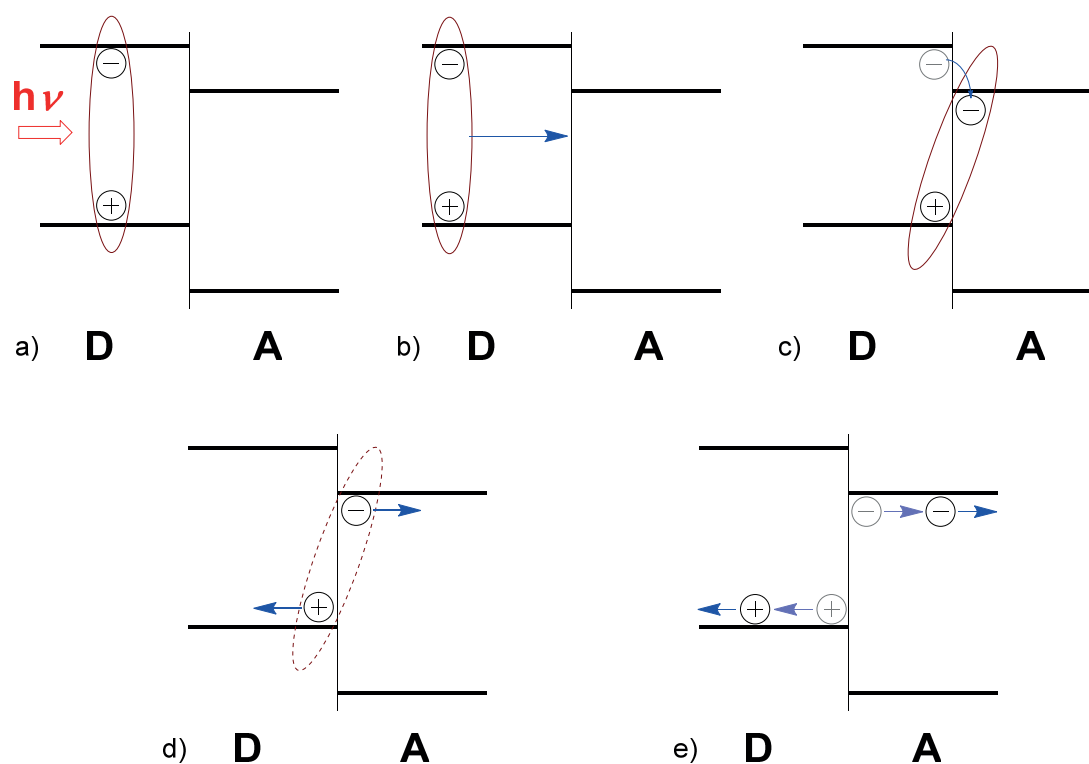


**Figure 2.4** Illustration of the principle of charge separation in a D/A heterojunction solar cell.

### 2.2.3 Photovoltaic Characteristics

In a single-junction photovoltaic cell, the power conversion efficiency (PCE), which is a measurement of how much electric power can be generated by conversion of the power provided from the light irradiation, is the most important performance quantity. It is characterized by three important parameters with a given incident power, namely open-circuit voltage ( $V_{OC}$ ), short-circuit current density ( $J_{SC}$ ), and fill factor (FF), as illustrated in **Figure 2.5**.

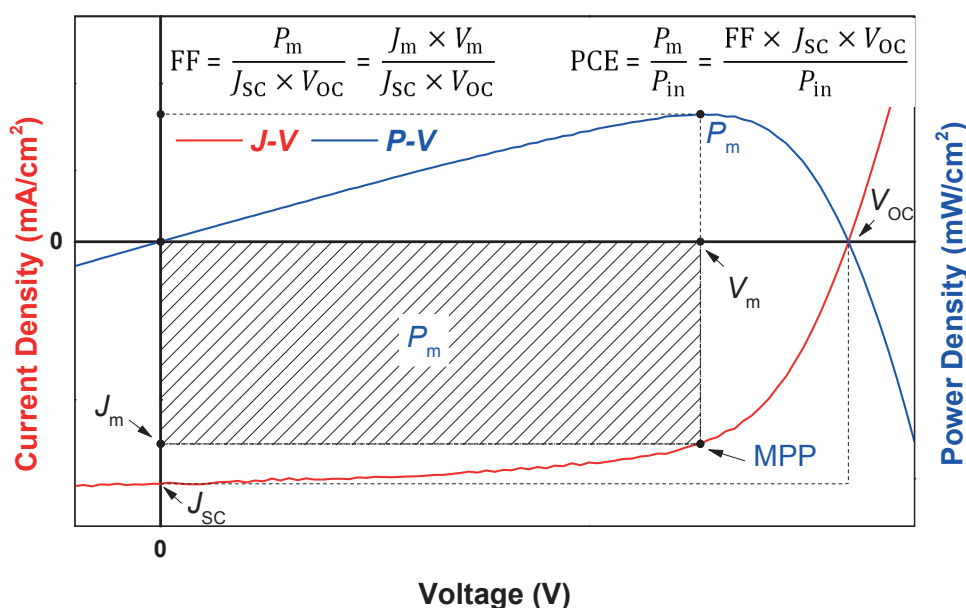


**Figure 2.5** Typical  $J$ - $V$  characteristics for a solar cell indicating the meaning of  $J_{SC}$ ,  $V_{OC}$ , FF, and PCE. The  $P$ - $V$  curve is also illustrated.  $J_m$  and  $V_m$  are respectively the current density and voltage at the maximum power point (MPP or  $P_m$ ), and  $P_{in}$  is the input irradiance.

Another way to evaluate the solar cell performance is to measure the external quantum efficiency (EQE). The EQE is a measurement of the ratio of the number of charge carriers collected by the solar cell to the number of incident photons of a given energy absorbed by the solar cell from outside.

In principle, to push the efficiency toward the theoretical limit in a single-junction photovoltaic cell, achieving both a high  $J_{SC}$  and a high  $V_{OC}$  is crucial, as well as a high FF. The FF characterizes how square-shaped the  $J$ - $V$  curve is and represents how easily the photogenerated carriers can be extracted out of a photovoltaic cell. To collect the photocurrent effectively, electrical transport must be adequate, and mobility of charge

carriers must be balanced to avoid formation of space charges, as in many materials generation and recombination of charge carriers is the limiting step. Many of these aspects are compressed in the FF of the device.<sup>34</sup> Therefore, understanding of the FF and the shape of a  $J-V$  curve can be helpful to probe what processes are occurring inside an OPV, especially when a new material is characterized.<sup>34</sup> Currently, a  $V_{OC}$  over 1 V,<sup>23b,27b,35</sup> a  $J_{SC}$  as high as 17–18 mA/cm<sup>2</sup>,<sup>16a,17d,36</sup> coupled with an EQE as high as 70–85%,<sup>16a,36c-h</sup> and a FF as high as 70–80%<sup>15a-d,16,17c,36c,37</sup> have been demonstrated in different single-junction organic solar cells. The challenge remains to combine all such promising photovoltaic characteristics in one solar cell, the success of which will bring the final efficiency of single-junction organic solar cells further to 12–15%.

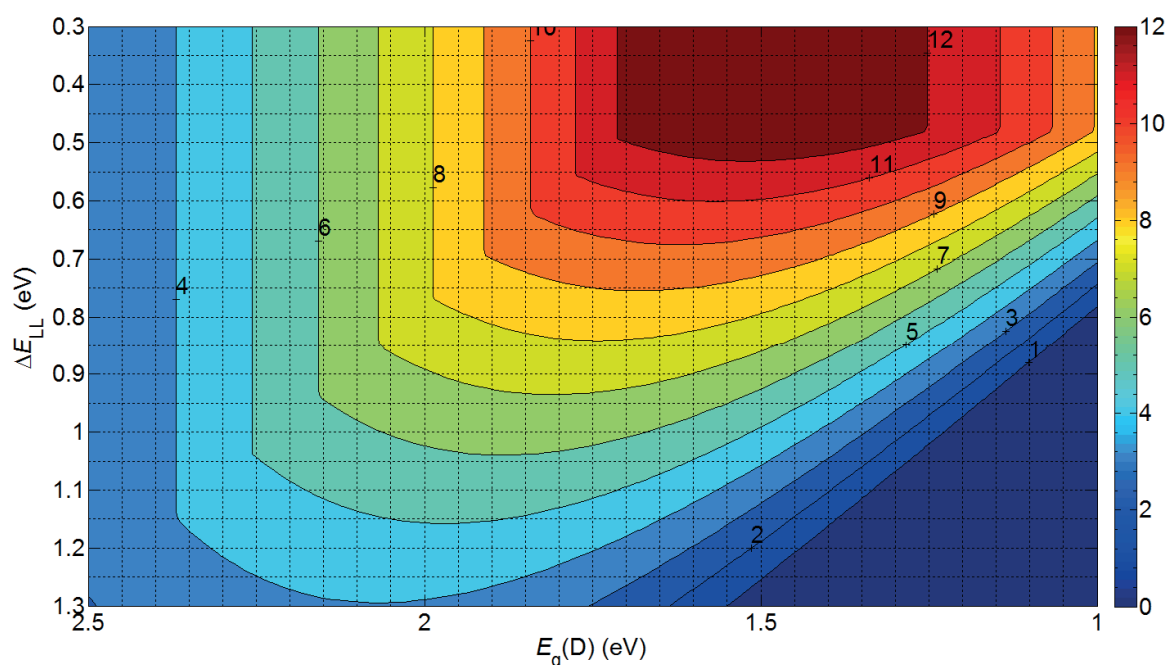


**Figure 2.6** Contour plot showing calculated efficiency (%) versus donor band gap (eV) & LUMO–LUMO level offset (eV) under AM1.5G illumination for a single-junction solar cell with PCBM as the acceptor material, assuming FF = 75% & EQE = 80%.

By assuming a FF of 75% and EQE of 80%, it is found possible to reach over 12% efficiency for polymer:fullerene solar cells (**Figure 2.6**),<sup>17b,38</sup> and very likely, a PCE of over 17% can be achieved by constructing double-junction tandem solar cells (**Figure 2.7**).

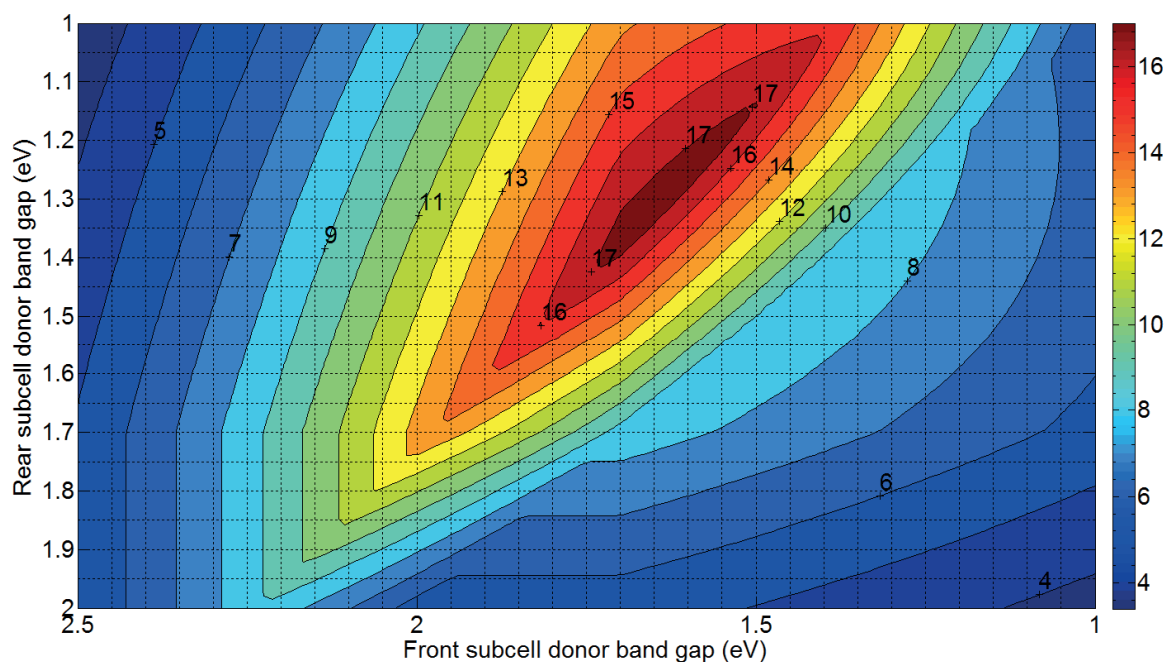


**Figure 2.7** Contour plot of calculated efficiency (%) under AM1.5G illumination for a double-heterojunction tandem device as a function of the band gaps of both donors, assuming  $\Delta E_{LL} = 0.3$  eV &  $E_g(A) = 1.7$  eV & FF = 75% & EQE = 80% for all subcells.

## 2.3 Band Gap and Energy Level Modulation

### 2.3.1 Band Gap and Optical Gap

The energy gap between the electronic levels of the highest occupied (HOMO) and lowest unoccupied (LUMO) molecular orbitals is a critical parameter determining the electronic, optical, redox, and electrical transport properties of a material.<sup>39</sup>

At the material level, the band gap ( $E_g$ ) is defined as the energy difference between the top of the valence band and the bottom of the conductive band. It corresponds to the energy difference between the ionization energy (IE) and electron affinity (EA) of the material. For a conductive material there would be no band gap due to the overlap of the two bands, allowing easy access for electrons in the valence band to move into the conductive band. Conversely, an insulator generally has a large band gap, making the electron moving between the two bands almost impossible. For a semiconductor, such as a conjugated polymer, the band gap is intermediate, enabling electrons to be excited to move from the valence band into the conductive band by various means. By measuring the ionization energy and electron affinity, it will be possible to assess the band gap of a material, but inconsistency in the values may occur with various methods and the results

should be used carefully.

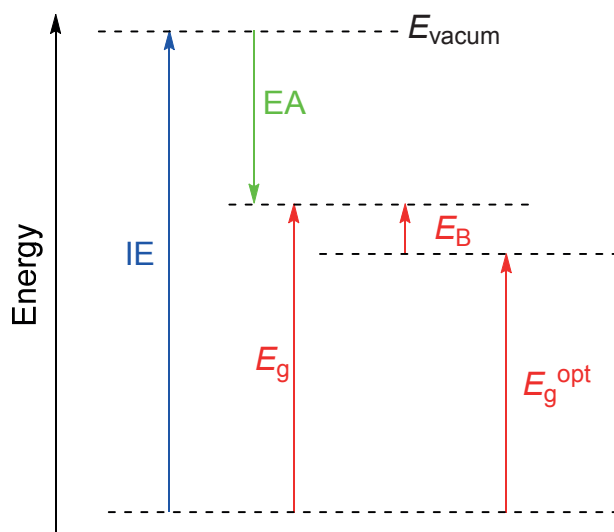


**Figure 2.8** Illustration of gap energies in the molecular case: the IE – EA difference represents the electronic band gap,  $E_g$ ; the electron–hole pair binding energy,  $E_B$ , is given by  $E_g - E_g^{\text{opt}}$ .<sup>39</sup>

The optical gap ( $E_g^{\text{opt}}$ ) is defined by the lowest optical transition upon photon absorption, that is, the energy threshold for photons to be absorbed. For conjugated polymers, the electron and hole remain electrostatically bound to one another in the excited state upon light absorption. This is different from the electronic band gap, which is defined by the minimum energy required to create an electron–hole pair that is not bound together. Thus, there will be an energy difference between the electronic band gap and the optical gap, which is termed as the exciton binding energy ( $E_B$ ), as shown in **Figure 2.8**. For conventional inorganic semiconductor crystals, the exciton binding energy is normally negligible, such that the optical gap and the electronic band gap become almost identical.

Different techniques may yield slightly different results in determination of the band gap. It can be noted that the optical gap of a conjugated polymer, as deduced from the onset of the UV–vis absorption spectrum, is often smaller than its electronic band gap, as accessed by electrochemical measurements such as square-wave voltammetry, which is commonly seen in the literature.<sup>27d,38b,39-40</sup> This can be due to the aforementioned fact that for conjugated polymers, the electron and hole remain electrostatically bound to one another in the excited state upon light absorption (contrary to the ionized state in the electrochemical measurements).<sup>39</sup> Besides that, polymer interchain interactions can generally result in a reduction in optical gaps in the solid state absorption, as compared to

electrochemical band gaps.<sup>27d,38b</sup> In addition, the interface barrier between the polymer film and the electrode surface can further cause a difference, making the electrochemical band gaps even larger than the optical gap.<sup>40</sup>

Since the band gap is such a critical parameter as mentioned above, being able to tune the band gap and the band edges will be of utmost importance in order to design new conjugated polymers for optoelectronic devices. For example, for a polymer solar cell, not only the band gap will influence the light absorption and thus the photocurrent generation, but also the position of its band edges may influence the photovoltage and photocurrent that can be extracted in the device.

### **2.3.2 Band Gap and Energy Level Modulation**

For a solar cell to perform well, the most important part of the solar radiation spectrum (**Figure 2.1**, Section 2.1.1) should be covered and efficiently absorbed, typically ranging from ~315–1400 nm (with photon energy of about 0.9–4 eV). Light-harvesting materials that have an optical gap between 1–2 eV are desired to maximize the solar cell efficiency.<sup>4,38a</sup> Clearly, to boost the efficiency toward the theoretical maximum in a single-junction photovoltaic cell, attaining both a high  $J_{SC}$  and a high  $V_{OC}$  is crucial, as well as a high FF. Both  $J_{SC}$  and  $V_{OC}$  are influenced by the band gap of the photoactive material and by the alignment of the HOMO and LUMO energy levels with respect to the acceptor material used in the donor–acceptor heterojunction. It has to be noted that the PCE is not monotonically correlated to either the band gap of the donor material or the LUMO-level offset of the donor material to the acceptor material (i.e.,  $LUMO_{Donor} - LUMO_{Acceptor}$ ), but both of them need to be optimized independently.<sup>17a,b,41</sup> Decreasing the band gap of the donor material will broaden the absorption spectrum, making it possible to harvest more photons for charge generation.<sup>5</sup> But decreasing the band gap of the donor material means that the HOMO level of the donor material ( $HOMO_{Donor}$ ) is raised or the LUMO level of the donor material ( $LUMO_{Donor}$ ) is lowered. Raising  $HOMO_{Donor}$  will decrease the maximum value for  $V_{OC}$ , approximated by  $(LUMO_{Acceptor} - HOMO_{Donor})/e$ .<sup>17b,41-42</sup> Lowering  $LUMO_{Donor}$  will reduce the LUMO-level offset of the donor material to the acceptor material used (i.e.,  $LUMO_{Donor} - LUMO_{Acceptor}$ ). The  $LUMO_{Donor} - LUMO_{Acceptor}$  difference is considered to provide the driving force for exciton dissociation as well as to prevent recombination of photogenerated charges.<sup>43</sup> A compromise is therefore needed to

## *Organic Photovoltaics*

balance the trade-off between the band gap of the donor material and the favorable alignment of HOMO/LUMO energy levels of the donor material with respect to the acceptor material.<sup>17b,41</sup> As a result, the effort to search for new electron donor polymers for OPVs is not merely directed to obtaining low band gaps but also to controlling the band gap by modulating the HOMO and LUMO energy levels to their optimal positions. Molecular engineering to carefully fine-tune the HOMO/LUMO energy levels and band gap is therefore of critical importance.

It is worth mentioning that energy level modulation is just one of the most important aspects in material design for organic solar cells. A good material design should try to take into account as fully as possible the whole process of the factors or properties that affect the photovoltaic device operation, such as absorption of light by the active layer, generation of excitons, diffusion of the excitons, CT-state dissociation of the excitons with generation of charge, mobility of charge carriers, charge collection at electrodes and so on.<sup>19,42</sup>

Even though the maximum attainable PCE can be predicted, the realization of this relies on the judicious molecular design and synthesis, especially in exploration of chemical methodologies.<sup>17b,44</sup> Furthermore, the design of efficient tandem solar cells requires an achievable high  $V_{OC}$  or high  $J_{SC}$  in conjunction with a high PCE from the donor components to be integrated, in order to exploit the overall performance.<sup>17b,c,18b</sup> All of these require a superior understanding of material design and device design.

## 3 Conjugated Polymers for Organic Solar Cells

### 3.1 Polymers and Dispersity

A polymer is a substance composed of macromolecules, usually in a range of molar masses (unit kg/mol), as not all of them are identical.<sup>45</sup> Generally the polymer chains can be portrayed as consisting of regular structural repeating units, along with end-groups.

The term “dispersity” has been recommended since 2009 by the IUPAC Polymer Division to describe the dispersions of distributions of properties such as molar masses (or relative molecular masses, or molecular weights) and degrees of polymerization.<sup>46</sup> Above all, molar-mass dispersity ( $D_M$ ) is defined as the ratio of the mass-average molar mass ( $\bar{M}_w$ , or  $\bar{M}_m$ ) to the number-average molar mass ( $\bar{M}_n$ ). Analogously, degree-of-polymerization dispersity ( $D_X$ ) is defined as the ratio of the mass-average degree of polymerization ( $\bar{X}_w$ ) to the number-average degree of polymerization ( $\bar{X}_n$ ). For a homopolymer or an alternating copolymer of sufficiently large molar masses, such that the effects of the distinct structures of the end-groups of the constituent macromolecules can be neglected, these dispersities will become identical to each other and can simply be referred to as  $D$  (i.e.,  $D_M = D_X = D$ ).

### 3.2 Conjugated Polymers

Polymers are typically insulators and may be used in power cables. In 1977, the exceptional conductivity ( $38 \text{ S cm}^{-1}$ ) of polyacetylene upon iodine doping was reported by Alan J. Heeger, Alan MacDiarmid and Hideki Shirakawa,<sup>47</sup> who were jointly awarded the Nobel Prize in Chemistry in 2000 for the discovery and development of conductive polymers. A conjugated polymer is a polymer composed of macromolecules with a sequence of conjugated multiple bonds in the main chains.<sup>48</sup> A conjugated polymer is referred to as a  $\pi$ -conjugated polymer if  $\pi$ -electrons are delocalized along the polymer main chain. Polyacetylene<sup>47,49</sup> is the simplest example as a  $\pi$ -conjugated polymer, consisting of alternating single and double bonds in its linear hydrocarbon chains.  $\pi$ -Conjugated polymers, such as poly(2,5-thiophene)s,<sup>50</sup> are widely used as photoactive materials with appropriate optical and electronic properties for optoelectronic applications due to their unique delocalized  $\pi$ -electron systems.

## Conjugated Polymers for Organic Solar Cells

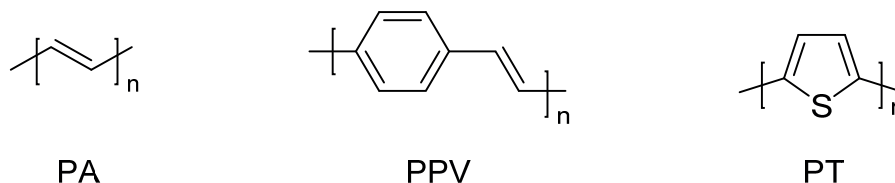


**Figure 3.1** Chemical structures of PA, PPV and PT.

It should be noted that a conjugated polymer may also be a  $\sigma$ -conjugated polymer (other than  $\pi$ -conjugated polymer), such as polysilanes<sup>51</sup> and polygermanes,<sup>48</sup> in molecules of which  $\sigma$ -electrons are delocalized along the main chain. Unless otherwise specified, the conjugated polymers discussed hereafter refer to those with delocalized  $\pi$ -electron systems.

### 3.3 Required Properties of Donor Materials

In general, an ideal organic electron donor component should present a broad spectral coverage of light absorption with a high absorption coefficient,<sup>52</sup> suitable frontier molecular orbital energies matching those of the acceptor to facilitate power generation,<sup>41</sup> a sufficient hole mobility to avoid formation of space charges,<sup>53</sup> and appropriate solution processability with film-forming and nano-structuring ability, once blended with the acceptor material, to form a beneficial morphology in the photoactive layer with nano-segregated and bicontinuous interpenetrating donor:acceptor domains, and long-term stability. The challenge, however, is to combine so many different properties into one single material. Therefore, conjugated polymers with fine-tuned HOMO and LUMO levels for efficient function in solar cells and for absorption covering the important part of the solar emission can be synthesized as a starting strategy of choice generally, while further structural modifications may be needed to tailor the other important properties for the material to perform well.<sup>3b,5,17a,38b,41,54</sup>

### 3.4 Material Design and Donor–Acceptor Strategy

#### 3.4.1 Donor Polymer Design

Generally, a conjugated polymer can be arbitrarily divided into three constituting components: the conjugated backbone, the side chains and the substituents.<sup>55</sup> The conjugated backbone is the most important component because it determines most of the physical properties related to photovoltaic performance and is of utmost importance in the

further development of polymer solar cells. The conjugation length of the polymer is quite important for conjugated polymers and is mostly dependent on the conjugated backbone. The longer the conjugation length of the polymer the smaller the band gap will be.<sup>56</sup> As the degree of polymerization reach high levels there will however be a saturation of this effect.<sup>57</sup> The conjugation could also be interrupted by torsion of the polymer backbone. For this reason a planar conformation of the backbone is preferred for achieving a small band gap.

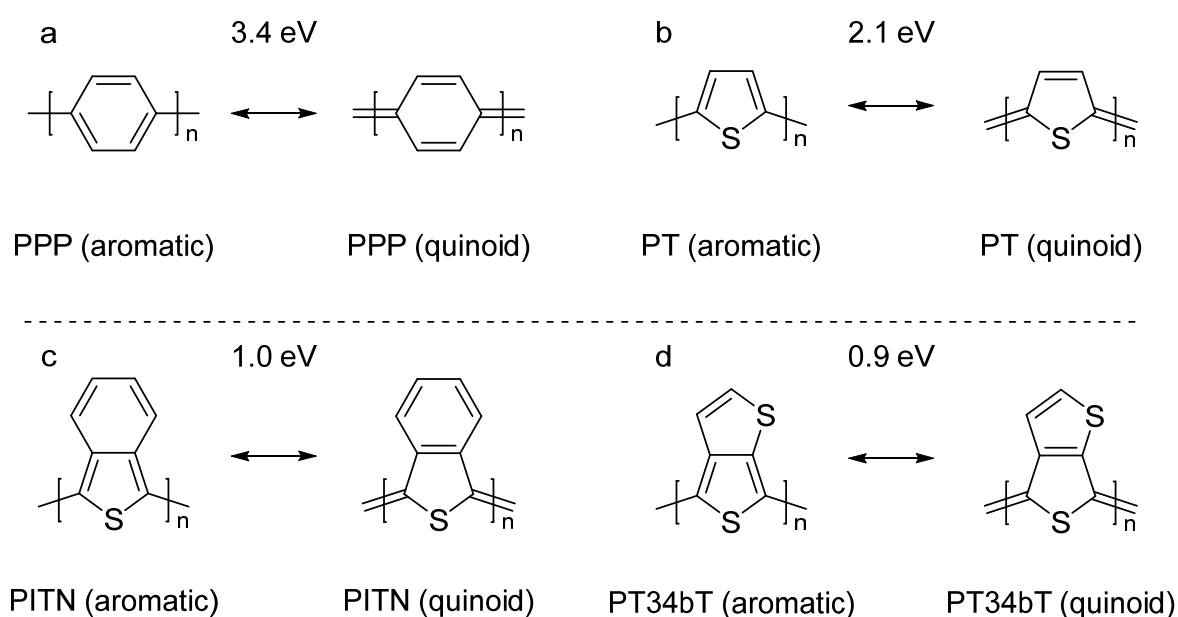


**Figure 3.2** Aromatic/quinoid forms and the optical gap of (a) PPP, (b) PT, (c) PITN and (d) PT34bT.

### 3.4.2 Aromatic and Quinoid Resonance

Generally conjugated polymers used in organic electronics consist of macromolecules containing various aromatic rings and/or fused heterocycles in the backbone. The inclusion of aromatic structures in the polymer backbone can improve the stability of the materials significantly. If we consider poly(*p*-phenylene) (PPP,  $E_g^{\text{opt}} = 3.4 \text{ eV}$ )<sup>58</sup> or poly(2,5-thiophene) (PT,  $E_g^{\text{opt}} = 2.1 \text{ eV}$ )<sup>59</sup> one quinoid resonance form can be derived apart from their energetically favored aromatic structure (**Figure 3.2**).<sup>60</sup> In the quinoid structure, the  $\pi$ -electrons are more delocalized. Properties of such a structure include smaller difference between single and double bond lengths, a more planar structure, a reduced band gap and a red-shifted absorption.<sup>61</sup> Upon chain extension via coupling of donor and acceptor monomers, to some extent the quinoid form is stabilized in the resulting polymer, strengthening the double bond character between the monomers and reducing the band

gap.

Improving the quinoid character of the backbone has been shown to be one effective way to narrow the band gap of a polymer. For example, fusing an aromatic benzene ring onto the parent thiophene in PT (**Figure 3.2**) resulted in poly(1,3-benzo[*c*]thiophene) (i.e., polyisothionaphthalene, PITN,  $E_g^{\text{opt}} = 1.0$  eV),<sup>62</sup> where the quinoid form is made more stable, which lowers the band gap by almost 50%.<sup>63</sup> Another similar example is poly(4,6-thieno[3,4-*b*]thiophene) (PT34bT), with an optical gap as low as 0.9 eV.<sup>64</sup>

### 3.4.3 Donor–Acceptor Motif

One well-established approach to obtain conjugated polymers is based on the strategy of donor–acceptor polymers,<sup>65</sup> which could not only form strong interchain interactions that favor charge transport, but also fine-tune the electronic structures of conjugated polymers, resulting in desired optoelectronic properties.

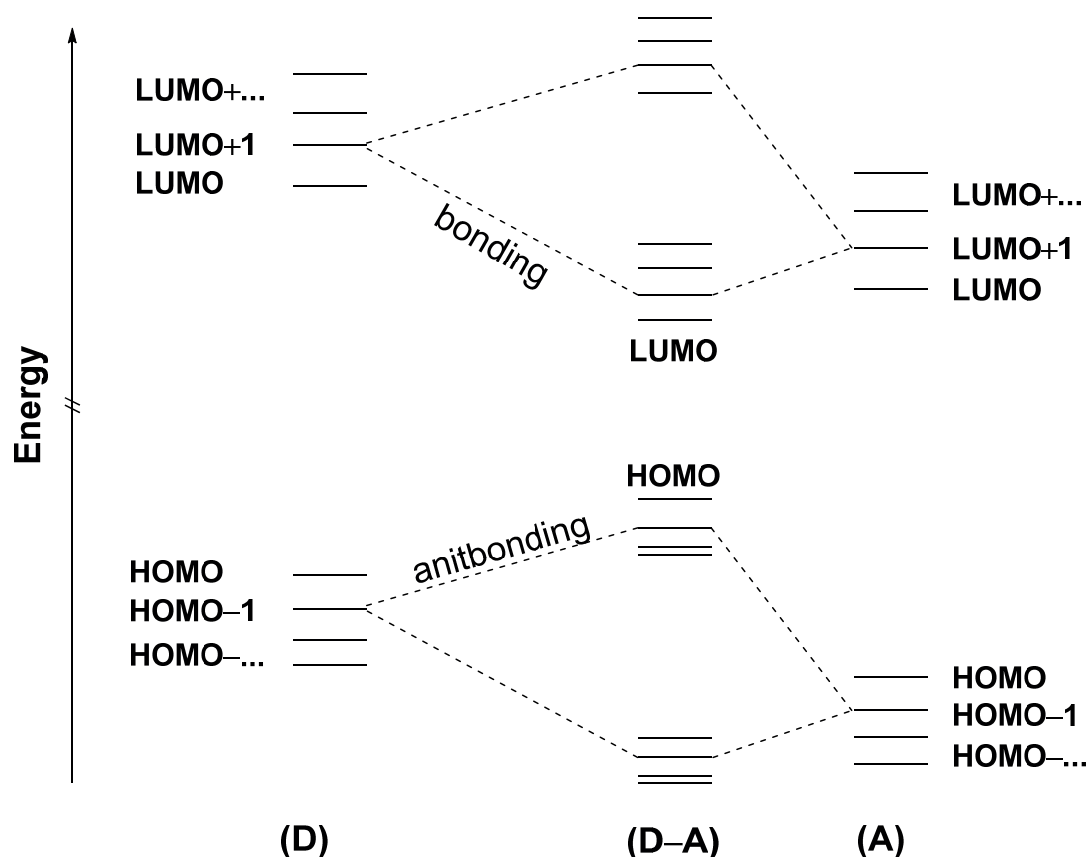


**Figure 3.3** Schematic representation of molecular orbital mixing in the alternating donor–acceptor motif in narrowing the effective band gap. Note that the resulting HOMO/LUMO do not necessarily originate from the frontier molecular orbitals of the respective segments.

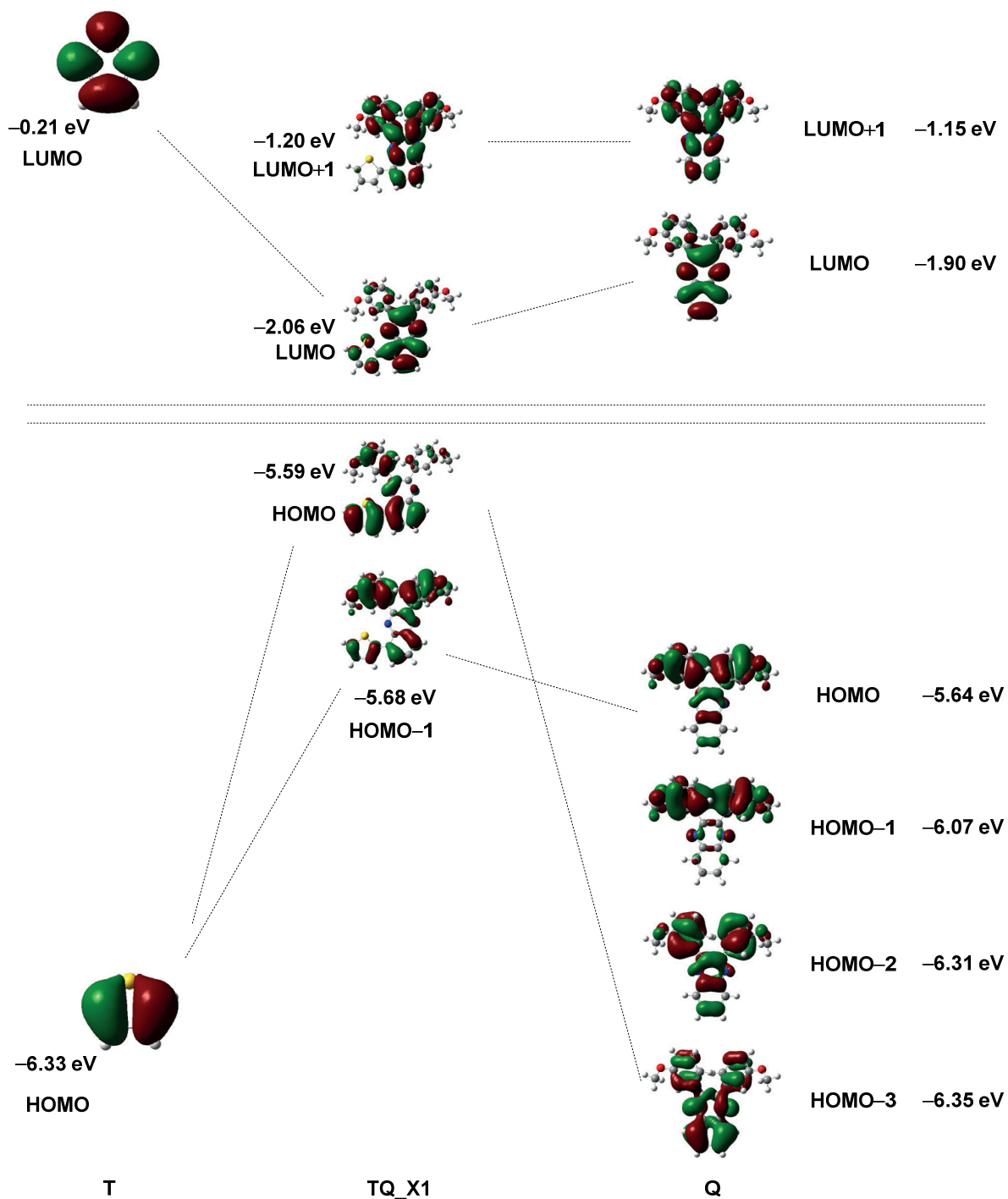


**Figure 3.4** Frontier orbitals of TQ1 monomer arising from the respective subunits (with isodensity plots, isovalue surface 0.02 au) as evaluated by DFT at the B3LYP/6-31G(d) level of theory.<sup>66</sup>

In this approach,  $\pi$ -electron-donating (donor) and  $\pi$ -electron-accepting (acceptor) conjugated moieties are combined into the backbones (i.e. the repeating units) of conjugated polymers, forming internal donor–acceptor structures. The energy levels and band gap of conjugated polymers can thus be controlled by choosing appropriate donor

and acceptor moieties, with the HOMO energy level determined synergistically by the donor and acceptor moieties, and the LUMO energy level by the acceptor moiety. A schematic representation of molecular orbital mixing to result in the HOMO and the LUMO of a donor–acceptor polymer is illustrated in **Figure 3.3**, which narrows the band gap.<sup>17b</sup> As an example in our study, **Figure 3.4** shows the molecular orbital contribution of the respective donor and acceptor moieties in the repeating unit of the donor–acceptor polymer **TQ1** (**Scheme 4.1**, Section **4.1**), as evaluated by DFT calculations.<sup>66</sup>

#### **3.4.4 Building Blocks**

As discussed in Section 3.4.1, the design of conjugated polymers relies first of all on the construction of the conjugated backbone (i.e. the repeating unit), which is the most important component because it determines most of the physical properties related to photovoltaic performance and is of utmost importance in the further development of polymer solar cells. In order to design a conjugated donor polymer that can combine as many desired properties as possible into one conjugated backbone, as noted in Section 3.3, appropriate building blocks are needed. With the well-established donor–acceptor polymers approach, a conjugated backbone can be arbitrarily divided into three constituting components: the donor moiety, the acceptor moiety and the  $\pi$ -conjugated bridge. In these donor–acceptor architectures, both the donor and acceptor units as well as the conjugated  $\pi$ -bridging groups, if used, inserted between them as spacers, play a fundamental role. In some cases, the  $\pi$ -conjugated bridges are also arbitrarily combined into the donor moiety, as often in these cases they are more electron-releasing as compared to the acceptor moiety. Nevertheless, the most important thing is to be able to identify the functions of their incorporation either more as the donor moiety or more as the  $\pi$ -conjugated bridge.

As can be noted in Section 4.3.4, for a rational material design based on energy level modulation, a common strategy is to first control the LUMO level of a conjugated polymer, even though it may end up with suboptimal band gap engineering due to the complex effect on the  $J_{SC}$  and the  $V_{OC}$ . Such unpredictable band gap engineering is very often accompanied with a careful choice of the acceptor units. Our efforts in Chapter 4 should be helpful to a better material design.

To begin with, an acceptor building block need be carefully chosen, which is of

paramount importance to achieve conjugated donor polymers for highly efficient solar cells. With decades of efforts in the OPV or related field, some promising acceptor units have been recognized. Quinoxaline<sup>36e,37q,67</sup> and isoindigo<sup>67d,68</sup> are among those that can be used to achieve state-of-the-art performance in conjunction with an efficient synthesis, which are very attractive for the future mass production of polymer solar cells. In the meantime, the potential of these acceptor units had not yet been fully explored at the beginning of our work, but was identified.<sup>35a,52,68a,69</sup> Hence, it is worth choosing these promising electron-deficient units as the acceptor moiety to construct donor–acceptor conjugated polymers and modulate their energy levels to the optimal positions. In Chapter 5, we will more focus on the influence of the donor moiety, while in Chapter 6 will we more discuss about the function of  $\pi$ -conjugated spacers. Finally, a discussion of side chain engineering will be included in Chapter 7.

Also, designing and synthesizing new building blocks is revolutionary to boost the photovoltaic performance of conjugated polymers and make them go through the benchmark for future commercialization of polymer solar cells and more, which has been evidenced by the research effort of design and synthesis of novel conjugated donor materials in boosting the rapid progress of BHJ OPVs. However, to identify novel promising building blocks as well as to make their synthesis efficient and cost-effective need a lot of research efforts.

### **3.5 Synthesis of Conjugated Polymers**

Over the past few decades, particularly in recent years, there has been significant progress in the synthesis of conjugated polymers.<sup>70</sup> The synthesis of conjugated polymers lies essentially in efficient carbon–carbon single bond formation between two unsaturated carbons in the unsaturated units (e.g., aryl–aryl coupling). Besides electrochemical and chemical oxidative polymerizations, transition-metal-catalyzed cross-coupling reactions provide a particularly powerful tool for  $Csp^2$ – $Csp^2$  and  $Csp$ – $Csp^2$  bond formation. Especially palladium-catalyzed cross-coupling reactions are often used for conjugated polymer synthesis, including the Heck,<sup>71</sup> Negishi,<sup>72</sup> Stille,<sup>73</sup> and Suzuki<sup>74</sup> coupling reactions. In 2010, Richard F. Heck, Ei-ichi Negishi and Akira Suzuki were awarded jointly the Nobel Prize in Chemistry for their work on palladium-catalyzed cross couplings in organic synthesis.

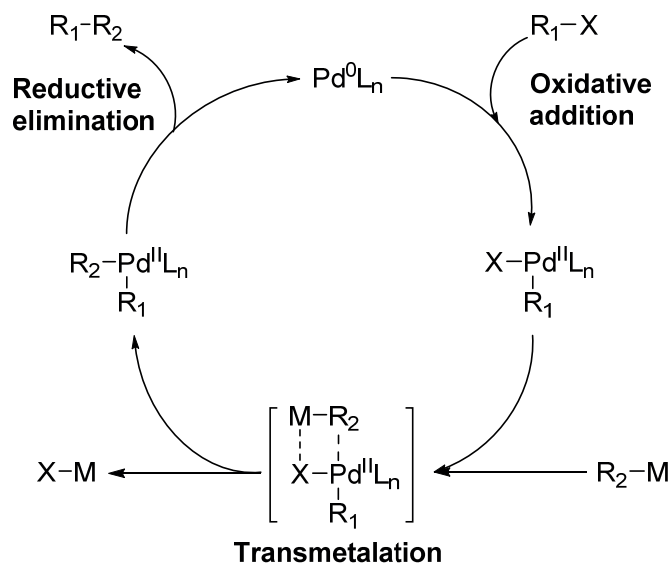


**Figure 3.5** Typical catalytic cycle of a Pd-catalyzed cross-coupling reaction.

Palladium-catalyzed cross-coupling polycondensation can be quite different from the condensation polymerization of non-conjugated polymers,<sup>75</sup> due to a unique reaction mechanism that involves a transition-metal catalyst system in a catalytic cycle (**Figure 3.5**).

In this work, either Suzuki<sup>27a</sup> or Stille<sup>27b-e</sup> polycondensation has been employed to synthesize the conjugated donor polymers studied.

### 3.5.1 Suzuki Polycondensation

The Suzuki reaction (or Suzuki coupling, or Suzuki–Miyaura reaction)<sup>74</sup> is a palladium-catalyzed cross-coupling reaction between an organoboron and a halide or pseudo-halide. The organoboron species can be an organoboronic acid or its ester, which needs to be activated for the reaction, usually in the presence of a base.<sup>27a,76</sup> This reaction is cheaper and less toxic than the Stille reaction. The Suzuki reaction can be used to perform step-growth polymerization catalyzed by Pd(PPh<sub>3</sub>)<sub>4</sub> or similar complexes.<sup>77</sup>

As illustrated in **Figure 3.6** (slightly different from **Figure 3.5**, due to the presence of a base to activate the organoboron compound), the mechanism of the Suzuki reaction involves the oxidative addition of an organic halide or pseudo-halide to give a palladium(II) intermediate, which undergoes transmetalation with the base-activated organoboron compound to give an organopalladium intermediate. This complex then

undergoes reductive elimination, giving the coupled product and regenerating the palladium(0) catalyst. Depending on the leaving groups, the oxidative addition step can be the rate-determining step of the catalytic cycle.

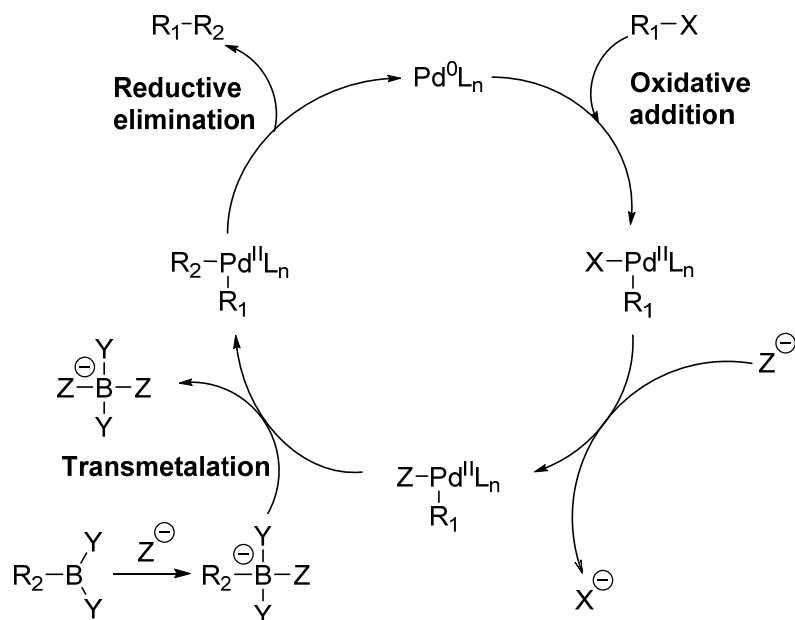


Figure 3.6 Reaction mechanism of the Suzuki reaction.

### 3.5.2 Stille Polycondensation

The Stille reaction (or Stille coupling, or Kosugi–Migita–Stille coupling)<sup>73,78</sup> is a chemical reaction that couples an organostannane with an organic halide or pseudo-halide catalyzed by palladium. The catalytic cycle of the Stille reaction is similar to that of the Suzuki reaction (*vide supra*, Section 3.5.1), except for the absence of a base in the Stille reaction.<sup>27b-d</sup> This allows the Stille reaction to have an exceptional tolerance for functional groups, which for example could be base-sensitive. It has also been shown that step-growth polymerization employing the Stille reaction with an electron-donating distannyl monomer and an electron-accepting dihalide monomer can yield high molar masses.<sup>79</sup> A major disadvantage with employing the Stille reaction is the involvement of highly toxic organostannane compounds,<sup>80</sup> which might pose a problem for future up-scaling of the synthetic process.

Following the unique catalytic cycle of palladium-catalyzed cross-coupling reactions as shown in **Figure 3.5**, the mechanism of the Stille reaction involves the oxidative addition of an organic halide or pseudo-halide to give a palladium(II) intermediate, which

undergoes transmetalation with the organostannane to give an organopalladium intermediate. This complex then undergoes reductive elimination, giving the coupled product and regenerating the palladium(0) catalyst. The transmetalation step is supposed to be the rate-determining step.

### **3.5.3 Degree of Polymerization Control for Synthesis of Conjugated Polymers**

It has been widely recognized that for polymer solar cells, the photovoltaic properties, in particular the photocurrent, can be very dependent on the chain length (i.e.,  $\bar{X}_n$  or  $\bar{M}_n$ ) of the donor polymers,<sup>36i,37t,57,81</sup> which can influence the microstructure of blend films and resulting optical and electrical properties, as also found in many related applications.<sup>36i,37t,57,81-82</sup> Therefore, obtaining a high molar mass, as well as an acceptable dispersity, on the basis of sufficient solubility for solution processing,<sup>83</sup> is one regular requirement of critical importance for conjugated polymers to perform efficiently.

In a polycondensation reaction using a step-growth mechanism, there is so-called Carothers Equation:<sup>75,84</sup>

$$p = \frac{2}{\bar{f}} \left( 1 - \frac{1}{\bar{X}_n} \right) \quad (3-1)$$

where  $\bar{X}_n$  is the number-average degree of polymerization,  $\bar{f}$  is the average degree of functionality, and  $p$  is the extent of reaction.<sup>75,84</sup> It can be rearranged to give the degree of polymerization in step-growth polymerization as follows:

$$\bar{X}_n = \frac{2}{(2 - p\bar{f})} \quad (3-2)$$

In step-growth polymerization, by controlling functionality ( $\bar{f}$ ) as well as the extent of reaction ( $p$ ) in the system, one can control the degree of polymerization  $\bar{X}_n$  to some limit (i.e.,  $\bar{X}_n = 1/(1 - p\bar{f}/2)$ ). This mechanism has been reported for many condensation polymerizations<sup>75,85</sup> including Suzuki polycondensation catalyzed by Pd(PPh<sub>3</sub>)<sub>4</sub> or similar complexes.<sup>77</sup>

Recently, many studies also suggest that a chain-growth-like mechanism can be developed for many transition-metal-catalyzed polymerizations (including Suzuki polycondensation) via catalyst-transfer polycondensation, which involves intramolecular

catalyst transfer during polymerization,<sup>77b,86</sup> making it more feasible to control the molar mass, dispersity and end groups of  $\pi$ -conjugated polymers,<sup>86e</sup> but the current monomer scope still remains largely limited to electron-donating monomers.<sup>86f</sup>

It can be concluded that obtaining high molar masses that ensure good conjugation lengths generally requires high purity and equimolar feed ratios of the monomers used, introduction of a sufficient amount of solubilizing side chains to the polymer backbone and use of an appropriate polymerization condition (e.g. solvent, catalyst system, temperature, etc.).<sup>86c,87</sup>

## **3.6 Polymer Characterization**

### **3.6.1 Gel Permeation Chromatography**

Gel permeation chromatography (GPC) is a type of size exclusion chromatography (SEC), which separates analytes on the basis of size. GPC is often used for the analysis of polymers to provide information about molar masses and dispersity, which are important properties of a polymer affecting the performance of polymer solar cells to some extent. It allows for the determination of  $\bar{M}_n$ ,  $\bar{M}_w$ ,  $D_M$  and so on (Section 3.1), with calibration relative to uniform polymer standards (e.g. polystyrene) or with universal calibration.

### **3.6.2 UV–Vis Spectroscopy**

As discussed in Section 2.3.1, the optical gap ( $E_g^{\text{opt}}$ ) is defined by the lowest optical transition upon photon absorption, that is, the energy threshold for photons to be absorbed. For organic photovoltaics to perform well, photoactive materials that can harvest the most important part of the solar radiation spectrum (**Figure 2.1**, Section 2.1.1) (typically ranging from ~315–1400 nm, with photon energy of about 0.9–4 eV) are desired to maximize the solar cell efficiency, preferably with an optical gap between 1–2 eV.<sup>4,38a</sup> Hence UV–vis spectroscopy is a useful and important measurement of the optical absorption properties to investigate and understand the performance of a conjugated polymer in solar cells.  $E_g^{\text{opt}}$  is usually deduced from the absorption edge (onset) of the UV–vis spectrum. By using Beer–Lambert law, one can also measure the absorptivity (or extinction coefficient) of a material or a blend, which is an important parameter (i.e. absorption strength) in determining the optical absorption efficiency apart from the absorption window.

### **3.6.3 Cyclic Voltammetry**

One way to assess the HOMO and LUMO energy levels of a conjugated polymer is electrochemical analysis by estimation of the respective ionization energy and electron affinity from the redox potentials. The most widely used electrochemical technique by OPV researchers is cyclic voltammetry.<sup>88</sup> This analytical method provides information of the redox processes of the investigated material as well as insight into their reversibility.

When an electrochemical analysis experiment is performed, the Faradic current (i.e., the current from the redox reaction) as well as the capacitive charging current which originates from the formed electric double layer at the working electrode is measured. The Faradic current decays more slowly than the capacitive current, which theoretically would make cyclic voltammetry ideal to evaluate the HOMO and LUMO positions. Usually the scan rate employed during cyclic voltammetry experiments is too fast for the capacitive charging current to decay sufficiently, making the redox waves recorded during the scans to be scan rate dependent.

As is known, electrochemical doping is complex and involves several simultaneous and/or consecutive chemical and physical processes like swelling of the polymer, charge transfer between the electrode and the polymer, insertion of compensating ions into the polymer bulk, conformational changes of the polymer chain and change of conductivity.<sup>88a</sup> The reverse reaction of the doping process cannot be equated to the de-doping reaction for the polymer, as conformational reorganization and variations of the energy levels are promoted by adding or removing an electron. Consequently, the electrochemical redox waves are often broad and asymmetric, and the onset potentials (the potentials for the initial injection of holes and electrons to the HOMO and LUMO, respectively) are thus generally used to estimate the electrochemical band gap.<sup>88a,89</sup> However, the onset of oxidation or reduction can vary with the scan rate, as polymers exhibit relatively slow electron transport properties.<sup>88b,89</sup> There may be inconsistencies such as how to define the onset position as well as how measurements relate to the vacuum level as found in literature.<sup>88a,b,89</sup> Also, there are uncertainties from such as the transport processes at the working electrode, the amount of energy contributed by solvation of electrochemical species, the complex interplay between Faradic current and capacitive current, the differences in conjugation length forming redox centers of varying potentials and

aggregation of polymer chains on the working electrode.

### **3.6.4 Square-Wave Voltammetry**

Square-wave voltammetry (SWV)<sup>69a,90</sup> is a pulse voltammetric technique where a square wave is superimposed upon a staircase. The idea behind the employment of pulse voltammetry is to alleviate the time dependence, in which the current is sampled at certain times after applying the potential to the working electrode. In SWV, the current is recorded at the end of each pulse, a forward current being recorded at the end of the first pulse and a reverse current being recorded at the end of the second pulse. By taking the difference in the forward and reverse currents a difference current, in theory it would minimize the contribution to the current signal from the capacitive or charging current and suppress background signals.<sup>91</sup> SWV is commonly used in trace analysis because of its high sensitivity.

Therefore, in our studies, SWV<sup>27a-d,69a,90</sup> was used to determine the oxidation and reduction potentials of the polymers more often than the traditional cyclic voltammetry,<sup>88c,d</sup> as SWV is more sensitive and more convenient to define the oxidation and reduction potentials based on the much clearer peaks in the voltammograms.

## **3.7 Computational Modelling**

### **3.7.1 Computationally Driven Material Design**

Computationally driven material design has been attracting interest to accelerate the search for optimal conjugated photovoltaic materials.<sup>92</sup> Computational modelling can provide a lot of useful physical insights about the whole process of the factors that affect photovoltaic device operation and properties that are crucial in material design as well, such as light absorption, chain conformations, electronic structures and so on,. Indeed, an improved understanding has been gained by incorporation of theoretical studies. In literature, many quantum-mechanical simulations on conjugated polymer systems have focused on the donor–acceptor polymer concept and physical insights extensively, but a comprehensive study of structural fine-tuning in relation to energy level modulation for future judicious design of conjugated donor polymers appears to be lacking, which can be useful for materials chemists in rational material design. Such work is needed to accelerate the search for chemical methodologies for example to control the frontier molecular orbital

energy levels and band gap in a judicious way and to meet the particular requirements of different device architectures (including tandem and ternary solar cells) on the donor components, such as a prominent photocurrent or photovoltage combined with a high efficiency, to further improve the overall performance of organic photovoltaics.<sup>66</sup>

### **3.7.2 Density Functional Theory**

Density functional theory (DFT) is a quantum-mechanical modelling method among the most popular and versatile ones available in condensed-matter physics, computational physics, and computational chemistry, to investigate the electronic structure of many-body systems, in particular atoms, molecules, and the condensed phases, using functionals (i.e., functions of another function) of the electron density. By expanding the theory and method in presence of time dimension, the so-called time-dependent density functional theory (TD-DFT) can be used to investigate the excited-state properties of many-body systems like excitation energies, oscillator strengths, and optical absorption spectra. In this thesis, DFT and TD-DFT have been the modelling methods of choice applied throughout the whole project focusing on the electronic properties of organic molecules and conjugated polymers.

### **3.7.3 General Computation Considerations**

Throughout this thesis, DFT calculations using the Gaussian 09 suite of programs<sup>93</sup> were performed to investigate the electronic structure of conjugated polymers by employing the B3LYP<sup>94</sup> hybrid density functional. The basis sets used for the calculations are the split valence 6-31G(d) basis set<sup>95</sup> for all the atoms except Te atoms for which effective core potential (ECP) corrected lanl2dz basis set<sup>96</sup> is employed. SCF tolerance is set so that the maximum remaining force on an atom in the system is less than  $4.5 \times 10^{-4}$  au and the maximum structural change of one coordinate is less than  $1.8 \times 10^{-3}$  au. In general, all of the optimized molecular structures are in a stable local minimum of the ground state potential energy surface, as ensured by analytical second derivatives of the Hessian matrix calculated at the same level of theory. TD-DFT calculations<sup>97</sup> were performed to assess the excited-state vertical transition energies and oscillator strengths based on the optimized molecular geometries at the same level of theory.

It has to be noted that the results from calculations should be used rigorously and should be compared to experimental data as much as possible, due to the existing

### *Conjugated Polymers for Organic Solar Cells*

limitations by the accuracy at different levels of theory and cost-effectiveness of these computational modelling methods in simulating the real world of organic/polymer optoelectronic materials and devices. In general, the accuracy and cost-effectiveness of any computation need be balanced on the basis that it can reasonably describe the trends of the properties investigated to give a systematic evaluation.

Hybrid functional B3LYP has been widely used to compute organic molecules successfully. It takes account of some dynamic correlation by mixing in the exact exchange from Hartree–Fock, which is important in order to describe long-range interactions like conjugation well.<sup>98</sup> It is worth mentioning that since the calculations reported in this study are performed within the same framework, we are able to provide a systematic evaluation of the intrinsic properties (e.g. electronic properties) of the organic molecules and polymers, by reasonable comparison of their respective trends. Our combined experimental and computational studies<sup>27b,c</sup> as well as many other studies<sup>92g,99</sup> show that the methods used here can be suitable for this purpose. In addition, some experimental data are also included in our discussion where available to compare with the trends of the calculated properties.

## 4 Energy Level Modulation

### 4.1 Introduction

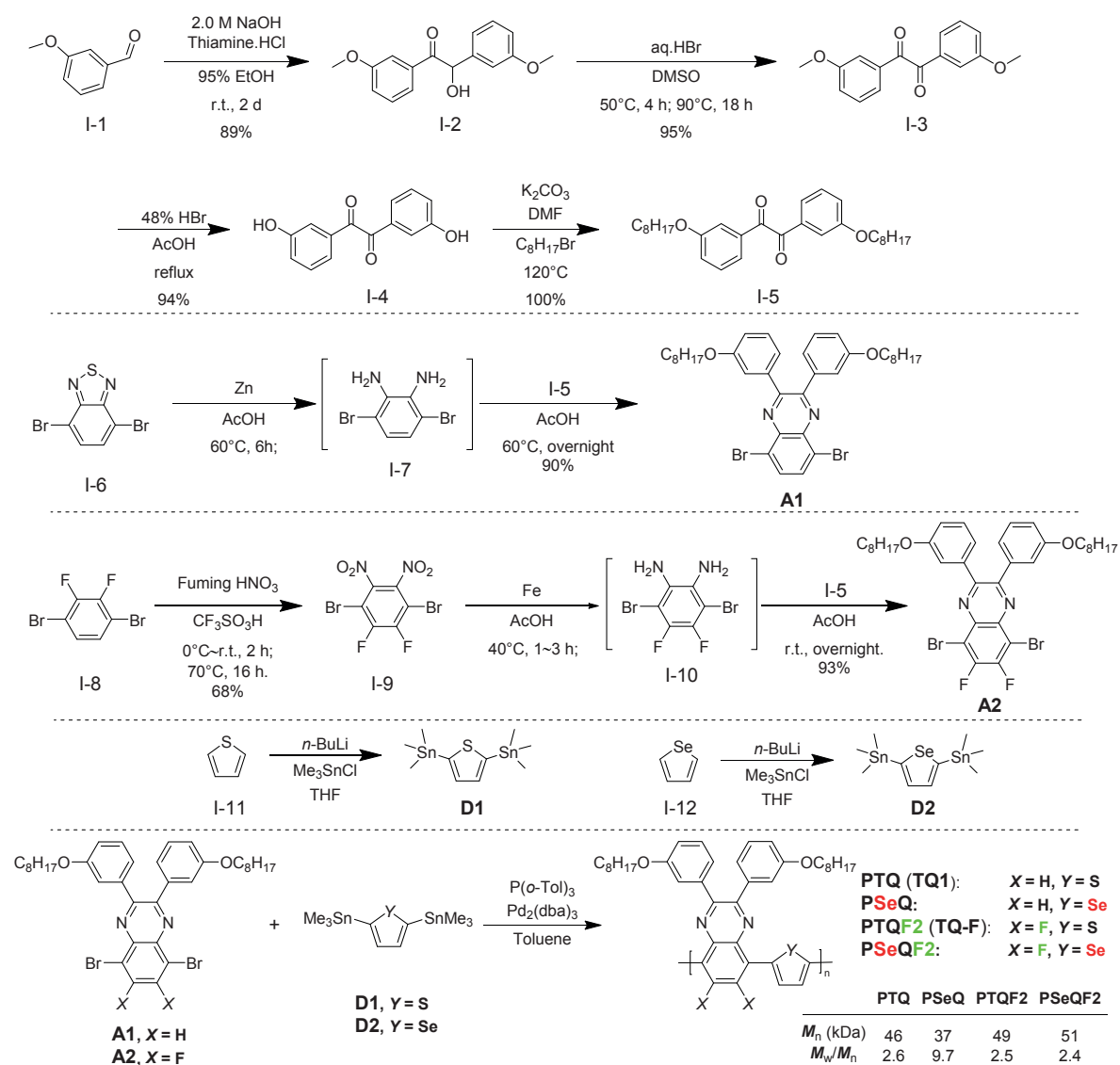
This chapter describes developing energy level modulation chemical strategies detailed in Paper I and II. The basics of energy gap and energy levels and their effect on the photovoltaic properties have been discussed in Sections 2.3.1 and 2.3.2. Here we use **TQ1 (PTQ)** as a model polymer to show how energy levels and band gap of conjugated polymers can be modulated and how such modulation can influence the resulting optoelectronic and photovoltaic properties. In particular, potential chemical methodologies for rational material design may be developed.

**TQ1 (PTQ)** is an alternating copolymer consisting of thiophene and quinoxaline. In the quinoxaline unit, two *meta*-octyloxyphenyl side groups are attached. This polymer was originally reported in 2003 by Yamamoto,<sup>100</sup> the backbone of which was already intensively studied back from 1995 by the same group,<sup>101</sup> but was never tested in solar cells until 2010 by our group.<sup>67a</sup> Very encouragingly, **TQ1** showed PCE up to 6% in conjunction with PC<sub>71</sub>BM,<sup>67a</sup> which can be further pushed to 7% by morphology control of the photoactive layer with an appropriate processing additive in 2013.<sup>67b</sup> The demonstrated high performance along with its efficient synthesis has drawn great interest due to a high perspective for mass production of polymer solar cells.<sup>67b,102</sup> The success of **TQ1** also further demonstrated the high potential of quinoxaline as the acceptor unit in conjugated polymer design.<sup>27a,35a,69a</sup> Very recently, more efficient polymer solar cells with quinoxaline-based conjugated polymers have been reported,<sup>36e,37q,67</sup> making them among the state-of-the-art promising candidates in conjunction with an efficient synthesis, which are very attractive for the future mass production of polymer solar cells.

The **TQ1** polymer has an optical gap of 1.70–1.75 eV (with an electrochemical band gap of 2.08–2.37 eV derived from SWV) and a LUMO-level offset of >0.8 eV with respect to PC<sub>71</sub>BM (based on SWV, corresponding to >0.6 eV as evaluated by DFT). The optical and electronic properties of **TQ1** suggest that the energetics of the polymer are suboptimal and that there may be still big room for improving the photovoltaic performance and for structural optimization.<sup>4,38a</sup> Modification on the chemical structure has been one focus of studies in recent years, to further understand the structure–property–performance

## Energy Level Modulation

relationships of conjugated donor materials and to further explore possibilities of improving the photovoltaic performance, such as modifications in chemical structures with fine-tuned molecular orbital energies, favorable side-chain architectures, and sufficient molar masses.<sup>27b,103</sup>



**Scheme 4.1** Synthetic route to polymers TQ1, PTQF2, PSeQ and PSeQF2.

## 4.2 Energy Level Modulation by Synergistically Combining Fluorine Substitution and Selenium Substitution

The synthetic route used in this study is outlined in **Scheme 4.1**. In this work, from our DFT and experimental study, we demonstrated an effective chemical approach to modulate the frontier molecular orbital energy levels by synergistically combining fluorine

## Energy Level Modulation

substitution and selenium substitution. This allows one to reduce the LUMO-level offset of the donor polymers to the acceptor materials while keeping the optical gap almost unchanged, accompanied by a deepening of the HOMO level. This approach may be suitable for the molecular design of new materials for the front subcell active layer in efficient tandem cells where a high photovoltage is very desirable.

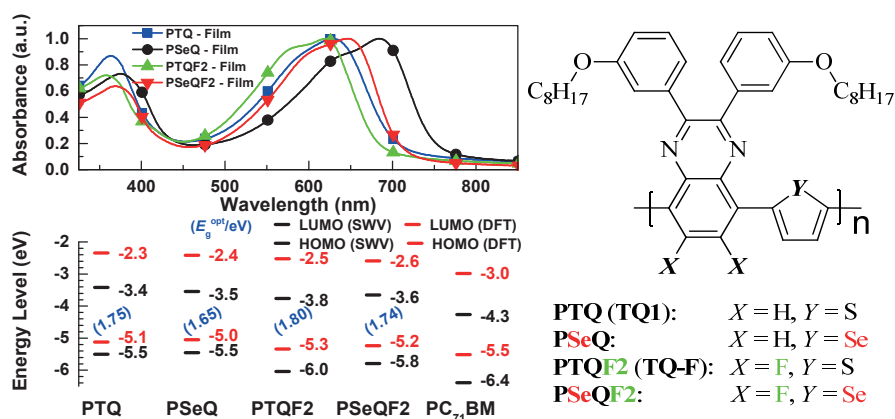


**Figure 4.1** Energy level modulation by synergistically combining F- and Se- substitutions.

### 4.2.1 Fluorine Substitution

Introduction of electron-withdrawing fluorine atoms into the polymer backbone is an effective chemical method to tune the energy levels of donor-acceptor polymers, by deepening the HOMO and LUMO levels simultaneously.<sup>104</sup> Meanwhile, as the smallest electron-withdrawing substituent in size, introduction of fluorine atoms can modulate the energy levels without disturbing the planar molecular structure of the conjugated backbone, as demonstrated by many highly-performing conjugated polymers, which is very essential and desirable for molecular design of donor materials. This approach has been employed to develop many new conjugated polymers that show efficiency exceeding 6%.<sup>15d-f,16,36e,37b,n,63b,67c,d,68d,105</sup> The record efficiency to date is registered with fluorinated conjugated polymers.<sup>15c-e,16</sup>

However, the fluorine substitution of the two protons on the quinoxaline ring in the **TQ1** repeating unit decreased the PCE to 1.6% for the TF<sub>2</sub>Q polymer (TQ-F, or **PTQF2**)<sup>103a</sup> even though a high  $V_{OC}$  of 0.99 V was obtained. When only one fluorine atom was introduced, the resulting TFQ polymer (FTQ)<sup>106</sup> was able to obtain a  $V_{OC}$  as high as 0.95 V with a PCE of 4%, close to that of the TQ polymer (**TQ1**, or **PTQ**). This

comparison suggests that the extent of fluorine substitution needs to be optimized. Very recently, it is also shown that the position of fluorine substitution can also influence the resulting photovoltaic performance.<sup>15e,105d</sup>

#### **4.2.2 Selenium Substitution**

The success of thiophene-based polymers has driven chemists to investigate the effect of substituting sulfur with other chalcogen analogues such as oxygen and selenium. The incorporation of selenophene into conjugated polymers has attracted increasing attention, which typically gives significant red-shifted UV–vis absorption as compared with its thiophene analogues, resulting in a narrowed optical gap.<sup>107</sup> Selenium substitution of sulfur on fused-thiophene units is also one direction of the attempts.<sup>81h,108</sup> Other selenium–sulfur exchange has also been attempted in the literature but is still less effective than the previous two in improving the photovoltaic performance, such as the replacement of benzo[*c*][1,2,5]thiadiazole with benzo[*c*][1,2,5]selenadiazole.<sup>109</sup>

The promising conjugated polymer **PTQ** also encouraged our focus on its selenium substitution on the thiophene moiety. Polymer synthesis of **PSeQ** is as straightforward as of **PTQ** (**Scheme 4.1**), even though the raw material cost may not be comparable. Comparable molar masses and good solubility were obtained. As a result, a red-shifted absorption is observed upon selenium substitution (**Figure 4.1**), giving an optical gap of 1.65 eV for **PSeQ**, as deduced from the film absorption edge, which is beneficial for a broader solar spectral coverage. This corresponds to a narrowing of around 0.1 eV in the band gap by substituting sulfur with selenium, as accompanied by a rise in the HOMO level and a lowering in the LUMO level to some extents, in agreement with literature.<sup>107</sup> Similar absorption coefficient is also recorded between **PSeQ** and **PTQ**, both from experimental optical absorption measurement and from TD-DFT calculations. A minimization of the large LUMO-level offset with respect to the fullerene acceptor is also preferable. All of these properties should favor the photocurrent generation. An estimate of the CT state energy gave very similar values, suggesting a comparable photovoltage may be obtainable. In summary, the resulting selenophene-based polymer is expected to be a promising candidate as an electron donor unless the fill factor in the corresponding BHJ photovoltaic devices would be reduced.

In fact, unexpectedly and disappointingly, a PCE of around 2% was registered with a

### *Energy Level Modulation*

$V_{OC}$  of  $\sim 0.76$  eV,  $J_{SC}$  of  $\sim 5.0$  mA/cm<sup>2</sup> and FF of 46%, which are concomitantly lower than the photovoltaic characteristics of devices based on **PTQ**. Based on our above discussion, it implies other parameters may be responsible for lower photovoltaic performance instead of the resulting optical and electronic properties of the polymer. Indeed, AFM studies show that the suboptimal morphology may be one reason for the poorer performance of **PSeQ** in the same device configuration, as also supported by the lower EQE over a wide wavelength range.

#### **4.2.3 Synergistic Effect of Fluorine and Selenium Substitutions**

The inferior performance upon chemical modification of **PTQ** either with difluorination on the acceptor unit or with selenium–sulfur exchange for the donor moiety was unexpected yet confirmed, although further studies may be needed to explore the potential of these polymers. However, we also tried to combine these two different modifications in one macromolecule of **PTQ**. The large LUMO-level offset of **PTQ** with respect to PC<sub>71</sub>BM allows and encourages us to further lower the LUMO level of the polymer. By combination of fluorination and selenophene-thiophene exchange from **PTQ** to **PSeQF2**, a lowering of around 0.2 eV in the LUMO level was observed, while a similar optical gap is retained ( $\sim 1.75$  eV). Similar to the unfluorinated **PSeQ**, favorable optical and electronic properties are observed for **PSeQF2**, along with a rise in the estimated  $E_{CT}$  by  $>0.2$  eV as compared to **PTQ**, which would be expected to result in an enhanced photovoltage.

The effect of fluorine substitution on the energy levels of **PTQ** and **PSeQ** were confirmed by both SWV and DFT in reducing both HOMO and LUMO levels. The band gap narrowing effect of selenium substitution was confirmed by DFT (showing an increase in the HOMO level along with a decrease in the LUMO level) and UV–vis absorption spectroscopy, as well as by SWV. It has to be mentioned that the similar LUMO levels deduced from SWV for **PTQF2** and **PSeQF2** may fall into the error margin of electrochemical measurements, which do not follow the same trend as seen by DFT calculations. Moreover, the combination of fluorine substitution and selenium substitution to modify **PTQ** significantly decreased the LUMO level by around 0.2 eV, but still gave a sufficient offset ( $\sim 0.6$  eV) to that of PC<sub>71</sub>BM (based on the reduction onsets),<sup>27a,110</sup> which is beneficial for charge transfer and dissociation at the polymer/fullerene interfaces.

We demonstrated that as a result of the synergic effect of fluorine substitution and

### *Energy Level Modulation*

selenium substitution on the energy level modulation while keeping the optical gap almost unchanged, the resulting fluorinated selenophene–quinoxaline alternating polymer, **PSeQF2**, achieved a high  $V_{OC}$  of 1.0 V while maintaining a high PCE ~4% that is comparable to **PTQ** (very sensitive to processing conditions with typical PCE of 3.1% or higher),<sup>103a,111</sup> which is a significant improvement compared to **PSeQ** or **PTQF2**. Here, the  $V_{OC}$  was increased by 0.1 V for **PSeQF2** compared to **PTQ**, which can be attributed to the increased charge-transfer state energy arising from the deepening of the HOMO level through the energy level modulation. Very recently, donor polymers that combine a high PCE above 6% with a high  $V_{OC}$  over 0.95 V have been reported,<sup>15c,35b,112</sup> but to the best of our knowledge, there are only a very few donor polymers with  $V_{OC}$  over 1.0 V that show PCE exceeding 3% when combined with PC<sub>61</sub>BM or PC<sub>71</sub>BM.<sup>35b-e</sup> In addition, **PSeQF2** and **PTQ**, consistent with their optical absorption profiles, resulted in similar  $J_{SC}$  and EQE, higher than **PSeQ** or **PTQF2**.<sup>103a</sup> Notably, the increased  $J_{SC}$  for **PSeQF2** compared to **PSeQ** can be explained by the improved EQE over a wide spectral range. This can be partially attributed to the more favorable morphology for the **PSeQF2**:PC<sub>71</sub>BM blend as evidenced by AFM on the active layer surface. The larger phase separation between the **PSeQ** donor and the PC<sub>71</sub>BM acceptor in the active layer could lead to inefficient exciton dissociation and/or charge transport, which limits the photocurrent generation and  $J_{SC}$ .<sup>23b,113</sup>

Hence, it can be concluded that we have demonstrated an effective chemical strategy through energy level modulation by synergistically introducing fluorine and selenium substitutions into conjugated polymers, which can lower the HOMO energy level while keeping the optical gap almost unchanged for achieving a high  $V_{OC}$ .<sup>27b</sup> This combination of modifications on existing promising donor polymers (especially thiophene-based conjugated polymers) may make them more suitable for use as donor components for the front subcell active layer in efficient tandem cells where a high photovoltage is very desirable, by the optimization of fluorine substitution together with selenium substitution. This new strategy further broadens the methodology of tuning the HOMO and LUMO energy levels of molecules and polymers, and opens one possibility for minimizing the LUMO-level offset of the donor polymers (especially thiophene-based conjugated polymers) to the acceptor materials.

### **4.3 Computational Modelling Tool in Search for Chemical Methodologies**

In our previous work, based on a combined experimental and DFT study, we successfully demonstrated an effective chemical strategy through energy level modulation by introducing fluorine and selenium substitutions into conjugated polymers, which can lower the HOMO energy level while keeping the optical gap almost unchanged for achieving a high  $V_{OC}$ .<sup>27b</sup> In fact, such chemical methodologies are very desired by the materials chemists for a rational material design in the OPV or related field. Hence, we turn to computational modelling as a tool to expand our exploration of chemical methodologies for a rational material design, especially to meet the particular requirements of different device architectures (including tandem and ternary solar cells) on the donor components, such as a prominent photocurrent or photovoltage combined with a high efficiency, to further maximize the overall performance of OPVs.

In this work, we present a systematic comparative DFT study for energy level modulation while keeping  $E_{HOMO}$ ,  $E_{LUMO}$  or  $E_g$  almost unchanged through engineered backbone structural fine-tuning for future judicious design of conjugated donor polymers. This appears to be the first report of systematic comparative studies to search for chemical methodologies of energy level modulation by theoretical calculations for designing conjugated materials with desirable photovoltaic characteristics through engineered backbone manipulations.

Based on the motif of donor–acceptor polymers, around 50 comparable polymers were constructed and investigated, derived from an easily accessible thiophene–quinoxaline alternating polymer donor showing power conversion efficiency up to 7%. We discussed and elucidated the heteroatom effects of combining fluorine, nitrogen and chalcogen substitutions onto the donor/acceptor units as well as the effect of extending  $\pi$ -conjugation in the donor moiety based on DFT calculations validated with experimental data where available. We found the trends in the energy levels and band gaps of these polymers correlate well to their corresponding structural modifications. Finally, we demonstrated three important ways of band gap and energy level tuning by showing potential chemical methodologies that can be applicable to further modify and optimize existing conjugated polymer backbones in different contexts.

## Energy Level Modulation

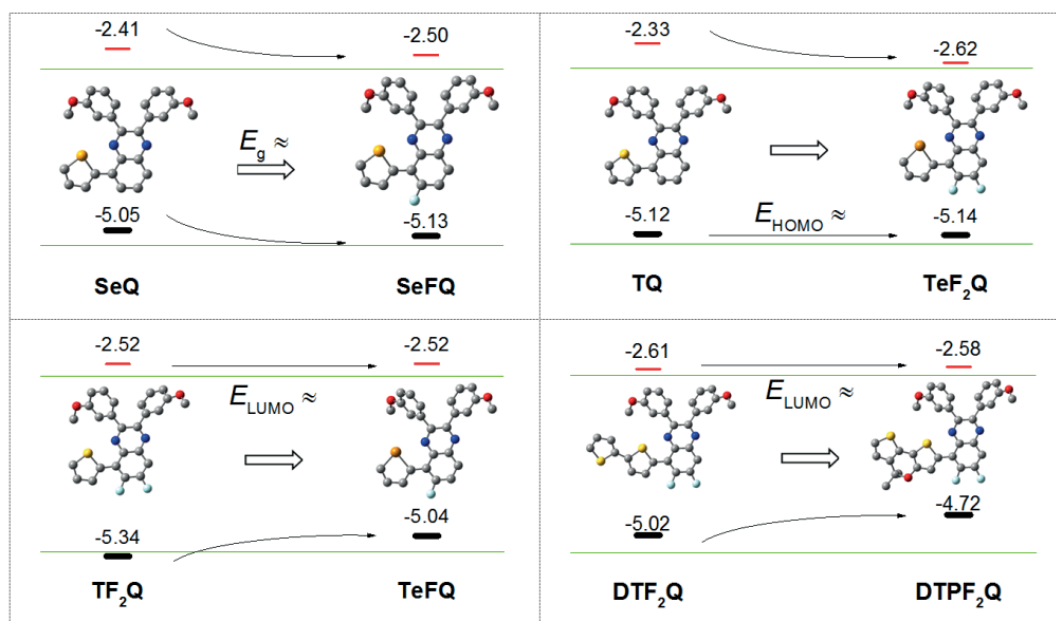


**Figure 4.2** Modelling in search for chemical methodologies for energy level modulation while keeping  $E_{\text{HOMO}}$ ,  $E_{\text{LUMO}}$  or  $E_{\text{g}}$  almost unchanged through engineered backbone structural fine-tuning.

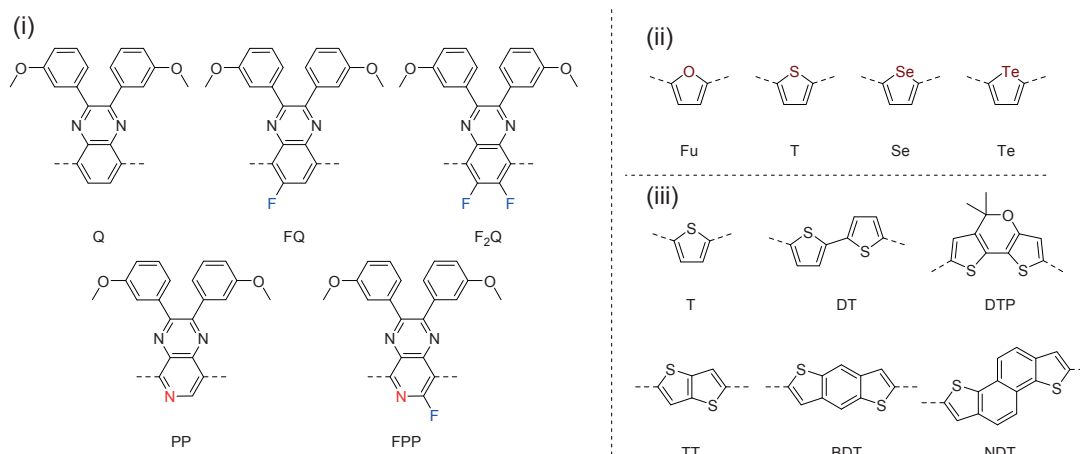


**Figure 4.3** Building units as donor/acceptor moieties with structural fine-tuning in this study.

### 4.3.1 Electronic Effect of Incorporating Fluorine and Nitrogen Atoms into the Acceptor Units

By varying the extent of fluorine substitutions and incorporation of imine nitrogen, five basic acceptor units bearing the same side chains (i.e. di(*meta*-alkoxyphenyl)) are studied (**Figure 4.3**). As shown in **Figure 4.4**, the LUMO levels of these units calculated by DFT follow the order  $Q > FQ > F_2Q > PP > FPP$ , which agrees with the effect of fluorine substitution on the energy levels in reducing both HOMO and LUMO levels. The HOMO levels follow the same trend as observed for the LUMO level, but the difference of the

## Energy Level Modulation

deepening is almost halved. As a result, the HOMO–LUMO gaps of these acceptor units also follow the same trend ( $Q > FQ > F_2Q > PP > FPP$ ).

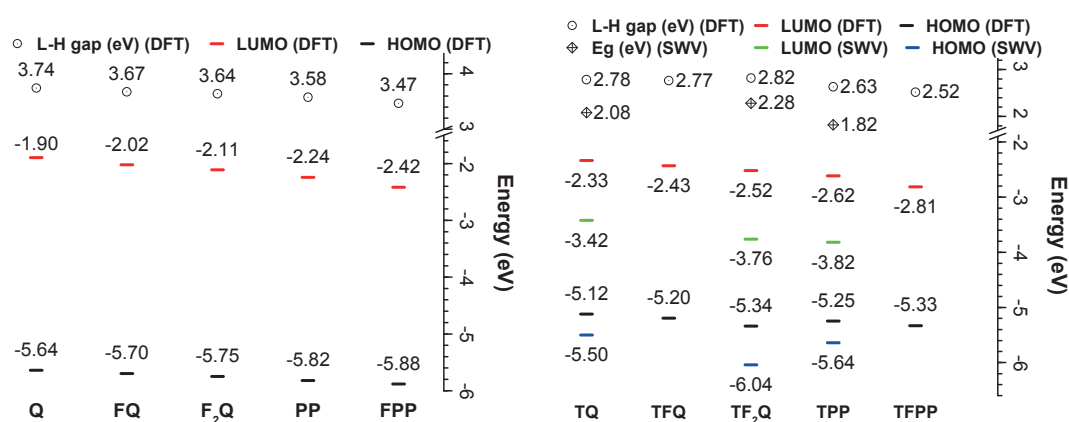


**Figure 4.4** Effect of incorporation of F-substituents and imine nitrogen on energy levels.

When donor–acceptor polymers are constructed based on these quinoxalines or pyridopyrazines as the acceptor unit with thiophene as the donor unit, DFT shows that the trend of the LUMO levels with various acceptor units is retained (**Figure 4.4**). By checking the frontier orbitals of these donor–acceptor structures (**Figure 3.4**), we find that their LUMOs are the bonding linear combination from the LUMOs of the respective segments (except LUMO+1 for tellurophene). Note that the resulting frontier molecular orbitals do not necessarily originate from the frontier molecular orbitals of the respective segments. Therefore, the structural changes (i.e. by incorporating electron-withdrawing fluorine or imine nitrogen) on the acceptor units will contribute to the LUMOs of the donor–acceptor polymers in the same way as to the LUMOs of the separated acceptor units, thereby retaining the trend of the LUMO levels with various acceptor units ( $Q > FQ > F_2Q > PP > FPP$ ).<sup>114</sup> The HOMOs of these donor–acceptor polymers arise from the antibonding linear combination from the highest occupied orbitals of the corresponding acceptor units with the right symmetry (HOMO–3) and the HOMOs of the corresponding donor units (except HOMO–1 for tellurophene) (**Figure 3.4**). As a result, a similar trend is followed, except that the difluorination still maintains a deeper HOMO level than the others. The HOMO–3 energies of these acceptor units follow the same trends of their HOMOs. As a consequence, the lower these HOMO–3 energies of the acceptor units are, the lower HOMO levels the donor–acceptor polymers would have, following the same trend as the HOMO levels of the separated acceptor units. However, in the cases with the inclusion of

## Energy Level Modulation

fluorine substituents on the acceptor units, there is an additional lowering of the HOMO due to through-space intramolecular stabilizing interactions between fluorine substituents and the neighboring donor unit in the donor–acceptor structures. We believe that the involvement of fluorine in the antibonding linear combination of the separated segments and interaction of the lone pair of fluorine with  $\pi$ -orbital of thiophene in the constructed donor–acceptor polymers (**Figure 4.5**) can stabilize the system that is not possible for the hydrogen or imine nitrogen atoms on the acceptor units, which is doubled for TF<sub>2</sub>Q compared to TFQ. This extra stabilization tends to increase the HOMO–LUMO gaps, which can counterpoise the opposite trend as seen on the separated acceptor units upon fluorination, resulting in variation of the trends of the HOMO levels and the HOMO–LUMO gaps, when these acceptor units are combined with different donor units.<sup>115</sup> Here for example, TF<sub>2</sub>Q has a slightly larger HOMO–LUMO gap than both TFQ and TQ, with TFQ very slightly lower than TQ. It is found that the chosen calculation methods in this study are indeed suitable for the investigated systems, by comparing these calculated results with the available electrochemical measurements of the synthesized polymers at hand (**Figure 4.4**).<sup>103a</sup>

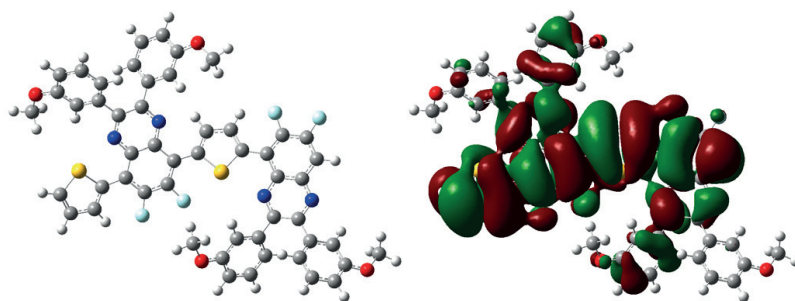


**Figure 4.5** Top view of molecular geometry and HOMO of TF<sub>2</sub>Q (isovalue surface 0.005 au).

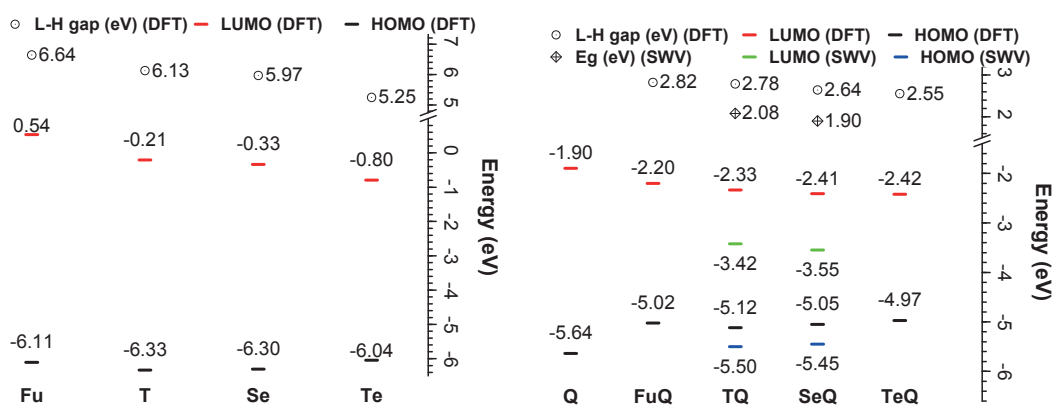


**Figure 4.6** Heteroatom effect of chalcogen substitutions to the donor moiety on energy levels.

### 4.3.2 Heteroatom Effect of Chalcogen Substitutions into the Donor Units

Here we will discuss the electronic difference by using different chalcogenophenes (**Figure 4.3**) as donor units in the donor–acceptor polymers.

The HOMO–LUMO energy gaps of these five-membered rings decrease with atomic numbers (**Figure 4.6**). The LUMO levels follow the same trend with the HOMO–LUMO energy gaps (decreasing with atomic numbers). The HOMO levels, however, follow a different trend, that is, sulfur < selenium < oxygen < tellurium. All of these trends agree well with previously reported experimental observations.<sup>116</sup> The LUMOs of these five-membered heterocycles can be attributed to the antibonding linear combination of the  $p_z$  orbital of the corresponding heteroatoms with the  $\pi^*$ -orbital of the carbon framework of the rings except tellurophene. For tellurophene, the molecular orbitals have a different order where the lowest  $\sigma^*$ -orbital is the LUMO and the antibonding linear combination of the  $p_z$  and  $\pi^*$  orbitals gives the LUMO+1, due to the smaller electronegativity of tellurium. Here we note that the order of the molecular orbitals of these chalcogenophene units has been observed experimentally before.<sup>116b</sup> The HOMOs can be assigned to the  $1a_2$   $\pi$ -orbital of these chalcogenophene units except tellurophene ( $2b_1$   $\pi$ -orbital, due to the smaller electronegativity of tellurium<sup>116a</sup>) (**Figure 3.4**). The  $1a_2$   $\pi$ -orbital does not mix with the heteroatom  $p_z$  orbital for symmetry reasons and therefore should have similar energy regardless of different chalcogen atoms.<sup>116a</sup> All these factors discussed here will contribute together to their HOMO–LUMO gaps (**Figure 4.6**). Interestingly, we find that these trends can be retained separately in most cases when constructed as donor–acceptor polymers, as seen in combination with quinoxaline (**Figure 4.6**) or fluorinated pyridopyrazine units. It is also noteworthy that comparison of the calculated results with the available electrochemical measurements of polymers<sup>27b</sup> (**Figure 4.6**) can further confirm the reasonable choice of calculation methods in this study.

### 4.3.3 Effect of Extended Conjugation and Fused Units in the Donor Moiety

Several fused thiophene-based units investigated here include thieno[3,2-*b*]thiophene (TT),<sup>117</sup> benzo[1,2-*b*:4,5-*b'*]dithiophene (BDT),<sup>15c,d,16a,36e,105b</sup> naphtho[1,2-*b*:5,6-*b'*]dithiophene (NDT),<sup>118</sup> and dithieno[3,2-*b*:2',3'-*d'*]pyran (DTP).<sup>17c,36i</sup> For comparison, 2,2'-bithiophene (DT) as well as thiophene (T)<sup>67a,b,119</sup> is also included (**Figure 4.3**).

## Energy Level Modulation

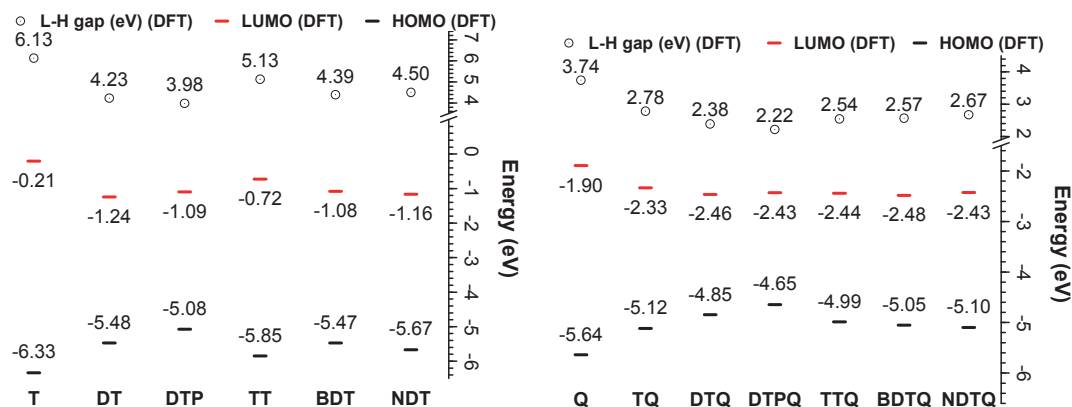


**Figure 4.7** Effect of extended conjugation in the donor moiety on energy levels.

First, a band gap narrowing is observed from  $\text{BDT} > \text{DT} > \text{DTP}$  when constructed as donor–acceptor polymers, as shown in combination with quinoxaline (**Figure 4.7**). This trend agrees well with the trend of these separated units, given their comparable conjugation path lengths. NDT-based donor–acceptor polymers show the largest HOMO–LUMO energy gaps given the largest conjugation path length within comparison. However, it may not be straightforward to further compare the HOMO–LUMO energy gaps of these separated donor units with the other donor units (T and TT). Indeed, for these single units, the conjugated path lengths of these donor units vary, from two double bonds for T, to three for TT, to four for DT, DTP and BDT, to five for NDT. Finally, by performing additional calculations with increased numbers of repeating units to obtain a comparable conjugation path length for indirect comparison, it can be concluded that the HOMO–LUMO energy gaps are narrowed generally following the order  $\text{NDT} > \text{BDT} > \text{T} > \text{TT} \approx \text{DT} > \text{DTP}$ . Furthermore, the resulting LUMO levels of donor–acceptor polymers based on these units are close to each other.

### 4.3.4 Implications and Guidance for Material Design

It is interesting to analyze how structural modifications can affect the electronic properties of the resulting molecules. Some first empirical rules may be drawn to provide insights to further modify and optimize other related semiconductors.

Firstly, one can modulate the energy levels while keeping the band gap almost unchanged through structural modifications. For this purpose, optimization of fluorine substitutions in conjunction with sulfur-selenium exchange may be considered.<sup>27b</sup> Lowering the LUMO level while keeping an identical band gap, along with a deepening in

## Energy Level Modulation

the HOMO level, may allow for a higher  $V_{OC}$  along with a comparable  $J_{SC}$  to result in a higher PCE. It may be applicable for designing the front subcell donor component in tandem solar cells where a high photovoltage is always highly desired, or for conjugated donor polymers in single-junction solar cells, to maximize the overall photovoltaic performance. By grouping the computed models with similar band gaps (**Figure 4.8**), one can see more clearly what kinds of chemical methodologies can be applicable for such energy level modulation. For example, single fluorination is usually an effective to lower the LUMO level without obviously changing the band gap of the polymer (e.g. from TQ to TFQ, or from SeQ to SeFQ). By taking optical gaps (slightly different from HOMO–LUMO gaps)<sup>39</sup> into account, we have previously shown that synergistically incorporating selenium and fluorine may in reality minimize the LUMO-level offset while keeping the optical gap almost unchanged.<sup>27b</sup>

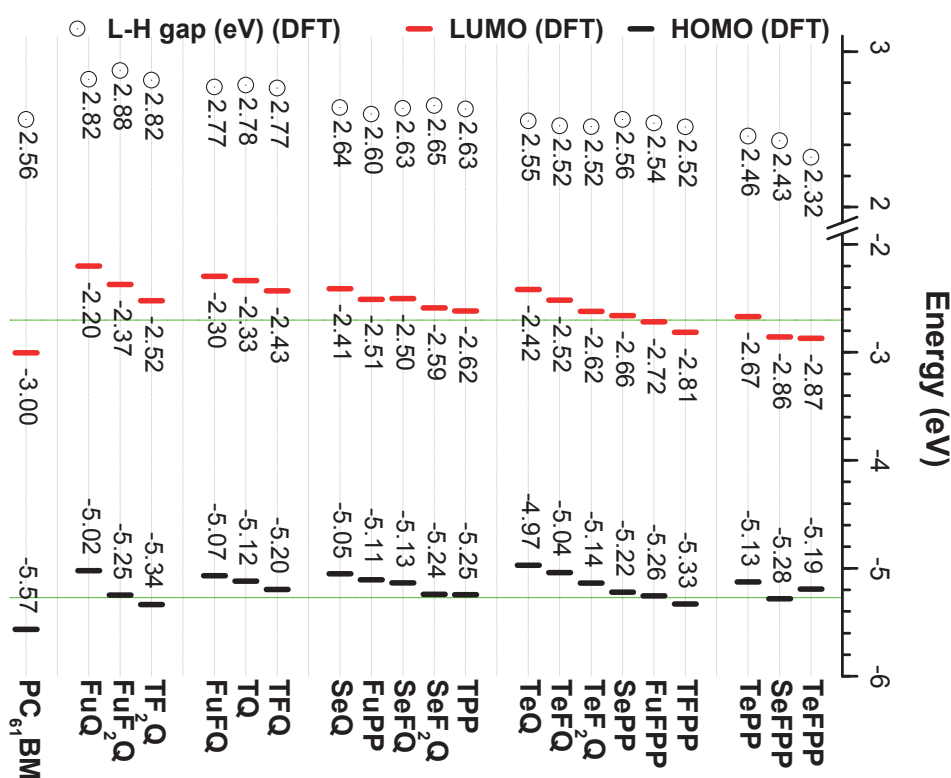


**Figure 4.8** Energy diagram of the different polymers grouped by similar band gaps.

Secondly, one can also tune the band gaps while maintaining an identical HOMO level modulated by chemical methods. Reducing the band gap while keeping a comparable HOMO level may allow for a similar photovoltage with a broader spectral coverage for



## 5 Engineering Donor Units in Isoindigo-Based Conjugated Polymers

In this chapter the influence of different electron-donating units in the donor–acceptor polymers will be discussed, in particular the influence of electron-donating units incorporated in isoindigo-based conjugated polymers. The exploration of new conjugated donor polymers that combine a high power conversion efficiency and a high open-circuit voltage is highly desirable in realizing efficient tandem solar cells, and the potential of isoindigo for organic solar cells has motivated us to further explore this possibility.

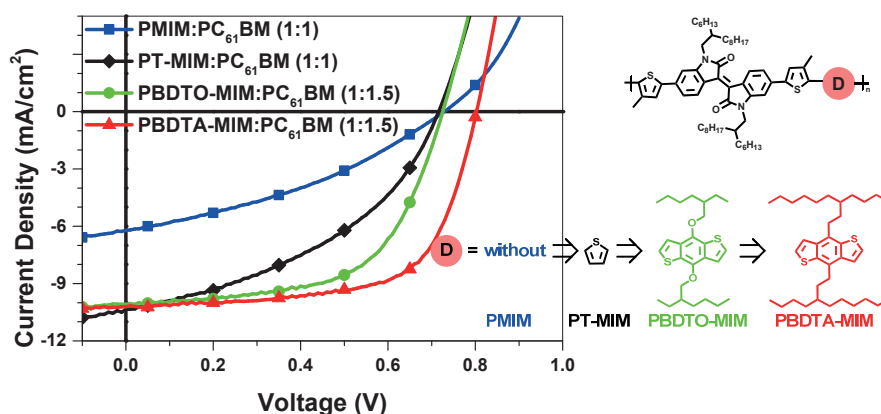


**Figure 5.1** Effect of incorporating different electron-donating thiophene-based units on the photovoltaic properties of isoindigo-based conjugated polymers.

Our recent studies demonstrated the potential of isoindigo as an efficient acceptor unit in donor–acceptor polymers for BHJ solar cells.<sup>52,68a,69b,120</sup> Among these, PTI-1, consisting of alternating thiophene and isoindigo units, with an optical gap of 1.6 eV, shows a PCE of 3.0% with a  $V_{OC}$  of 0.89 V,  $J_{SC}$  of 5.4 mA/cm<sup>2</sup> and FF of 63% when combined with PC<sub>71</sub>BM ([6,6]-phenyl-C<sub>71</sub>-butyric acid methyl ester) as the acceptor in BHJ devices.<sup>69b</sup> Extending the conjugation length of the donor unit in PTI-1 from thiophene to a terthiophene derivative resulted in a more efficient donor polymer, P3TI, with a reduced optical gap (1.5 eV). P3TI shows a PCE of 6.3% in the same device configuration, with a  $V_{OC}$ ,  $J_{SC}$  and FF of 0.70 V, 13.1 mA/cm<sup>2</sup> and 69%, respectively.<sup>68a</sup> Notably, even though a high PCE was achieved for P3TI, the  $V_{OC}$  was not prominent, while for PTI-1, even though a  $V_{OC}$  up to 0.9 V was obtained, the PCE was moderate. The initial success of isoindigo-

based polymers for organic solar cells<sup>52,68a,69b,120-121</sup> motivated us to further explore the possibility of improving the photovoltaic performance in these systems, especially by combining a high PCE and a high  $V_{OC}$  into one single isoindigo-based polymer, as well as to investigate their structure–property relationships. A series of novel donor–acceptor conjugated alternating copolymers based on the isoindigo acceptor moiety (**PMIM**, **PT-MIM**, **PBDTO-MIM** and **PBDTA-MIM**, **Figure 5.1**) were therefore designed, synthesized and characterized, in order to explore the potential of isoindigo for efficient donor materials with high photovoltages in solar cells.

We have systematically investigated the influence of the different electron-donating units on the structural, optical, electrochemical and photovoltaic properties. Mobility measurements, morphological studies and quantum-chemical calculations including DFT and TD-DFT were carried out to find out the insights into the differences. We find that the PCEs of the resulting PSCs can be improved by over 3-fold through a rational structural modification of the donor moiety, which highlights the importance of carefully choosing appropriate chemical structure to design efficient donor–acceptor polymers for solar cells. Among these polymers, PBDA-MIM exhibits a PCE of 5.4%, which is the highest value obtained for isoindigo-based polymers for conventional BHJ PSCs combined with PC<sub>61</sub>BM as the acceptor to date. This further emphasizes the use of isoindigo as an effective acceptor unit for designing active donor materials and demonstrates the potential of this class of polymers as donor candidates for bottom cells in tandem devices, which combine low optical gaps (1.5–1.7 eV), promising efficiencies and desirable open-circuit voltages (at least 0.8 V) into isoindigo-based polymers with PC<sub>61</sub>BM as the acceptor.

## **5.1 Material Design, Synthesis and Structural Characterization**

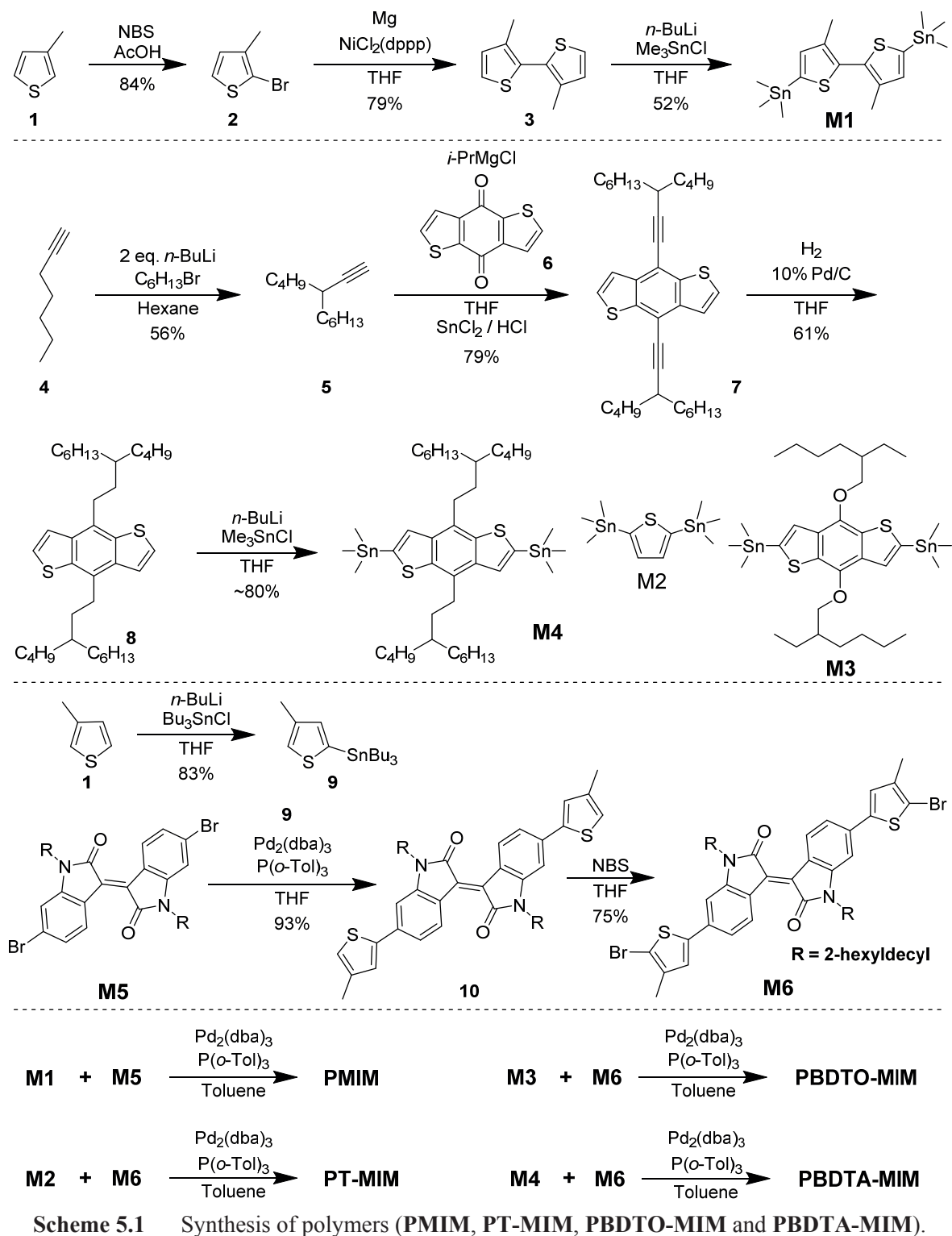
Previous work on isoindigo polymers has shown that extending the conjugation in the donor moieties from a single thiophene (PTI-1)<sup>69b</sup> to terthiophene (P3TI)<sup>68a</sup> resulted in a decreased  $V_{OC}$  by ~0.2 V, even though the PCE was more than doubled. In this study, the bithiophene unit was employed to have an intermediate  $\pi$ -conjugation length in the donor moiety, resulting in donor–acceptor polymer **PMIM**. The introduction of methyl groups on the bithiophene unit would be expected to give a slightly twisted backbone, which should increase the band gap and thus the  $V_{OC}$ .<sup>122</sup> Meanwhile, a beneficial intermolecular stacking might still occur by adopting conformations where the two methyl substituents on the

adjacent thiophene units are away from each other,<sup>123</sup> favoring a linear backbone in the solid state.<sup>124</sup> For comparison, a thiophene ring was inserted in between the two alkylthiophene units to have the same polymer backbone as P3TI (the best-performing isoindigo-based polymer reported so far)<sup>68a</sup>, resulting in **PT-MIM**. To further extend the  $\pi$ -conjugation length of the donor unit, benzo[1,2-*b*:4,5-*b'*]dithiophene (BDT) was also incorporated. Recently, BDT has been widely used as an effective electron-donating building block thanks to its desirable properties such as structural rigidity, planarity and favorable interchain  $\pi$ - $\pi$  stacking, along with the presence of additional substitution sites for the incorporation of side chains.<sup>36e,h,37b,63b,105a-c,107a,125</sup> Here the BDT unit with two 2-ethylhexyloxy side chains was used to replace the middle thiophene in the terthiophene unit in **PT-MIM**, resulting in **PBDTO-MIM**. Notably, similar polymers with identical backbones (**PBDT-TIT** and **PBDT-OIO**) showed promising device performance with a  $V_{OC}$  up to 0.79 V,  $J_{SC}$  of 7.87 mA/cm<sup>2</sup>, FF of 68% and a PCE of 4.22%.<sup>52</sup> Furthermore, it is known that removal of oxygen from the side chains of the donor unit can reduce the electron density, to allow for a deeper HOMO energy level, which in principle should enhance the  $V_{OC}$  of the resulting PSCs.<sup>126</sup> Hence the alkoxy side chains on the BDT unit were replaced with branched alkyl chains, resulting in **PBDTA-MIM**.

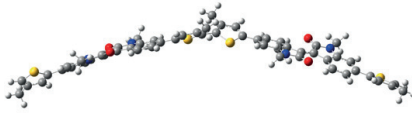
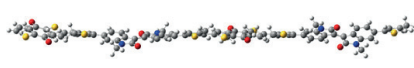
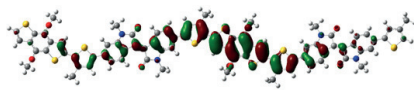
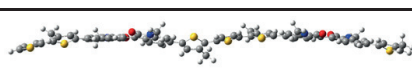
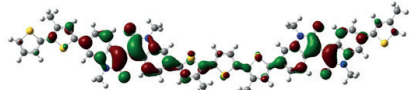
The synthesis of the monomers is outlined in **Scheme 5.1**. All the polymers were synthesized *via* Stille coupling reaction<sup>79</sup> from the corresponding monomers as shown in **Scheme 5.1**. After the reaction mixture was precipitated into methanol, the polymers were collected and washed *via* Soxhlet extraction with methanol, acetone, ether, hexane, dichloromethane and chloroform successively. The chloroform fraction was precipitated into methanol, and the final products were collected by filtration and dried under vacuum. **PMIM** had a  $\bar{M}_n$  of 20.1 kDa with a  $D_M$  of 2.1 ( $\bar{X}_n = 22.3$ ). It should be mentioned that a hot chlorobenzene fraction after chloroform extraction gave a comparable yield of **PMIM**, with a much higher  $\bar{M}_n$  of 62.8 kDa ( $D_M = 1.9$ ,  $\bar{X}_n = 69.7$ ), which is not considered for comparison in this work because it was not processable from common organic solvents at the concentrations needed for devices preparation. Going from **PMIM** to **PT-MIM** resulted in a slightly lower  $\bar{M}_n$  of 13.4 kDa for **PT-MIM** ( $D_M = 1.8$ ,  $\bar{X}_n = 13.6$ ), indicating a decreased solubility. By replacing the unsubstituted thiophene with a BDT unit with alkoxy or alkyl branched side chains, a dramatic improvement in terms of solubility and molar masses of the polymers occurred (**PBDTO-MIM**:  $\bar{M}_n = 63.5$  kDa,  $D_M = 3.0$ ,  $\bar{X}_n =$

Engineering Donor Units in Isoindigo-Based Conjugated Polymers

47.2; PBDTA-MIM:  $\bar{M}_n = 69.3$  kDa,  $D_M = 4.0$ ,  $\bar{X}_n = 47.7$ ).<sup>127</sup>



**Table 5.1** The LUMO and HOMO for the four polymers and their molecular geometries from side view (Isovalue Surface 0.02 au) evaluated by DFT at the B3LYP/6-31G(d) level

	PMIM	PBDTO-MIM
Side View		
LUMO		
HOMO		
	PT-MIM	PBDTA-MIM
Side View		
LUMO		
HOMO		

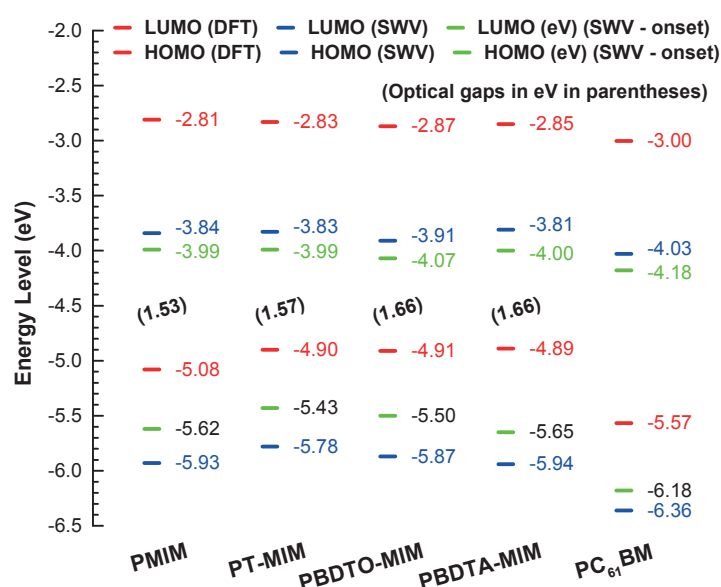
## 5.2 Electronic Structures and Optoelectronic Properties

The optimized molecular geometries of the models and their calculated frontier orbitals are depicted in **Table 5.1**. Without insertion of additional donor units, **PMIM** gives the most twisted (ca. 50°) optimized molecular geometry as can be seen from **Table 5.1**. The other three polymers can have a more coplanar conformation than **PMIM**. The torsion angles between the flanking methylthiophene and inserted donor units are more or less the same, around 20°. For **PT-MIM**, it is also possible to give a flat angle of  $\theta_3$  similar to the BDT-based polymers, given the rigidity and symmetry of the inserted units. As the side chains on the flanking thiophene are very short (just methyl groups for the synthesized **PT-MIM**), they do not force the terthiophene units to adopt conformations that place the side chains away from each other.<sup>122</sup> The high planarity of the backbones in these three conjugation-extended polymeric systems, which was also shown for **PBDT-TIT** in our recent modeling work,<sup>92h</sup> could favor the  $\pi$ - $\pi$  stacking interactions that occur among the polymer backbones in the solid state, which could in turn enhance the charge mobility (see below mobility measurements in **Table 5.2**).<sup>122</sup>

**Table 5.2** Photovoltaic parameters of the BHJ PSCs and corresponding charge mobilities

Polymer: PC <sub>61</sub> BM ratio (w/w)	Solvent	DIO (% v/v)	T <sub>Ann.</sub> (°C) <sup>a</sup>	J <sub>SC</sub> (mA cm <sup>-2</sup> )	V <sub>OC</sub> (V)	FF (%)	PCE <sup>b</sup> (%)	μ <sub>h</sub> <sup>c</sup> (cm <sup>2</sup> V <sup>-1</sup> s <sup>-1</sup> )
<b>PMIM</b> (1:1)	CF	2	90	6.24	0.73	36	1.64 (1.5)	7.4 × 10 <sup>-5</sup>
<b>PT-MIM</b> (1:1)	CF	1	--	10.41	0.71	43	3.14 (3.1)	1.0 × 10 <sup>-4</sup>
<b>PBDTO-MIM</b> (1:1.5)	CF:DCB (1:1)	3	110	10.09	0.73	59	4.36 (3.9)	1.5 × 10 <sup>-4</sup>
<b>PBDTA-MIM</b> (1:1.5)	CF:DCB (1:1)	3	--	10.20	0.80	65	5.36 (5.1)	2.7 × 10 <sup>-4</sup>

<sup>a</sup>) Annealing time: 10 min; <sup>b</sup>) Power conversion efficiencies of the best devices, with average values based on over six devices given in parentheses; <sup>c</sup>) Hole mobility estimated by space charge limited current (SCLC) method.

**Figure 5.2** Energy levels estimated from DFT-B3LYP/6-31G(d) and from SWV and optical gaps.

We also extended the DFT calculation for **PMIM** to three repeating units to have a similar conjugation path length to the BDT-based oligomers. The DFT-computed HOMO and LUMO energy levels are -5.06 eV and -2.86 eV, respectively. Indeed, this will result in slightly different orders of the values, but we can further confirm that the LUMO levels are governed by the acceptor units and that **PMIM** has the lowest HOMO level and the largest LUMO–HOMO energy gap among the four isoindigo-based polymers in the gas phase. Energy levels deduced from the onsets of the first oxidation and reduction potentials

were included in **Figure 5.2** for comparison. The trend of LUMO levels from these onsets is consistent with the calculated trend, which is **PBDTO-MIM** < **PBDTA-MIM** < **PT-MIM**  $\approx$  **PMIM**. The measured HOMO levels and band gaps follow the trends from DFT calculations except for **PBDTA-MIM** due to the aforementioned reasons.

### 5.3 Photovoltaic Performance

**Table 5.2** summarizes the photovoltaic responses of optimized PSCs using a conventional device configuration (glass/ITO/PEDOT:PSS/polymer:PC<sub>61</sub>BM/LiF/Al). Representative  $J-V$  plots are shown in **Figure 5.1**. The best-performing BHJ solar cells were obtained again when processed with DIO as the solvent additive. It is worth noting that the PCEs for **PBDTO-MIM** and **PBDTA-MIM** together with our previously reported **PBDT-TIT** and **PBDT-OIO**<sup>52</sup> follow the order: **PBDT-OIO** (1.26%) < **PBDT-TIT** (4.22%) < **PBDTO-MIM** (4.36%) < **PBDTA-MIM** (5.36%). This indicates that the introduction of methyl groups on the flanking thiophenes is indeed a simple and effective alternative synthetic strategy without sacrificing the photovoltaic performance or suffering the synthetic difficulty for example to make **PBDT-TIT**.<sup>52</sup> This strategy also allows one to design and synthesize new isoindigo-based polymers that combine many other different donor moieties in order to further explore possibilities of improving the photovoltaic performance without having to stay with the low-yielding synthesis of the dibromide monomer (i.e. *N,N'*-disubstituted-6,6'-bis(5-bromothiophen-2-yl)isoindigo).

The insertion of the thiophene into the backbone, going from **PMIM** to **PT-MIM**, resulted in a decreased  $V_{OC}$  due to the raised HOMO level, but an almost doubled PCE was achieved coupled with a greatly increased  $J_{SC}$  due to the increased hole mobility. In addition, the replacement of a thiophene ring with a BDT moiety increased the  $V_{OC}$  and FF without losses in  $J_{SC}$ , leading to an enhanced PCE. More importantly, when alkoxy side chains on the BDT unit were replaced with analogous alkyl chains, the  $V_{OC}$  was further improved due to the deepening in the HOMO level, and the FF was further improved as well probably thanks to a modified morphological D:A blend arrangement. As a result, **PBDTA-MIM**, blended with PC<sub>61</sub>BM, stands out as the best-performing photoactive material among these polymers, with a  $V_{OC}$  of 0.80 V,  $J_{SC}$  of 10.20 mA/cm<sup>2</sup>, FF of 65% and a PCE of 5.36%. This synergistically demonstrates the potential of isoindigo-based polymers as suitable donor candidates for use in front subcells of efficient tandem devices.

## 6 Engineering $\pi$ -Bridges in Quinoxaline-Based Polymers

In this chapter we focus on a discussion on the function and influence of  $\pi$ -conjugated bridges in conjugated polymers, in particular acting as  $\pi$ -conjugated spacers between benzodithiophene donor and fluorinated quinoxaline acceptor moieties in the main chain.

### 6.1 Highlights

In this work, two new easily accessible conjugated polymers (**PBDTFQ-T** and **PBDTFQ-TT**, **Figure 6.1**) based on benzodithiophene donor and fluorinated quinoxaline acceptor moieties with thiophene or thieno[3,2-*b*]thiophene as  $\pi$ -conjugated bridges were designed and synthesized to explore the relationships between the molecular structures, optoelectronic properties and photovoltaic performances. We demonstrated that doctor-blading technique can be used to fabricate efficient photovoltaic devices in air based on these two new polymers, which represents an important step for future mass production of PSCs, with minimized material losses and low-cost processes. Through the control of different parameters, it was possible to achieve PCE up to  $\sim 5.6\%$  with  $V_{OC}$  exceeding 0.82 V and  $J_{SC}$  reaching 11 mA/cm<sup>2</sup>.

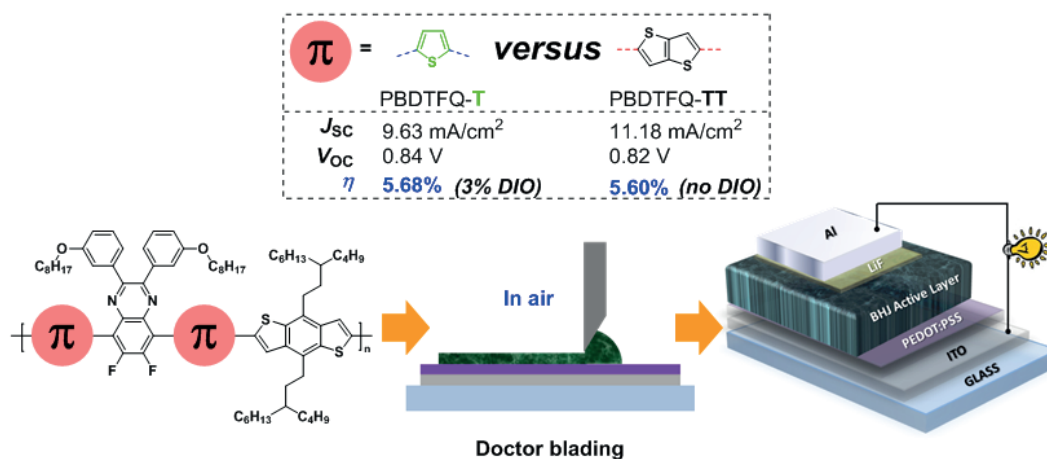


**Figure 6.1** Replacing thiophene with thieno[3,2-*b*]thiophene as  $\pi$ -conjugated spacers in electron donor polymers eases the solution processing for high-performance organic photovoltaic cells.

The synthesis of polymers is outlined in **Scheme 6.1**. The characterized properties are summarized in **Table 6.1**. Here, the replacement of thiophene with thieno[3,2-*b*]thiophene as spacer resulted in a narrowing of the optical gap of the polymer, which favors a higher

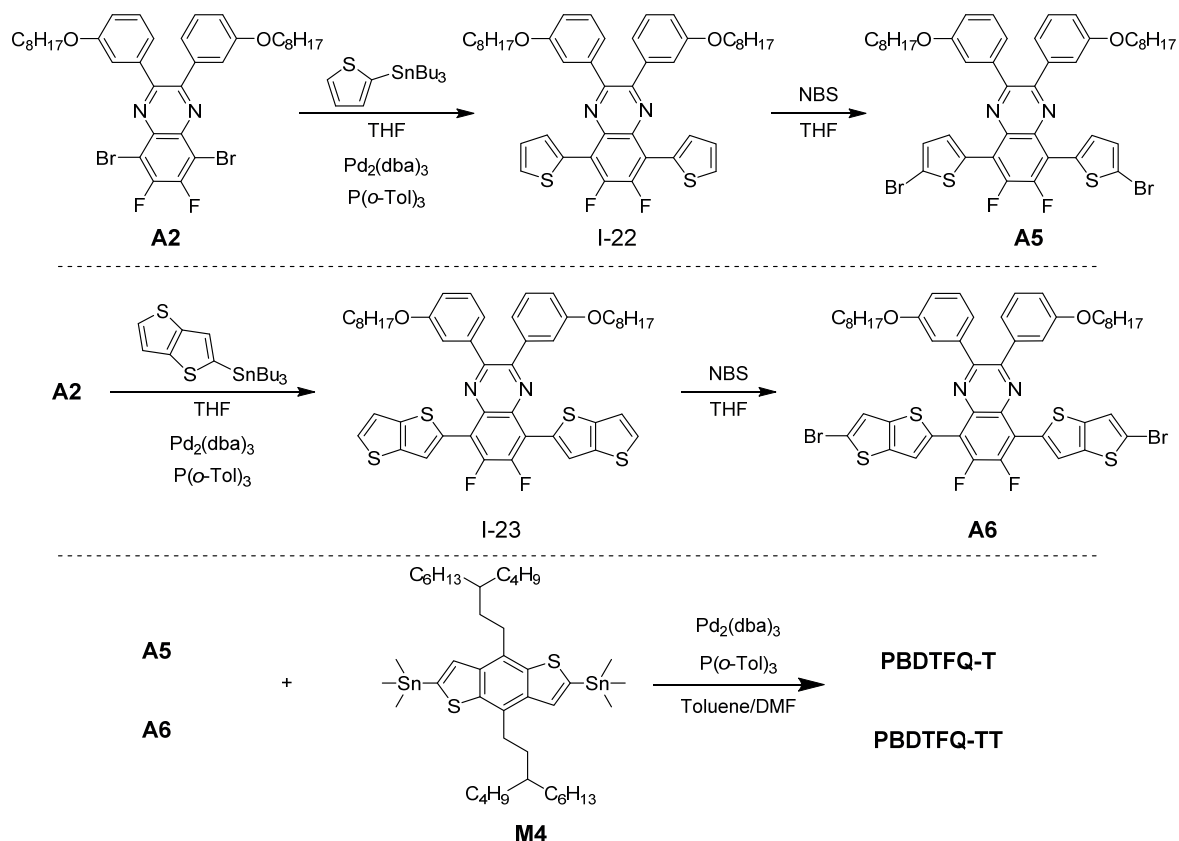
photocurrent generation in photovoltaic devices. Moreover, the use of thieno[3,2-*b*]thiophene as spacer resulted in a more linear and planar polymer chain (as confirmed by DFT calculations), which facilitates the polymer chains to pack well in the solid state and to have a higher hole mobility as compared to the thiophene analogue. As the result, a 1:1 blend of **PBDTFQ-TT** and PC<sub>61</sub>BM showed up to ~5.6% PCE in a device fabricated by blade coating without the need to add any solvent additive (**Table 6.2**). On the other hand, the use of thiophene as spacer imparted the polymer (**PBDTFQ-T**) with higher molar masses due to the better solubility of the monomer and the polymer, which enhanced the light absorption and the photocurrent generation in devices. In the meantime, devices fabricated from a blend of **PBDTFQ-T** and PC<sub>61</sub>BM (1:1 ratio) processed with DCB showed improved fill factor and photocurrent through appropriate control of active layer morphology using solvent additive (3% DIO) which resulted in comparable device efficiency to what was obtained by the thieno[3,2-*b*]thiophene based polymer. Finally, we would like to emphasize that the use of thieno[3,2-*b*]thiophene as  $\pi$ -conjugated bridges in donor–acceptor structures is a facile method for obtaining highly performing polymers in BHJ solar cells without the need of any additional processing solvent additives.

**Table 6.1** Molar masses, optical and electrochemical properties of **PBDTFQ-T** and **PBDTFQ-TT**.

Polymer	$\bar{M}_n$ [kDa]	$\bar{M}_w$ [kDa]	Film (solution) <sup>a</sup>			SWV (DFT) <sup>b</sup>		
			$\lambda_{\max}$ [nm]	$\lambda_{\text{on}}$ [nm]	$E_g^{\text{opt } c}$ [eV]	$E_{\text{HOMO}}$ [eV]	$E_{\text{LUMO}}$ [eV]	$E_g^d$ [eV]
<b>PBDTFQ-T</b>	101	270	622 (605)	700 (668)	1.77 (1.85)	-6.00 (-4.90)	-3.63 (-2.59)	2.37 (2.31)
<b>PBDTFQ-TT</b>	15	42	596 (598)	725 (714)	1.71 (1.74)	-5.90 (-4.85)	-3.52 (-2.68)	2.38 (2.17)

<sup>a</sup>) The values in parentheses are those determined in chloroform solution. <sup>b</sup>) The values in parentheses are those obtained from DFT calculations at the B3LYP/6-31G(d) level. <sup>c</sup>)  $E_g^{\text{opt}} = 1240 / \lambda_{\text{on}}$ . <sup>d</sup>)  $E_g = E_{\text{LUMO}} - E_{\text{HOMO}}$ .

## Engineering $\pi$ -Bridges in Quinoxaline-Based Polymers



**Scheme 6.1** Synthetic route to **PBDTFQ-T** and **PBDTFQ-TT**.

**Table 6.2** Photovoltaic parameters of polymer:PC<sub>61</sub>BM BHJ OPV devices. The results reported are averaged over 10 cells, while the values in parentheses represent the best device parameters

Polymer:PC <sub>61</sub> BM ratio (w/w)	Thickness (nm)	DIO (% v/v)	$J_{\text{SC}}$ (mA/cm <sup>2</sup> )	$V_{\text{OC}}$ (V)	FF (%)	PCE (%)
<b>PBDTFQ-T (1:1.5)</b>	141	3	-9.29	0.81	68	5.12
<b>PBDTFQ-T (1.5:1)</b>	151	3	-8.64	0.85	67	4.91
<b>PBDTFQ-T (1:1)</b>	162	-	-5.46	0.87	46	2.18
<b>PBDTFQ-T (1:1)</b>	168	3	-9.18 (-9.63)	0.84 (0.84)	67 (70)	5.30 (5.68)
<b>PBDTFQ-TT (1:1.5)</b>	127	-	-9.27	0.81	62	4.62
<b>PBDTFQ-TT (1.5:1)</b>	142	-	-10.48	0.83	58	5.05
<b>PBDTFQ-TT (1:1)</b>	149	-	-10.87 (-11.18)	0.82 (0.82)	59 (61)	5.29 (5.60)
<b>PBDTFQ-TT (1:1)</b>	150	3	-9.53	0.75	45	3.19

## 6.2 Chain Conformations and Optoelectronic Properties

For computational simplification, the alkoxy side chains on the quinoxaline acceptor unit were replaced with methoxy groups, the branched alkyl side chains on the BDT unit were replaced with methyl groups, and the backbones were simplified to two repeating units.

In order to obtain more accurate results, we first needed to determine the conformations of the structure units of the two polymers. As the BDT unit is a centrosymmetric fused unit, we assume a *trans* conformation between the BDT unit and the bridging group (i.e. thiophene or thieno[3,2-*b*]thiophene), to minimize the steric hindrance as well as the potential energy of the whole systems.<sup>105f</sup> More attention was given to analyze the conformation between the quinoxaline unit and the bridging group. Notably, even if different conformations (i.e. *syn*-conformation defects) may be adopted between the BDT unit and the bridging group, they still result in the same conclusions which can be made in our below computational analysis of the conformation between the quinoxaline unit and the bridging group (i.e. thiophene or thieno[3,2-*b*]thiophene). As shown in **Figure 6.2**, there are three possible conformers to be resolved for each  $\pi$ -bridge flanking FQ ( $\pi$ -A- $\pi$ ) segment. We performed DFT calculations for these possible conformations by using the two-repeating-unit model, because there are two joints in the  $\pi$ -A- $\pi$  segment for the BDT units to bond with. The potential energies of the three conformers of the  $\pi$ -A- $\pi$  segments decrease in the order 121>112>111 (**Figure 6.2**) for both the different spacers.

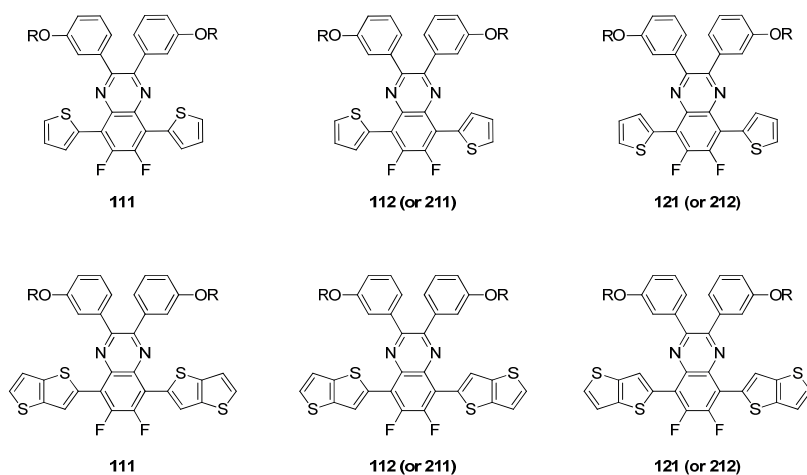


**Figure 6.2** Possible conformers of  $\pi$ -bridge flanking FQ ( $\pi$ -A- $\pi$ ) segments.

However, in the optimized geometries of the corresponding dimers, additional factors could determine the lower conformation energy, other than that of the  $\pi$ -A- $\pi$  segment, such

as the presence of bulky side chains. For example, the lowering of the potential energy through the minimization of the steric hindrance between the bulky side chains on the BDT unit and on the FQ one may prevail. In fact, for polymer **PBDTFQ-T**, the distance between the benzyl carbon on the BDT unit and the closest oxygen atom on the adjacent quinoxaline units,  $L_2$ , is 4.0 Å for the dimer with  $\pi$ -A- $\pi$  conformations 111 or 112, while it is 9.5 Å for the dimer with the  $\pi$ -A- $\pi$  conformation 121 (**Table 6.3**). We therefore postulate that, for polymer **PBDTFQ-T**, the conformation 121 of the  $\pi$ -A- $\pi$  segment is favored because it allows a minimum steric hindrance in the presence of adjacent bulky side chains. Such conformation preference may already occur in the polymerization of **PBDTFQ-T**. On the other hand, in the case of the dimers with thieno[3,2-*b*]thiophene bridge, the steric hindrance of lateral alkyl chains is strongly reduced: the distance between the benzyl carbon atom on the BDT unit and the closest oxygen atom on the adjacent quinoxaline units,  $L_2$ , is in any case comparable (9.4 Å). As a consequence, thanks to the rigidity and centrosymmetry of the thieno[3,2-*b*]thiophene unit, the three possible conformations of the dimers are all linear and have similar spatial orientation of the side chains. Then for polymer **PBDTFQ-TT** is favored the conformation where the  $\pi$ -A- $\pi$  unit has the lowest potential energy, which is conformation 111. It has to be mentioned that for **PBDTFQ-TT**, other possible conformations between the quinoxaline unit and the  $\pi$ -bridge may exist, as well as between the BDT unit and the  $\pi$ -bridge, but the polymer backbone linearity would be maintained. The linear backbone of **PBDTFQ-TT**, compared to the curved backbone of **PBDTFQ-T**, presumably favors inter-chain stacking/packing and leads to improved charge mobility.<sup>128</sup>

The optimized molecular geometries of the two-repeating-unit models (**PBDTFQ-T\_121** and **PBDTFQ-TT\_111**) and their frontier molecular orbitals are shown in **Figure 6.3**. The computed HOMO and LUMO energy levels for **PBDTFQ-T\_121** are -4.90 eV and -2.59 eV respectively, with an energy gap of 2.31 eV, while for **PBDTFQ-TT\_111** the HOMO and LUMO levels are -4.85 eV and -2.68 eV, respectively, with an energy gap of 2.17 eV (**Table 6.1**). The HOMO levels agree with the ionization energies estimated by SWV, with a slight increase in energy when passing from the thiophene to the thieno[3,2-*b*]thiophene based polymer. On the other hand, the decrease in the LUMO energy, computed by DFT, when going from thiophene to thieno[3,2-*b*]thiophene cases, was not observed by SWV. The band gap narrowing when going from the thiophene to the

thieno[3,2-*b*]thiophene based polymers observed by DFT calculations is in agreement with the optical gap deduced from the UV-vis absorption spectra. This band gap difference can be explained through the increased charge-transfer-like interactions of the **PBDTFQ-TT** polymer compared to **PBDTFQ-T**. This is confirmed by the shortening of the bond length between the  $\pi$ -bridge and the FQ unit in the  $\pi$ -A- $\pi$  segment when passing from the optimized structure **PBDTFQ-T\_121** to the **PBDTFQ-TT\_111** one.

**Table 6.3** The C-C-C torsion angles (deg), the C-C-C angles  $\Phi(C_aC_bC_c)$  (deg) between the closest BDT units, the bond lengths (Å) between FQ and  $\pi$ -bridges, and the distances (Å) between the benzyl carbon on BDT and the closest oxygen atom on the adjacent FQ units of the polymers.

	$\theta_1$	$\theta_2$	$\theta_3$	$\theta_4$	$\theta_5$	$\theta_6$	$\theta_7$	$\Phi$	$L_1$	$L_2$
<b>PBDTFQ-T_121</b>	161	-173	-173	-160	-11	-12	159	150	1.461	9.52
<b>PBDTFQ-TT_111</b>	171	-172	-169	171	-5	-3	170	177	1.458	9.43

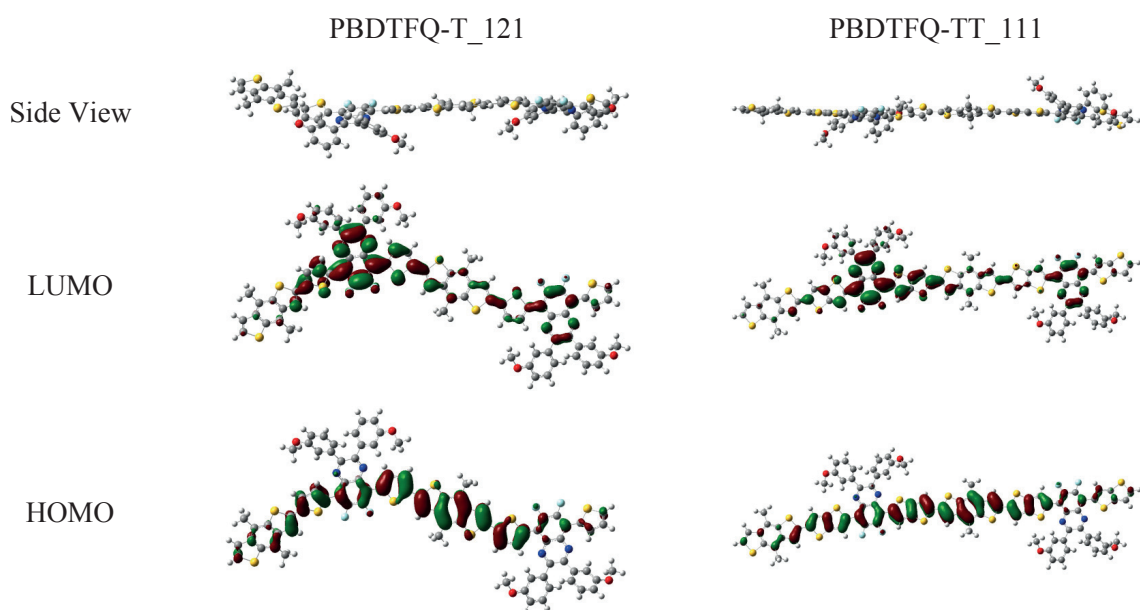


**Figure 6.3** Illustrations of the frontier orbitals of the polymers and their molecular geometries from side view (isovalue surface 0.02 au) evaluated by DFT at the B3LYP/6-31G(d) level.

Different  $\pi$ -bridge units significantly affect the molecular architecture. As can be seen from **Table 6.3**, both polymers have an optimized structure with in-plane backbones, with a slightly more planar geometry for the model of **PBDTFQ-TT** than that of **PBDTFQ-T**. For example, as shown in **Table 6.3**, the torsion angles ( $\theta_5$  and  $\theta_6$ ) between the quinoxaline and BDT units along the backbone are ca. 2.6–4.7° for **PBDTFQ-TT** vs. ca. 11.4–12.4° for **PBDTFQ-T**. Moreover, for **PBDTFQ-TT** a linear backbone conformation can be adopted while **PBDTFQ-T** shows a backbone curvature. For instance, the angles ( $\Phi$ ) between the two closest BDT units along the backbone are ca. 173.5° and ca. 147.3° for **PBDTFQ-TT** and **PBDTFQ-T**, respectively (**Table 6.3**). This may result in a significant difference in interchain stacking and charge mobility, as confirmed by the broader absorption band with a red-shifted onset for **PBDTFQ-TT** compared to **PBDTFQ-T** and by the mobility measurements under the same conditions ( $1.1 \times 10^{-4} \text{ cm}^2/(\text{V}\cdot\text{s})$  for **PBDTFQ-T** vs.  $3.7 \times 10^{-4} \text{ cm}^2/(\text{V}\cdot\text{s})$  for **PBDTFQ-TT**).<sup>129</sup>

In conclusion, we have synthesized two easily accessible conjugated polymers (**PBDTFQ-T** and **PBDTFQ-TT**) consisting of benzodithiophene donor and fluorinated quinoxaline acceptor units spaced with either thiophene or thieno[3,2-*b*]thiophene  $\pi$ -bridges, respectively. The influence of thiophene or thieno[3,2-*b*]thiophene as  $\pi$ -bridge on the resulting solubility, molar masses, backbone conformations, optical and electronic properties were investigated. A first comparison between the electrical and photovoltaic properties of the two synthesized polymers, blended with PC<sub>61</sub>BM as the acceptor and processed under the same conditions with doctor-blading (without using solvent additives), reveals an improved performance of the polymer with the thieno[3,2-*b*]thiophene as the  $\pi$ -bridge (with a PCE of 5.29% on average and 5.60% at maximum) compared to the thiophene  $\pi$ -bridged analogue (with an average PCE of 2.18%). This can be ascribed to enhanced light absorption, charge mobility and improved blend film nanomorphology, despite the lower molar mass. It is worth emphasizing that the facile method for obtaining highly performing polymers by simply varying the  $\pi$ -spacer in donor–acceptor structures and obtaining efficient BHJ solar cells without the need of any additional processing solvent additives suggests the importance of a further and deeper investigation on the use of thieno[3,2-*b*]thiophene or similar  $\pi$ -bridges inserted in other polymeric structures.

# 7 Side-Chain Engineering in 2,7-Carbazole- and Quinoxaline-Based Polymers

## 7.1 Introduction

This chapter features a discussion on the effect of side-chain engineering on photovoltaic performance in 2,7-carbazole-<sup>130</sup> and quinoxaline-based<sup>35a,67a,69a</sup> polymers. Alkyl or alkoxy side-chains are commonly incorporated onto the backbones of donor–acceptor polymers to ensure good solubility to allow solution processing. It was found that the proper placement of alkyl or alkoxy groups is important and this can have a pronounced effect on the performance of the resulting PSCs.<sup>63b,88c,125b,131</sup> To gain more insight into the influence of alkyl or alkoxy groups in the photophysical, electrochemical and photovoltaic properties of 2,7-carbazole-based polymers, we designed and synthesized three polymers (**EWC1**, **EWC2**, and **EWC3**) with a common carbazole–thiophene–quinoxaline–thiophene backbone but with different side chains. This kind of direct comparison between 2,7-carbazole-based polymers with branched and straight side chains on the carbazole moieties<sup>130c-e</sup> bearing the same acceptor segments was rarely noted before. The devices based on **EWC3** showed the best performance with a PCE of 3.7%.

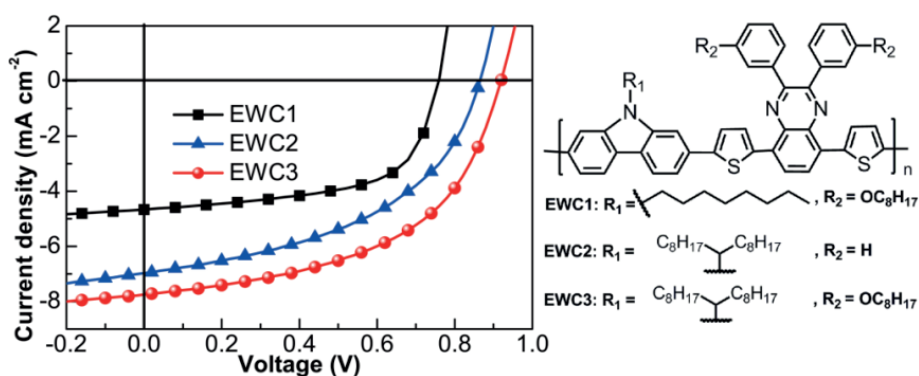


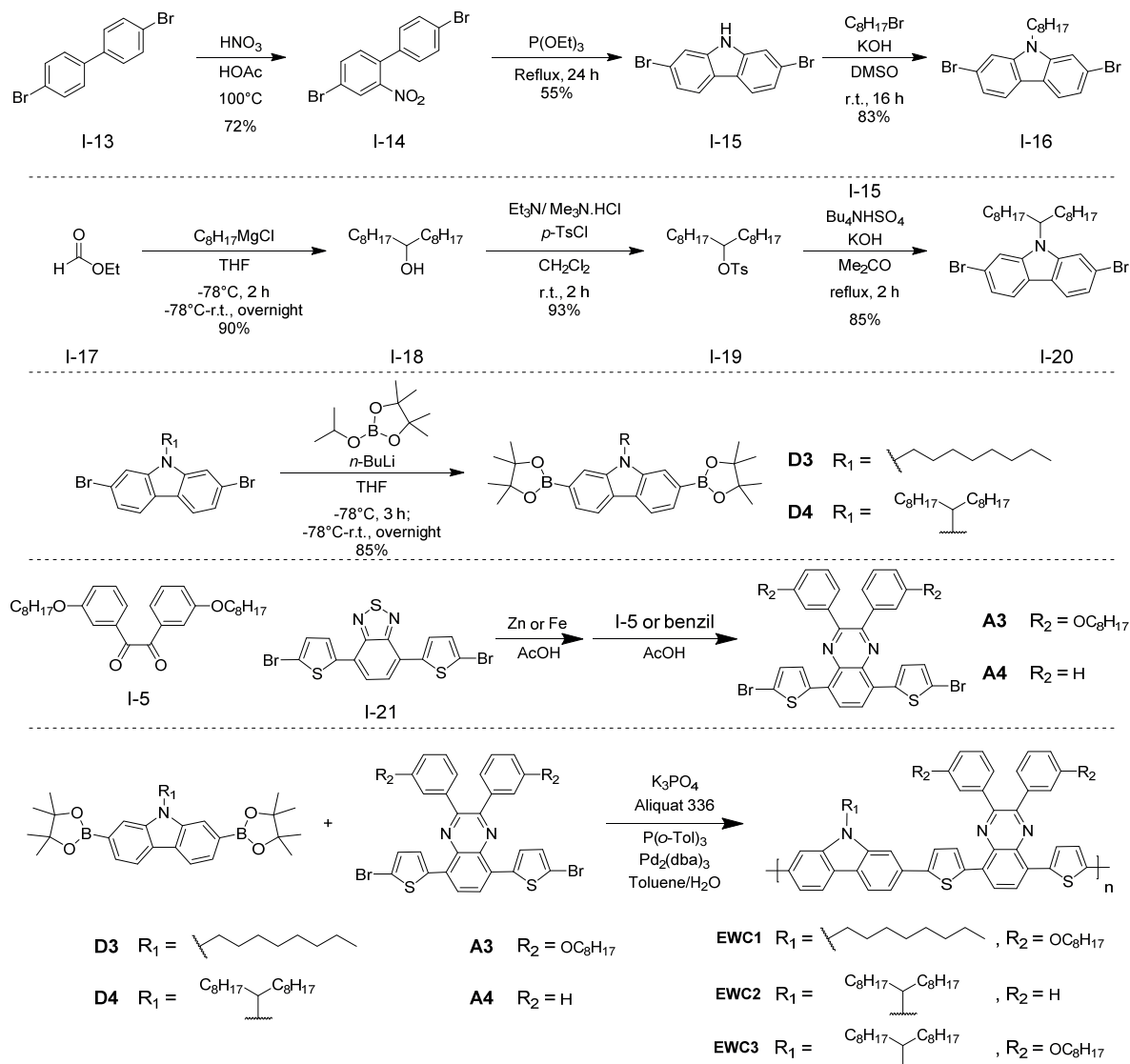
Figure 7.1 Influence of side chains on photovoltaic properties of 2,7-carbazole-based polymers.

## 7.2 Material Synthesis and Characterization

The synthesis of polymers is outlined in **Scheme 7.1**. All the three polymers were obtained by coupling the corresponding carbazole-based and quinoxaline-based monomers *via* a modified Suzuki reaction.<sup>132</sup> The obtained molar masses are summarized in **Table 7.1**. It was noted that the GPC spectrum of **EWC1** presents two peaks with a low  $\bar{M}_n$  of 14 kDa

## Side-Chain Engineering in 2,7-Carbazole- and Quinoxaline-Based Polymers

and large  $D_M$  of 7.3 if it was washed in the Soxhlet extractor only with diethyl ether before being extracted with chloroform. By additionally washing with dichloromethane after using diethyl ether, **EWC1** showed an improved  $\bar{M}_n$  of 34 kDa and narrowed  $D_M$  of 2.9.



**Scheme 7.1** Synthetic route to the three carbazole-based polymers.

## 7.3 Optical and Electrochemical Properties

The UV-vis absorption spectra of the polymers in chloroform solution and in the solid state are shown in **Figure 7.2**. All three polymers present two absorption bands. The band at longer wavelength can be attributed to the ground-state-to-excited-state transitions with intramolecular charge-transfer-like character. The almost identical absorption spectra of **EWC2** and **EWC3**, both in solution and in the solid state, respectively, indicate that the

octyloxy groups on the quinoxaline segments of **EWC3** have no influence in the absorption spectra of the resulting polymers. In contrast, the side chains on the carbazole units have an obvious effect on the absorption spectra of the resulting polymers, as can be seen from the fact that **EWC1** ( $\lambda_{\text{on}} = 680 \text{ nm}$ ,  $E_{\text{g}}^{\text{opt}} = 1.82 \text{ eV}$ ) showed a visible red shift compared to **EWC3** ( $\lambda_{\text{on}} = 644 \text{ nm}$ ,  $E_{\text{g}}^{\text{opt}} = 1.92 \text{ eV}$ ) (**Table 7.1**). Note that there is only very limited red shift for the absorption spectra of all the synthesized polymers when going from the solution to the solid state, indicating that the polymers are amorphous and there is no obvious aggregation or long-range orderly  $\pi$ - $\pi$  stacking formed in the solid state.

**Table 7.1** Molar masses, optical and electrochemical properties of the polymers.

polymer	$\bar{M}_n$		$\lambda_{\text{max}}$ (nm)		$\lambda_{\text{on}}$ (nm) film	$E_{\text{g}}^{\text{opt}}$ (eV)	$E^{\text{ox}}$ (V)	$E^{\text{red}}$ (V)	HOMO (eV)	LUMO (eV)
	kDa	$D_M$	solution	film						
EWC1	34	2.9	405,554	404,558	680	1.82	0.43	-1.84	-5.56	-3.29
EWC2	9	1.7	386,521	390,533	649	1.91	0.56	-1.80	-5.69	-3.33
EWC3	23	2.7	385,521	390,536	644	1.92	0.60	-1.81	-5.73	-3.32

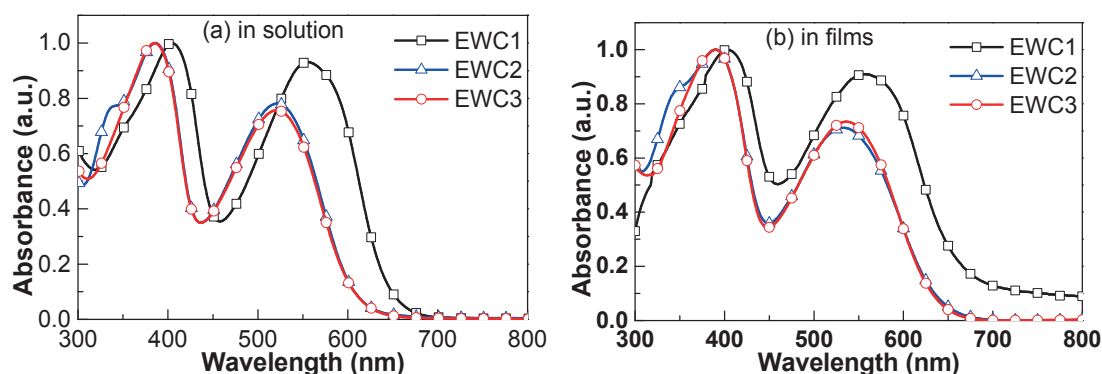


**Figure 7.2** UV-vis absorption spectra of the polymers (a) in chloroform solution and (b) in films.

The three polymers present almost the same reduction potentials (of *ca.* -1.8 V), but different oxidation potentials as determined by SWV (**Table 7.1**). The high LUMO levels of the three polymers can ensure enough driving force for charge transfer in the resulting PSCs utilizing PC<sub>71</sub>BM (LUMO -4.13 eV) as acceptor.<sup>41</sup> Based on the above data, it was concluded that the side chains on both carbazole and quinoxaline segments have no influence on the LUMO levels of the polymers but a clear impact on their HOMO levels.

**Table 7.2** Summary of photovoltaic parameters of the solar cells from the three polymers

polymer	additive	weight ratio polymer: PC <sub>71</sub> BM	Thickness (nm)	$V_{OC}$ (V)	$J_{SC}$ (mA cm <sup>-2</sup> )	FF	PCE (%)
<b>EWC1</b>	none	1:1	60	0.74	3.8	0.58	1.7
		1:2	65	0.75	5.4	0.55	2.2
		1:3	65	0.75	4.7	0.60	2.2
		1:4	60	0.73	4.2	0.60	2.0
	DIO	1:3	65	0.72	4.7	0.55	1.9
<b>EWC2</b>	none	1:1	80	0.90	6.9	0.44	2.7
		1:2	65	0.85	6.9	0.53	3.1
		1:3	60	0.81	7.1	0.54	3.1
		1:4	95	0.80	7.1	0.51	2.9
	DIO	1:3	70	0.79	4.3	0.54	1.9
<b>EWC3</b>	none	1:1	85	0.96	5.7	0.37	2.1
		1:2	95	0.92	6.1	0.46	2.6
		1:3	70	0.92	7.7	0.52	3.7
		1:4	85	0.87	7.0	0.48	2.9
	DIO	1:3	70	0.94	2.7	0.57	1.4

## 7.4 Photovoltaic Properties

PSCs were fabricated with a sandwich configuration of glass/ITO/PEDOT:PSS/active layer/LiF/Al. The active layers of the solar cells were spin-coated from DCB solutions of polymer:PC<sub>71</sub>BM. The results are listed in **Table 7.2**. All the three polymers achieved their best performances with a polymer:PC<sub>71</sub>BM ratio of 1:3.

**EWC3** exhibited the highest PCE of 3.7% with  $V_{OC}$  of 0.92 V,  $J_{SC}$  of 7.7 mA cm<sup>-2</sup> and fill factor of 0.52, exhibiting 0.17 V higher  $V_{OC}$  values than devices made of **EWC1**. It is striking to find that branched side chains on the carbazole units are beneficial in achieving higher  $V_{OC}$  in the resulting devices. This result is consistent with the recent reports about the effect of side chains based on other polymer backbones and it is believed that branched side chains can reduce intermolecular interactions and lead to higher  $V_{OC}$ .<sup>105a,131c,d</sup> This observation may be of importance in designing carbazole-based polymers for high-efficiency PSCs.

## 8 Concluding Remarks

The past five years have witnessed a rapid progress of bulk heterojunction organic photovoltaics boosted by (i) design and synthesis of novel conjugated donor materials, (ii) control and optimization of device fabrication, and (iii) the development of new device architectures such as tandem and ternary solar cells. The current challenges for OPVs remain to further improve photovoltaic efficiency as well as durability and cost-effectiveness, to compete with silicon-based solar cells. The work described in this thesis deals with the design, synthesis, characterization, and computational modelling of conjugated polymers for bulk heterojunction organic photovoltaics. It focused on material design of conjugated donor polymers through band gap engineering via rational structural modifications such as engineered backbone manipulations and side-chain engineering, as well as incorporation of newly developed building blocks. This thesis also established structure–property relationships of the polymer systems here studied, and explored potential chemical methodologies for future judicious material design. Many conjugated polymers were synthesized, by the Stille or Suzuki reactions, which were designed for use as donors in polymer:fullerene solar cells, and were partly included in this thesis.

Chapter 4 describes energy level modulation with chemical strategies detailed in Paper I and II. It is known that material design through band gap and energy level tuning has been playing a key role in developing new donor materials for efficient organic solar cells. The studies included here will be aimed at a more rational material design with controllable photovoltaic characteristics which are desired for the material to be integrated into the modern device design. Both experimental and modelling efforts were devoted for this purpose and three different ways of energy level modulation were discussed to explore chemical methodologies that may be suitable in pushing the efficiency further toward the theoretical limit.

From Chapter 5 to Chapter 7, we demonstrated the experimental studies in designing conjugated donor polymers via structural modifications such as engineered backbone manipulations and side-chain engineering. In order to design a conjugated donor polymer that can combine as many desired properties as possible into one conjugated backbone, appropriate building blocks are needed. Quinoxaline and isoindigo are among the acceptor

### *Concluding Remarks*

units that can be used to achieve state-of-the-art performance in conjunction with an efficient synthesis, which can be very attractive for the future mass production of polymer solar cells. Hence, they were chosen as the acceptor moiety to construct donor–acceptor conjugated polymers, to first control the LUMO level of a conjugated polymer, even though it may end up with suboptimal band gap engineering due to the complex effect on the  $J_{SC}$  and the  $V_{OC}$ . The influence of different donor units in the donor–acceptor polymers based on isoindigo was investigated and discussed in Chapter 5, which is based on Paper III. This work emphasizes the use of isoindigo as an effective acceptor unit for designing active donor materials and demonstrates the potential of this class of polymers as a front subcell donor component in tandem devices, which combine low optical gaps (1.5–1.7 eV), promising efficiencies and desirable open-circuit voltages (at least 0.8 V) into isoindigo-based polymers with PC<sub>61</sub>BM as the acceptor. Chapter 6 discussed the influence of conjugated bridges in the donor polymer design based on fluorinated quinoxaline featured in Paper IV, in which it shows replacing thiophene with thieno[3,2-*b*]thiophene as  $\pi$ -conjugated spacers in electron donor polymers eases the solution processing for high-performance organic photovoltaic cells without the need of additional solvent additives. Chapter 7 features a discussion on the effect of side-chain engineering on photovoltaic performance based on 2,7-carbazole and quinoxaline that originates from work presented in Paper V, where it was found that branched side chains on the carbazole units are beneficial in achieving higher  $V_{OC}$  in the resulting devices.

Worth mentioning is that designing and synthesizing new building blocks is revolutionary to boost the photovoltaic performance of conjugated polymers and make it possible for future commercialization of polymer solar cells in terms of efficiency, lifetime and cost-effectiveness. However, to identify novel promising building blocks as well as to make their synthesis efficient and cost-effective need a lot of research efforts. More efforts will be needed to speed up this process. All of these require a superior understanding of material design and device design.

## Acknowledgments

I truly appreciate all the organizations, grants, institutions, and people who have helped me scientifically and socially during my doctoral studies here.

First and foremost, I would like to express my sincere gratitude to my doctoral advisor Prof. Mats R. Andersson, for taking me as his PhD student in Polymer Technology, Chalmers. I want to thank him for his instruction, understanding and encouragement through all time.

I want to acknowledge all my co-authors for their contributions and help in publications and all the collaborators within Sweden and in Europe. I especially want to thank Dr. Hongyu Zhen, Zheng Tang, Prof. Fengling Zhang and Prof. Olle Inganäs from Linköping University; Dr. Mirko Seri, Dr. Margherita Bolognesi, Marta Tessarolo and Prof. Michele Muccini from CNR, Italy. All of your contributions have together made this thesis possible. I am very grateful to all your valuable contributions and discussions and I also look forward to our continued collaborations in the future.

I would also like to thank all the present and past members of Polymer Technology for a lot of valuable discussions, help and enjoyment. In particular, I want to acknowledge Dr. Ergang Wang for all his help and for all the past time we experienced; Dr. Renee Kroon for all the discussions, afterwork, cake-baking, scientific input and more; Dr. Timothy T. Steckler for all the discussions from labwork to afterwork and all his generous help; Dr. Desta Gedefaw for all the discussions and help in research and life; Dr. Angelica Lundin for the modelling work and discussions and all I have learnt from her; Prof. Wendimagegn Mammo for his help in chemistry and life and for the unforgotten conference trip to France; Stefan Hellström and Patrik Henriksson for all the electrochemical measurements and Anders Mårtensson for numerous SEC measurements. I also want to thank Camilla Lindqvist for both being a nice officemate during all my whole PhD studies here and being always ready to help. I really appreciate what I have learnt to make cakes from Dr. Sandra Fusco for her kindness and patience as well as from Renee and others. I also thank Dr. Christian Müller for a better understanding of polymer physics and for all the discussions and help. I also thank Markus Jarvid for all the help with modelling and proof reading.

### *Acknowledgments*

Thanks also go to Zandra George, Zelalem Abdissa Gerba, Amaia Diaz de Zerio Mendaza, Dr. Helena Andersson, Mattias Andersson, Dr. Harald Wutzel, and many master students and visiting students (Tianqi Cai, Zhen Zhang, Wenjun Sun, Xun Pan, Ching-Chiao Feng, Volodymyr Kuzmenko, ...), for all together contributing to the working atmosphere in the group and for all their help. Dr. Anders Lennartsson and Dr. Kasper Moth-Poulsen were respectively acknowledged for all the interesting discussions and help.

I want to thank Anne Wendel, Roger Forsberg, Ann Jakobsson, Christina Meyer, Carina Pettersson, Frida Andersson, Prof. Bo Albinsson, Prof. Sten Eriksson and Prof. Sven Engström, for helping me through my PhD studies. There are also many other previous and present colleagues in Floor 8 to be acknowledged for contributing to the working atmosphere at Floor 8 and for their help. I would like to thank Tina Gschneidner and Lanlan Sun for a lot of enjoyment they brought.

I also want to thank Isabella Leung, Andy Tang, Audrey Goh, Yun Zhou, and their better halves, and many others (including neighbors and the “Goodminton” members) for making my time in Sweden better and for their help. I also appreciate the help and experience on travelling in Europe.

I also want to thank my friends in China who have never forgotten me but always forgiven me for being absent during the past four years!

Last but not least, I would like to thank my family for their love and support. I especially thank my parents, my parents-in-law, my wife and my son for all their love and spiritual support. My work without you would be meaningless.

Wenliu Zhuang

Gothenburg, December 2013

## References

1. N. S. Lewis and D. G. Nocera, *Proc. Natl. Acad. Sci. U. S. A.*, 2006, **103**, 15729–15735.
2. Y. Chen, X. Wan and G. Long, *Acc. Chem. Res.*, 2013, **46**, 2645–2655.
3. (a) G. Li, R. Zhu and Y. Yang, *Nature Photon.*, 2012, **6**, 153–161; (b) C. J. Brabec, *Sol. Energy Mater. Sol. Cells*, 2004, **83**, 273–292.
4. W. Shockley and H. J. Queisser, *J. Appl. Phys.*, 1961, **32**, 510–519.
5. E. Bundgaard and F. C. Krebs, *Sol. Energy Mater. Sol. Cells*, 2007, **91**, 954–985.
6. E. Becquerel, *Comptes Rendus*, 1839, **9**, 561–567.
7. C. E. Fritts, *Am. J. Sci.*, 1883, **26**, 465.
8. *U.S. Pat.*, US2,402,662, 1946.
9. D. M. Chapin, C. S. Fuller and G. L. Pearson, *J. Appl. Phys.*, 1954, **25**, 676–677.
10. (a) M. A. Green, K. Emery, Y. Hishikawa, W. Warta and E. D. Dunlop, *Prog. Photovolt: Res. Appl.*, 2013, **21**, 827–837; (b) J. H. Zhao, A. H. Wang, M. A. Green and F. Ferrazza, *Appl. Phys. Lett.*, 1998, **73**, 1991–1993; (c) A. Shah, P. Torres, R. Tscharnner, N. Wyrsh and H. Keppner, *Science*, 1999, **285**, 692–698.
11. (a) C. J. Brabec, N. S. Sariciftci and J. C. Hummelen, *Adv. Funct. Mater.*, 2001, **11**, 15–26; (b) F. C. Krebs, *Sol. Energy Mater. Sol. Cells*, 2009, **93**, 394–412; (c) E. Wang, L. Wang, L. Lan, C. Luo, W. Zhuang, J. Peng and Y. Cao, *Appl. Phys. Lett.*, 2008, **92**, 033307.
12. C. W. Tang, *Appl. Phys. Lett.*, 1986, **48**, 183–185.
13. (a) G. Yu and A. J. Heeger, *J. Appl. Phys.*, 1995, **78**, 4510–4515; (b) J. J. M. Halls, C. A. Walsh, N. C. Greenham, E. A. Marseglia, R. H. Friend, S. C. Moratti and A. B. Holmes, *Nature*, 1995, **376**, 498–500; (c) G. Yu, J. Gao, J. C. Hummelen, F. Wudl and A. J. Heeger, *Science*, 1995, **270**, 1789–1791.
14. R. F. Service, *Science*, 2011, **332**, 293.
15. (a) J. Zhou, Y. Zuo, X. Wan, G. Long, Q. Zhang, W. Ni, Y. Liu, Z. Li, G. He, C. Li, B. Kan, M. Li and Y. Chen, *J. Am. Chem. Soc.*, 2013, **135**, 8484–8487; (b) D. H. Wang, A. K. K. Kyaw, V. Gupta, G. C. Bazan and A. J. Heeger, *Adv. Energy Mater.*, 2013, **3**, 1161–1165; (c) C. Cabanetos, A. El Labban, J. A. Bartelt, J. D. Douglas, W. R. Mateker, J. M. J. Frechet, M. D. McGehee and P. M. Beaujuge, *J. Am. Chem. Soc.*, 2013, **135**, 4656–4659; (d) Z. He, C. Zhong, X. Huang, W.-Y. Wong, H. Wu, L. Chen, S. Su and Y. Cao, *Adv. Mater.*, 2011, **23**, 4636–4643; (e) M. Zhang, X. Guo, S. Zhang and J. Hou, *Adv. Mater.*, 2013, DOI: 10.1002/adma.201304427; (f) N. Wang, Z. Chen, W. Wei and Z. Jiang, *J. Am. Chem. Soc.*, 2013, **135**, 17060–17068.
16. (a) Z. C. He, C. M. Zhong, S. J. Su, M. Xu, H. B. Wu and Y. Cao, *Nature Photon.*, 2012, **6**, 591–595; (b) S.-H. Liao, H.-J. Jhuo, Y.-S. Cheng and S.-A. Chen, *Adv. Mater.*, 2013, **25**, 4766–4771.

## References

17. (a) G. Dennler, M. C. Scharber, T. Ameri, P. Denk, K. Forberich, C. Waldauf and C. J. Brabec, *Adv. Mater.*, 2008, **20**, 579–583; (b) G. Dennler, M. C. Scharber and C. J. Brabec, *Adv. Mater.*, 2009, **21**, 1323–1338; (c) J. You, L. Dou, K. Yoshimura, T. Kato, K. Ohya, T. Moriarty, K. Emery, C.-C. Chen, J. Gao, G. Li and Y. Yang, *Nature Commun.*, 2013, **4**, 1446; (d) W. Li, A. Furlan, K. H. Hendriks, M. M. Wienk and R. A. J. Janssen, *J. Am. Chem. Soc.*, 2013, **135**, 5529–5532; (e) O. Adebajo, P. Maharjan, P. Adhikary, M. Wang, S. Yang and Q. Qiao, *Energy Environ. Sci.*, 2013, **6**, 3150–3170.
18. (a) L. Q. Yang, H. X. Zhou, S. C. Price and W. You, *J. Am. Chem. Soc.*, 2012, **134**, 5432–5435; (b) T. Ameri, P. Khoram, J. Min and C. J. Brabec, *Adv. Mater.*, 2013, **25**, 4245–4266.
19. P. W. M. Blom, V. D. Mihailetschi, L. J. A. Koster and D. E. Markov, *Adv. Mater.*, 2007, **19**, 1551–1566.
20. H. W. Kroto, J. R. Heath, S. C. O'Brien, R. F. Curl and R. E. Smalley, *Nature*, 1985, **318**, 162–163.
21. (a) N. S. Sariciftci, D. Braun, C. Zhang, V. I. Srdanov, A. J. Heeger, G. Stucky and F. Wudl, *Appl. Phys. Lett.*, 1993, **62**, 585–587; (b) N. S. Sariciftci, L. Smilowitz, A. J. Heeger and F. Wudl, *Science*, 1992, **258**, 1474–1476.
22. (a) J. J. M. Halls, K. Pichler, R. H. Friend, S. C. Moratti and A. B. Holmes, *Appl. Phys. Lett.*, 1996, **68**, 3120–3122; (b) A. Haugeneder, M. Neges, C. Kallinger, W. Spirkl, U. Lemmer, J. Feldmann, U. Scherf, E. Harth, A. Gugel and K. Mullen, *Phys. Rev. B*, 1999, **59**, 15346–15351; (c) J. J. M. Halls and R. H. Friend, *Synth. Met.*, 1997, **85**, 1307–1308; (d) D. E. Markov, E. Amsterdam, P. W. M. Blom, A. B. Sieval and J. C. Hummelen, *J. Phys. Chem. A*, 2005, **109**, 5266–5274; (e) D. Veldman, O. Ipek, S. C. J. Meskers, J. Sweelssen, M. M. Koetse, S. C. Veenstra, J. M. Kroon, S. S. van Bavel, J. Loos and R. A. J. Janssen, *J. Am. Chem. Soc.*, 2008, **130**, 7721–7735.
23. (a) M. M. Wienk, M. Turbiez, J. Gilot and R. A. J. Janssen, *Adv. Mater.*, 2008, **20**, 2556; (b) F. L. Zhang, K. G. Jespersen, C. Bjorstrom, M. Svensson, M. R. Andersson, V. Sundstrom, K. Magnusson, E. Moons, A. Yartsev and O. Inganäs, *Adv. Funct. Mater.*, 2006, **16**, 667–674.
24. (a) G. Li, V. Shrotriya, J. S. Huang, Y. Yao, T. Moriarty, K. Emery and Y. Yang, *Nature Mater.*, 2005, **4**, 864–868; (b) S. Y. Heriot and R. A. L. Jones, *Nature Mater.*, 2005, **4**, 782–786.
25. (a) Y. Yao, J. H. Hou, Z. Xu, G. Li and Y. Yang, *Adv. Funct. Mater.*, 2008, **18**, 1783–1789; (b) J. K. Lee, W. L. Ma, C. J. Brabec, J. Yuen, J. S. Moon, J. Y. Kim, K. Lee, G. C. Bazan and A. J. Heeger, *J. Am. Chem. Soc.*, 2008, **130**, 3619–3623.
26. W. L. Ma, C. Y. Yang, X. Gong, K. Lee and A. J. Heeger, *Adv. Funct. Mater.*, 2005, **15**, 1617–1622.
27. (a) E. Wang, L. Hou, Z. Wang, Z. Ma, S. Hellström, W. Zhuang, F. Zhang, O. Inganäs and M. R. Andersson, *Macromolecules*, 2011, **44**, 2067–2073; (b) W. Zhuang, H. Zhen, R. Kroon, Z. Tang,

## References

- S. Hellström, L. Hou, E. Wang, D. Gedefaw, O. Inganäs, F. Zhang and M. R. Andersson, *J. Mater. Chem. A*, 2013, **1**, 13422–13425; (c) W. Zhuang, M. Bolognesi, M. Seri, P. Henriksson, D. Gedefaw, R. Kroon, M. Jarvid, A. Lundin, E. Wang, M. Muccini and M. R. Andersson, *Macromolecules*, 2013, **46**, 8488–8499; (d) M. Bolognesi, D. Gedefaw, D. Dang, P. Henriksson, W. Zhuang, M. Tessarolo, E. Wang, M. Muccini, M. Seri and M. R. Andersson, *RSC Adv.*, 2013, **3**, 24543–24552; (e) D. Gedefaw, M. Tessarolo, W. Zhuang, R. Kroon, E. Wang, M. Bolognesi, M. Seri, M. Muccini and M. R. Andersson, *Polym. Chem.*, DOI: 10.1039/C3PY01519J.
28. S. Kirchmeyer and K. Reuter, *J. Mater. Chem.*, 2005, **15**, 2077–2088.
29. (a) T. W. Holcombe, J. E. Norton, J. Rivnay, C. H. Woo, L. Goris, C. Piliago, G. Griffini, A. Sellinger, J.-L. Bredas, A. Salleo and J. M. J. Frechet, *J. Am. Chem. Soc.*, 2011, **133**, 12106–12114; (b) V. Lemaire, M. Steel, D. Beljonne, J. L. Bredas and J. Cornil, *J. Am. Chem. Soc.*, 2005, **127**, 6077–6086; (c) A. Liscio, G. De Luca, F. Nolde, V. Palermo, K. Muellen and P. Samori, *J. Am. Chem. Soc.*, 2008, **130**, 780–781; (d) T. M. Clarke and J. R. Durrant, *Chem. Rev.*, 2010, **110**, 6736–6767.
30. (a) G. Grancini, M. Maiuri, D. Fazzi, A. Petrozza, H. J. Egelhaaf, D. Brida, G. Cerullo and G. Lanzani, *Nature Mater.*, 2013, **12**, 29–33; (b) J. Lee, K. Vandewal, S. R. Yost, M. E. Bahlke, L. Goris, M. A. Baldo, J. V. Manca and T. Van Voorhis, *J. Am. Chem. Soc.*, 2010, **132**, 11878–11880; (c) Y. P. Yi, V. Coropceanu and J. L. Bredas, *J. Am. Chem. Soc.*, 2009, **131**, 15777–15783; (d) X. D. Yang, C. L. Lee, S. Westenhoff, X. P. Zhang and N. C. Greenham, *Adv. Mater.*, 2009, **21**, 916–919; (e) A. Petersen, A. Ojala, T. Kirchartz, T. A. Wagner, F. Wurthner and U. Rau, *Phys. Rev. B*, 2012, **85**, 245208.
31. (a) S. Gunes, H. Neugebauer and N. S. Sariciftci, *Chem. Rev.*, 2007, **107**, 1324–1338; (b) R. Noriega, J. Rivnay, K. Vandewal, F. P. V. Koch, N. Stingelin, P. Smith, M. F. Toney and A. Salleo, *Nature Mater.*, 2013, **12**, 1038–1044; (c) N. Tessler, Y. Preezant, N. Rappaport and Y. Roichman, *Adv. Mater.*, 2009, **21**, 2741–2761; (d) V. Coropceanu, J. Cornil, D. A. da Silva, Y. Olivier, R. Silbey and J. L. Bredas, *Chem. Rev.*, 2007, **107**, 926–952; (e) R. J. Kline and M. D. McGehee, *Polym. Rev. (Philadelphia, PA, U. S.)*, 2006, **46**, 27–45.
32. C. Deibel, T. Strobel and V. Dyakonov, *Adv. Mater.*, 2010, **22**, 4097–4111.
33. (a) K. Vandewal, A. Gadisa, W. D. Oosterbaan, S. Bertho, F. Banishoeib, I. Van Severen, L. Lutsen, T. J. Cleij, D. Vanderzande and J. V. Manca, *Adv. Funct. Mater.*, 2008, **18**, 2064–2070; (b) K. Vandewal, K. Tvingstedt, A. Gadisa, O. Inganäs and J. V. Manca, *Nature Mater.*, 2009, **8**, 904–909; (c) K. Vandewal, K. Tvingstedt, J. V. Manca and O. Inganäs, *IEEE J. Sel. Top. Quantum Electron.*, 2010, **16**, 1676–1684; (d) K. Vandewal, S. Himmelberger and A. Salleo, *Macromolecules*, 2013, **46**, 6379–6387.
34. B. Y. Qi and J. Z. Wang, *Phys. Chem. Chem. Phys.*, 2013, **15**, 8972–8982.

## References

35. (a) A. Gadisa, W. Mammo, L. M. Andersson, S. Admassie, F. Zhang, M. R. Andersson and O. Inganäs, *Adv. Funct. Mater.*, 2007, **17**, 3836–3842; (b) J. Yuan, Z. Zhai, H. Dong, J. Li, Z. Jiang, Y. Li and W. Ma, *Adv. Funct. Mater.*, 2013, **23**, 885–892; (c) Q. D. Zheng, B. J. Jung, J. Sun and H. E. Katz, *J. Am. Chem. Soc.*, 2010, **132**, 5394–5404; (d) W. D. Cheng, Z. H. Wu, S. P. Wen, B. Xu, H. Li, F. R. Zhu and W. J. Tian, *Org. Electron.*, 2013, **14**, 2124–2131; (e) Y. J. Cheng, S. W. Cheng, C. Y. Chang, W. S. Kao, M. H. Liao and C. S. Hsu, *Chem. Commun.*, 2012, **48**, 3203–3205; (f) E. T. Hoke, K. Vandewal, J. A. Bartelt, W. R. Mateker, J. D. Douglas, R. Noriega, K. R. Graham, J. M. J. Fréchet, A. Salleo and M. D. McGehee, *Adv. Energy Mater.*, 2013, **3**, 220–230; (g) M. Wang, X. W. Hu, P. Liu, W. Li, X. Gong, F. Huang and Y. Cao, *J. Am. Chem. Soc.*, 2011, **133**, 9638–9641.
36. (a) R. C. Coffin, J. Peet, J. Rogers and G. C. Bazan, *Nature Chem.*, 2009, **1**, 657–661; (b) M. Lv, S. Li, J. J. Jasieniak, J. Hou, J. Zhu, Z. a. Tan, S. E. Watkins, Y. Li and X. Chen, *Adv. Mater.*, 2013, DOI: 10.1002/adma.201302726; (c) S. Liu, K. Zhang, J. Lu, J. Zhang, H.-L. Yip, F. Huang and Y. Cao, *J. Am. Chem. Soc.*, 2013, **135**, 15326–15329; (d) L. Lu, T. Xu, W. Chen, J. M. Lee, Z. Luo, I. H. Jung, H. I. Park, S. O. Kim and L. Yu, *Nano Lett.*, 2013, **13**, 2365–2369; (e) H.-C. Chen, Y.-H. Chen, C.-C. Liu, Y.-C. Chien, S.-W. Chou and P.-T. Chou, *Chem. Mater.*, 2012, **24**, 4766–4772; (f) T. Yang, M. Wang, C. Duan, X. Hu, L. Huang, J. Peng, F. Huang and X. Gong, *Energy Environ. Sci.*, 2012, **5**, 8208–8214; (g) X. Li, W. C. H. Choy, L. Huo, F. Xie, W. E. I. Sha, B. Ding, X. Guo, Y. Li, J. Hou, J. You and Y. Yang, *Adv. Mater.*, 2012, **24**, 3046–3052; (h) L. Huo, S. Zhang, X. Guo, F. Xu, Y. Li and J. Hou, *Angew. Chem. Int. Ed.*, 2011, **50**, 9697–9702; (i) L. Dou, C.-C. Chen, K. Yoshimura, K. Ohya, W.-H. Chang, J. Gao, Y. Liu, E. Richard and Y. Yang, *Macromolecules*, 2013, **46**, 3384–3390; (j) D. C. Lim, K.-D. Kim, S.-Y. Park, E. M. Hong, H. O. Seo, J. H. Lim, K. H. Lee, Y. Jeong, C. Song, E. Lee, Y. D. Kim and S. Cho, *Energy Environ. Sci.*, 2012, **5**, 9803–9807; (k) E. Zhou, J. Cong, K. Hashimoto and K. Tajima, *Energy Environ. Sci.*, 2012, **5**, 9756–9759.
37. (a) A. P. Zoombelt, S. G. J. Mathijssen, M. G. R. Turbiez, M. M. Wienk and R. A. J. Janssen, *J. Mater. Chem.*, 2010, **20**, 2240–2246; (b) S. C. Price, A. C. Stuart, L. Yang, H. Zhou and W. You, *J. Am. Chem. Soc.*, 2011, **133**, 4625–4631; (c) X. Guo, N. Zhou, S. J. Lou, J. Smith, D. B. Tice, J. W. Hennek, R. P. Ortiz, J. T. L. Navarrete, S. Li, J. Strzalka, L. X. Chen, R. P. H. Chang, A. Facchetti and T. J. Marks, *Nature Photon.*, 2013, **7**, 825–833; (d) V. D. Mihaletchi, H. X. Xie, B. de Boer, L. J. A. Koster and P. W. M. Blom, *Adv. Funct. Mater.*, 2006, **16**, 699–708; (e) J. Wagner, M. Gruber, A. Hinderhofer, A. Wilke, B. Broker, J. Frisch, P. Amsalem, A. Vollmer, A. Opitz, N. Koch, F. Schreiber and W. Brütting, *Adv. Funct. Mater.*, 2010, **20**, 4295–4303; (f) M. Zhang, Y. Gu, X. Guo, F. Liu, S. Zhang, L. Huo, T. P. Russell and J. Hou, *Adv. Mater.*, 2013, **25**, 4944–9; (g) Q. Xu, F. Wang, Z. a. Tan, L. Li, S. Li, X. Hou, G. Sun, X. Tu, J. Hou and Y. Li, *ACS Appl. Mater. Interfaces*, 2013, **5**, 10658–10664; (h) J.-M. Jiang, H.-C. Chen, H.-K. Lin, C.-

## References

- M. Yu, S.-C. Lan, C.-M. Liu and K.-H. Wei, *Polym. Chem.*, 2013, **4**, 5321–5328; (i) G. Marotta, M. A. Reddy, S. P. Singh, A. Islam, L. Han, F. De Angelis, M. Pastore and M. Chandrasekharam, *ACS Appl. Mater. Interfaces*, 2013, **5**, 9635–9647; (j) K. Li, Z. Li, K. Feng, X. Xu, L. Wang and Q. Peng, *J. Am. Chem. Soc.*, 2013, **135**, 13549–13557; (k) J. H. Heo, S. H. Im, J. H. Noh, T. N. Mandal, C. S. Lim, J. A. Chang, Y. H. Lee, H. J. Kim, A. Sarkar, M. K. Nazeeruddin, M. Gratzel and S. I. Seok, *Nature Photon.*, 2013, **7**, 487–492; (l) D. Qian, W. Ma, Z. Li, X. Guo, S. Zhang, L. Ye, H. Ade, Z. a. Tan and J. Hou, *J. Am. Chem. Soc.*, 2013, **135**, 8464–8467; (m) W. Li, K. H. Hendriks, W. S. C. Roelofs, Y. Kim, M. M. Wienk and R. A. J. Janssen, *Adv. Mater.*, 2013, **25**, 3182–3186; (n) J. R. Tumbleston, A. C. Stuart, E. Gann, W. You and H. Ade, *Adv. Funct. Mater.*, 2013, **23**, 3463–3470; (o) H. Li, T. M. Koh, A. Hagfeldt, M. Gratzel, S. G. Mhaisalkar and A. C. Grimsdale, *Chem. Commun.*, 2013, **49**, 2409–2411; (p) K. H. Hendriks, W. Li, M. M. Wienk and R. A. J. Janssen, *Adv. Energy Mater.*, 2013, **3**, 674–679; (q) X. Guo, M. Zhang, J. Tan, S. Zhang, L. Huo, W. Hu, Y. Li and J. Hou, *Adv. Mater.*, 2012, **24**, 6536–6541; (r) J. Min, Z. G. Zhang, S. Y. Zhang and Y. F. Li, *Chem. Mater.*, 2012, **24**, 3247–3254; (s) L. Ye, S. Zhang, W. Ma, B. Fan, X. Guo, Y. Huang, H. Ade and J. Hou, *Adv. Mater.*, 2012, **24**, 6335–6341; (t) T.-Y. Chu, J. Lu, S. Beaupré, Y. Zhang, J.-R. Pouliot, J. Zhou, A. Najari, M. Leclerc and Y. Tao, *Adv. Funct. Mater.*, 2012, **22**, 2345–2351; (u) B. R. Aïch, J. Lu, S. Beaupré, M. Leclerc and Y. Tao, *Org. Electron.*, 2012, **13**, 1736–1741; (v) L. Dou, J. You, J. Yang, C.-C. Chen, Y. He, S. Murase, T. Moriarty, K. Emery, G. Li and Y. Yang, *Nature Photon.*, 2012, **6**, 180–185; (w) C.-Y. Chang, C.-E. Wu, S.-Y. Chen, C. Cui, Y.-J. Cheng, C.-S. Hsu, Y.-L. Wang and Y. Li, *Angew. Chem. Int. Ed.*, 2011, **50**, 9386–9390; (x) G. Zhao, Y. He and Y. Li, *Adv. Mater.*, 2010, **22**, 4355; (y) M. Shahid, R. S. Ashraf, Z. Huang, A. J. Kronemeijer, T. McCarthy-Ward, I. McCulloch, J. R. Durrant, H. Sirringhaus and M. Heeney, *J. Mater. Chem.*, 2012, **22**, 12817–12823.
38. (a) M. C. Scharber and N. S. Sariciftci, *Prog. Polym. Sci.*, 2013, **38**, 1929–1940; (b) D. Veldman, S. C. J. Meskers and R. A. J. Janssen, *Adv. Funct. Mater.*, 2009, **19**, 1939–1948; (c) M. A. Faist, T. Kirchartz, W. Gong, R. S. Ashraf, I. McCulloch, J. C. de Mello, N. J. Ekins-Daukes, D. D. C. Bradley and J. Nelson, *J. Am. Chem. Soc.*, 2012, **134**, 685–692.
39. J.-L. Bredas, *Mater. Horiz.*, 2014, **1**, 17–19.
40. Z. K. Chen, W. Huang, L. H. Wang, E. T. Kang, B. J. Chen, C. S. Lee and S. T. Lee, *Macromolecules*, 2000, **33**, 9015–9025.
41. M. C. Scharber, D. Wuhlbacher, M. Koppe, P. Denk, C. Waldauf, A. J. Heeger and C. L. Brabec, *Adv. Mater.*, 2006, **18**, 789–794.
42. R. A. J. Janssen and J. Nelson, *Adv. Mater.*, 2013, **25**, 1847–1858.
43. J. J. M. Halls, J. Cornil, D. A. dos Santos, R. Silbey, D. H. Hwang, A. B. Holmes, J. L. Bredas and R. H. Friend, *Phys. Rev. B*, 1999, **60**, 5721–5727.

## References

44. L. Dou, J. You, Z. Hong, Z. Xu, G. Li, R. A. Street and Y. Yang, *Adv. Mater.*, 2013, DOI: 10.1002/adma.201302563.
45. R. C. Hiorns, R. J. Boucher, R. Duhlev, K. H. Hellwich, P. Hodge, A. D. Jenkins, R. G. Jones, J. Kahovec, G. Moad, C. K. Ober, D. W. Smith, R. F. T. Stepto, J. P. Vairon and J. Vohlidal, *Pure Appl. Chem.*, 2012, **84**, 2167–2169.
46. R. F. T. Stepto, *Pure Appl. Chem.*, 2009, **81**, 351–353.
47. H. Shirakawa, E. J. Louis, A. G. Macdiarmid, C. K. Chiang and A. J. Heeger, *J. Chem. Soc.-Chem. Commun.*, 1977, 578–580.
48. M. Baron, K. H. Hellwich, M. Hess, K. Horie, A. D. Jenkins, R. G. Jones, J. Kahovec, P. Kratochvil, W. V. Metanomski, W. Mormann, R. F. T. Stepto, J. Vohlidal and E. S. Wilks, *Pure Appl. Chem.*, 2009, **81**, 1131–1183.
49. (a) C. K. Chiang, M. A. Druy, S. C. Gau, A. J. Heeger, E. J. Louis, A. G. Macdiarmid, Y. W. Park and H. Shirakawa, *J. Am. Chem. Soc.*, 1978, **100**, 1013–1015; (b) J. H. Burroughes, C. A. Jones and R. H. Friend, *Nature*, 1988, **335**, 137–141.
50. (a) R. D. McCullough, *Adv. Mater.*, 1998, **10**, 93–116; (b) Z. Bao, A. Dodabalapur and A. J. Lovinger, *Appl. Phys. Lett.*, 1996, **69**, 4108–4110.
51. (a) R. G. Kepler, *Synth. Met.*, 1989, **28**, 573–580; (b) S. Hayase, *Prog. Polym. Sci.*, 2003, **28**, 359–381.
52. Z. F. Ma, E. G. Wang, M. E. Jarvid, P. Henriksson, O. Inganäs, F. L. Zhang and M. R. Andersson, *J. Mater. Chem.*, 2012, **22**, 2306–2314.
53. J. T. Shieh, C. H. Liu, H. F. Meng, S. R. Tseng, Y. C. Chao and S. F. Horng, *J. Appl. Phys.*, 2010, **107**, 084503.
54. B. Kippelen and J. L. Bredas, *Energy Environ. Sci.*, 2009, **2**, 251–261.
55. (a) H. Zhou, L. Yang and W. You, *Macromolecules*, 2012, **45**, 607–632; (b) Z.-G. Zhang and J. Wang, *J. Mater. Chem.*, 2012, **22**, 4178–4187; (c) H. J. Son, F. He, B. Carsten and L. P. Yu, *J. Mater. Chem.*, 2011, **21**, 18934–18945; (d) X. W. Zhan and D. B. Zhu, *Polym. Chem.*, 2010, **1**, 409–419; (e) J. Roncali, *Macromol. Rapid Commun.*, 2007, **28**, 1761–1775.
56. (a) R. Hoffmann, C. Janiak and C. Kollmar, *Macromolecules*, 1991, **24**, 3725–3746; (b) C. Winder and N. S. Sariciftci, *J. Mater. Chem.*, 2004, **14**, 1077–1086.
57. C. Müller, E. Wang, L. M. Andersson, K. Tvingstedt, Y. Zhou, M. R. Andersson and O. Inganäs, *Adv. Funct. Mater.*, 2010, **20**, 2124–2131.
58. L. W. Shacklette, H. Eckhardt, R. R. Chance, G. G. Miller, D. M. Ivory and R. H. Baughman, *J. Chem. Phys.*, 1980, **73**, 4098–4102.
59. T. C. Chung, J. H. Kaufman, A. J. Heeger and F. Wudl, *Phys. Rev. B*, 1984, **30**, 702–710.
60. J. L. Bredas, B. Themans, J. G. Fripiat, J. M. Andre and R. R. Chance, *Phys. Rev. B*, 1984, **29**, 6761–6773.

## References

61. M. Kertesz and Y. S. Lee, *J. Phys. Chem.*, 1987, **91**, 2690–2692.
62. (a) F. Wudl, M. Kobayashi and A. J. Heeger, *J. Org. Chem.*, 1984, **49**, 3382–3384; (b) M. Kobayashi, N. Colaneri, M. Boysel, F. Wudl and A. J. Heeger, *J. Chem. Phys.*, 1985, **82**, 5717–5723; (c) J. Kurti, P. R. Surjan and M. Kertesz, *J. Am. Chem. Soc.*, 1991, **113**, 9865–9867.
63. (a) J. L. Bredas, A. J. Heeger and F. Wudl, *J. Chem. Phys.*, 1986, **85**, 4673–4678; (b) Y. Y. Liang, D. Q. Feng, Y. Wu, S. T. Tsai, G. Li, C. Ray and L. P. Yu, *J. Am. Chem. Soc.*, 2009, **131**, 7792–7799.
64. B. Lee, M. S. Yavuz and G. A. Sotzing, *Macromolecules*, 2006, **39**, 3118–3124.
65. E. E. Havinga, W. ten Hoeve and H. Wynberg, *Polym. Bull.*, 1992, **29**, 119–126.
66. W. Zhuang, A. Lundin and M. R. Andersson, *J. Mater. Chem. A*, DOI: 10.1039/C3TA14456A.
67. (a) E. Wang, L. Hou, Z. Wang, S. Hellström, F. Zhang, O. Inganäs and M. R. Andersson, *Adv. Mater.*, 2010, **22**, 5240–5244; (b) Y. Kim, H. R. Yeom, J. Y. Kim and C. Yang, *Energy Environ. Sci.*, 2013, **6**, 1909–1916; (c) H.-C. Chen, Y.-H. Chen, C.-H. Liu, Y.-H. Hsu, Y.-C. Chien, W.-T. Chuang, C.-Y. Cheng, C.-L. Liu, S.-W. Chou, S.-H. Tung and P.-T. Chou, *Polym. Chem.*, 2013, **4**, 3411–3418; (d) D. Dang, W. Chen, R. Yang, W. Zhu, W. Mammo and E. Wang, *Chem. Commun.*, 2013, **49**, 9335–9337.
68. (a) E. G. Wang, Z. F. Ma, Z. Zhang, K. Vandewal, P. Henriksson, O. Inganäs, F. L. Zhang and M. R. Andersson, *J. Am. Chem. Soc.*, 2011, **133**, 14244–14247; (b) Z. Ma, W. Sun, S. Himmelberger, K. Vandewal, Z. Tang, J. Bergqvist, A. Salleo, J. W. Andreasen, O. Inganäs, M. R. Andersson, C. Müller, F. Zhang and E. Wang, *Energy Environ. Sci.*, 2014, DOI: 10.1039/C3EE42989J; (c) Z. Ma, D. Dang, Z. Tang, D. Gedefaw, J. Bergqvist, W. Zhu, W. Mammo, M. R. Andersson, O. Inganäs, F. Zhang and E. Wang, *Adv. Energy Mater.*, 2013, DOI: 10.1002/aenm.201301455; (d) Y. Yang, R. Wu, X. Wang, X. Xu, Z. Li, K. Li and Q. Peng, *Chem. Commun.*, 2014, DOI: 10.1039/C3CC47677D; (e) E. H. Jung and W. H. Jo, *Energy Environ. Sci.*, 2013, DOI: 10.1039/C3EE42297F; (f) Y. Deng, J. Liu, J. Wang, L. Liu, W. Li, H. Tian, X. Zhang, Z. Xie, Y. Geng and F. Wang, *Adv. Mater.*, 2013, DOI: 10.1002/adma.201303586; (g) C. Wang, Z. Cao, Y. Huang, P. Shen, B. Zhao, Z. Tan, X. Li and S. Tan, *Chem. Commun.*, 2013, **49**, 3857–3859.
69. (a) L. J. Lindgren, F. L. Zhang, M. Andersson, S. Barrau, S. Hellström, W. Mammo, E. Perzon, O. Inganäs and M. R. Andersson, *Chem. Mater.*, 2009, **21**, 3491–3502; (b) E. G. Wang, Z. F. Ma, Z. Zhang, P. Henriksson, O. Inganäs, F. L. Zhang and M. R. Andersson, *Chem. Commun.*, 2011, **47**, 4908–4910.
70. (a) Y. J. Cheng, S. H. Yang and C. S. Hsu, *Chem. Rev.*, 2009, **109**, 5868–5923; (b) B. Carsten, F. He, H. J. Son, T. Xu and L. Yu, *Chem. Rev.*, 2011, **111**, 1493–1528; (c) J. Roncali, *Chem. Rev.*, 1997, **97**, 173–206; (d) J. Sakamoto, M. Rehahn, G. Wegner and A. D. Schlüter, *Macromol. Rapid Commun.*, 2009, **30**, 653–687.

## References

71. (a) T. Mizoroki, K. Mori and A. Ozaki, *Bull. Chem. Soc. Jpn.*, 1971, **44**, 581; (b) R. F. Heck and J. P. Nolley, *J. Org. Chem.*, 1972, **37**, 2320–2322.
72. (a) E. Negishi, A. O. King and N. Okukado, *J. Org. Chem.*, 1977, **42**, 1821–1823; (b) A. O. King, N. Okukado and E. I. Negishi, *J. Chem. Soc.-Chem. Commun.*, 1977, 683–684; (c) E. I. Negishi, *Acc. Chem. Res.*, 1982, **15**, 340–348.
73. D. Milstein and J. K. Stille, *J. Am. Chem. Soc.*, 1978, **100**, 3636–3638.
74. (a) N. Miyaura, K. Yamada and A. Suzuki, *Tetrahedron Lett.*, 1979, **20**, 3437–3440; (b) N. Miyaura and A. Suzuki, *J. Chem. Soc., Chem. Commun.*, 1979, 866–867; (c) A. Suzuki, *J. Organomet. Chem.*, 1999, **576**, 147–168; (d) N. Miyaura, T. Yanagi and A. Suzuki, *Synth. Commun.*, 1981, **11**, 513–519.
75. P. J. Flory, *Chem. Rev.*, 1946, **39**, 137–197.
76. (a) W. Zhuang, Y. Zhang, Q. Hou, L. Wang and Y. Cao, *J. Polym. Sci. Part A: Polym. Chem.*, 2006, **44**, 4174–4186; (b) E. Wang, C. Li, W. Zhuang, J. Peng and Y. Cao, *J. Mater. Chem.*, 2008, **18**, 797–801.
77. (a) A. D. Schluter, *J. Polym. Sci., Part A Polym. Chem.*, 2001, **39**, 1533–1556; (b) T. Beryozkina, K. Boyko, N. Khanduyeva, V. Senkovskyy, M. Horecha, U. Oertel, F. Simon, M. Stamm and A. Kiriy, *Angew. Chem. Int. Ed.*, 2009, **48**, 2695–2698.
78. (a) D. Azarian, S. S. Dua, C. Eaborn and D. R. M. Walton, *J. Organomet. Chem.*, 1976, **117**, C55–C57; (b) M. Kosugi, K. Sasazawa, Y. Shimizu and T. Migita, *Chem. Lett.*, 1977, 301–302; (c) M. Kosugi, Y. Shimizu and T. Migita, *Chem. Lett.*, 1977, 1423–1424.
79. Z. N. Bao, W. K. Chan and L. P. Yu, *J. Am. Chem. Soc.*, 1995, **117**, 12426–12435.
80. I. J. Boyer, *Toxicology*, 1989, **55**, 253–298.
81. (a) B. N. Kang, L. D. Wang, Y. Yang and Y. Qiu, *Chin. Sci. Bull.*, 2004, **49**, 2259–2261; (b) P. Schilinsky, U. Asawapirom, U. Scherf, M. Biele and C. J. Brabec, *Chem. Mater.*, 2005, **17**, 2175–2180; (c) W. Ma, J. Y. Kim, K. Lee and A. J. Heeger, *Macromol. Rapid Commun.*, 2007, **28**, 1776–1780; (d) A. M. Ballantyne, L. Chen, J. Dane, T. Hammant, F. M. Braun, M. Heeney, W. Duffy, I. McCulloch, D. D. C. Bradley and J. Nelson, *Adv. Funct. Mater.*, 2008, **18**, 2373–2380; (e) M. Koppe, C. J. Brabec, S. Heiml, A. Schausberger, W. Duffy, M. Heeney and I. McCulloch, *Macromolecules*, 2009, **42**, 4661–4666; (f) M. H. Tong, S. Cho, J. T. Rogers, K. Schmidt, B. B. Y. Hsu, D. Moses, R. C. Coffin, E. J. Kramer, G. C. Bazan and A. J. Heeger, *Adv. Funct. Mater.*, 2010, **20**, 3959–3965; (g) I. Osaka, M. Saito, H. Mori, T. Koganezawa and K. Takimiya, *Adv. Mater.*, 2012, **24**, 425–430; (h) J. J. Intemann, K. Yao, H.-L. Yip, Y.-X. Xu, Y.-X. Li, P.-W. Liang, F.-Z. Ding, X. Li and A. K. Y. Jen, *Chem. Mater.*, 2013, **25**, 3188–3195; (i) C. Liu, K. Wang, X. Hu, Y. Yang, C.-H. Hsu, W. Zhang, S. Xiao, X. Gong and Y. Cao, *ACS Appl. Mater. Interfaces*, 2013, **5**, 12163–12167.

## References

82. (a) T. G. Fox and P. J. Flory, *J. Appl. Phys.*, 1950, **21**, 581–591; (b) M. Trznadel, A. Pron and M. Zagorska, *Macromolecules*, 1998, **31**, 5051–5058; (c) D. M. Johansson, M. Theander, G. Srdanov, G. Yu, O. Inganäs and M. R. Andersson, *Macromolecules*, 2001, **34**, 3716–3719; (d) M. J. Banach, R. H. Friend and H. Sirringhaus, *Macromolecules*, 2003, **36**, 2838–2844; (e) R. J. Kline, M. D. McGehee, E. N. Kadnikova, J. Liu and J. M. J. Fréchet, *Adv. Mater.*, 2003, **15**, 1519–1522; (f) Y. F. Ding, V. N. Novikov, A. P. Sokolov, A. Cailliaux, C. Dalle-Ferrier, C. Alba-Simionesco and B. Frick, *Macromolecules*, 2004, **37**, 9264–9272; (g) R. J. Kline, M. D. McGehee, E. N. Kadnikova, J. S. Liu, J. M. J. Fréchet and M. F. Toney, *Macromolecules*, 2005, **38**, 3312–3319; (h) J. F. Chang, J. Clark, N. Zhao, H. Sirringhaus, D. W. Breiby, J. W. Andreasen, M. M. Nielsen, M. Giles, M. Heeney and I. McCulloch, *Phys. Rev. B*, 2006, **74**, 12; (i) K. Koynov, A. Bahtiar, T. Ahn, R. M. Cordeiro, H. H. Horhold and C. Bubeck, *Macromolecules*, 2006, **39**, 8692–8698; (j) M. Brinkmann and P. Rannou, *Macromolecules*, 2009, **42**, 1125–1130; (k) F. P. V. Koch, J. Rivnay, S. Foster, C. Müller, J. Downing, E. Buchaca-Domingo, P. Westacott, L. Yu, M. Yuan, M. Baklar, Z. Fei, C. Luscombe, M. A. McLachlan, M. Heeney, G. Rumbles, C. Silva, A. Salleo, J. Nelson, P. Smith and N. Stingelin, *Prog. Polym. Sci.*, 2013, **38**, 1978–1989.
83. B. A. Miller-Chou and J. L. Koenig, *Prog. Polym. Sci.*, 2003, **28**, 1223–1270.
84. W. H. Carothers, *Trans. Faraday Soc.*, 1936, **32**, 0039–0053.
85. W. H. Carothers, *Chem. Rev.*, 1931, **8**, 353–426.
86. (a) A. Yokoyama, H. Suzuki, Y. Kubota, K. Ohuchi, H. Higashimura and T. Yokozawa, *J. Am. Chem. Soc.*, 2007, **129**, 7236–7237; (b) Z. Xue, A. D. Finke and J. S. Moore, *Macromolecules*, 2010, **43**, 9277–9282; (c) B. Hohl, L. Bertschi, X. Y. Zhang, A. D. Schluter and J. Sakamoto, *Macromolecules*, 2012, **45**, 5418–5426; (d) W. Huang, L. Su and Z. Bo, *J. Am. Chem. Soc.*, 2009, **131**, 10348–10349; (e) T. Yokozawa, H. Kohno, Y. Ohta and A. Yokoyama, *Macromolecules*, 2010, **43**, 7095–7100; (f) Z. J. Bryan and A. J. McNeil, *Macromolecules*, 2013, **46**, 8395–8405; (g) A. Yokoyama, R. Miyakoshi and T. Yokozawa, *Macromolecules*, 2004, **37**, 1169–1171; (h) E. E. Sheina, J. S. Liu, M. C. Iovu, D. W. Laird and R. D. McCullough, *Macromolecules*, 2004, **37**, 3526–3528; (i) R. Miyakoshi, A. Yokoyama and T. Yokozawa, *Macromol. Rapid Commun.*, 2004, **25**, 1663–1666; (j) R. Miyakoshi, A. Yokoyama and T. Yokozawa, *J. Am. Chem. Soc.*, 2005, **127**, 17542–17547.
87. J. Murage, J. W. Eddy, J. R. Zimbalist, T. B. McIntyre, Z. R. Wagner and F. E. Goodson, *Macromolecules*, 2008, **41**, 7330–7338.
88. (a) T. Johansson, W. Mammo, M. Svensson, M. R. Andersson and O. Inganäs, *J. Mater. Chem.*, 2003, **13**, 1316–1323; (b) C. M. Cardona, W. Li, A. E. Kaifer, D. Stockdale and G. C. Bazan, *Adv. Mater.*, 2011, **23**, 2367–2371; (c) E. G. Wang, M. Wang, L. Wang, C. H. Duan, J. Zhang, W. Z. Cai, C. He, H. B. Wu and Y. Cao, *Macromolecules*, 2009, **42**, 4410–4415; (d) W.

## References

- Mammo, S. Admassie, A. Gadisa, F. L. Zhang, O. Inganäs and M. R. Andersson, *Sol. Energy Mater. Sol. Cells*, 2007, **91**, 1010–1018.
89. S. Admassie, O. Inganäs, W. Mammo, E. Perzon and M. R. Andersson, *Synth. Met.*, 2006, **156**, 614–623.
90. S. Hellström, F. L. Zhang, O. Inganäs and M. R. Andersson, *Dalton Trans.*, 2009, 10032–10039.
91. A. J. Bard and L. R. Faulkner, *Electrochemical Methods: Fundamentals and Applications*, 2nd edn., John Wiley & Sons, New York, 2001.
92. (a) J. Gierschner, J. Cornil and H. J. Egelhaaf, *Adv. Mater.*, 2007, **19**, 173–191; (b) B. G. Sumpter and V. Meunier, *J. Polym. Sci., Part B: Polym. Phys.*, 2012, **50**, 1071–1089; (c) G. L. Gibson, T. M. McCormick and D. S. Seferos, *J. Am. Chem. Soc.*, 2012, **134**, 539–547; (d) I. Y. Kanal, S. G. Owens, J. S. Bechtel and G. R. Hutchison, *J. Phys. Chem. Lett.*, 2013, **4**, 1613–1623; (e) N. Berube, V. Gosselin, J. Gaudreau and M. Cote, *J. Phys. Chem. C*, 2013, **117**, 7964–7972; (f) C. Risko, M. D. McGehee and J. L. Bredas, *Chem. Sci.*, 2011, **2**, 1200–1218; (g) L. Pandey, C. Risko, J. E. Norton and J.-L. Brédas, *Macromolecules*, 2012, **45**, 6405–6414; (h) P. Salvatori, E. Mosconi, E. Wang, M. R. Andersson, M. Muccini and F. De Angelis, *J. Phys. Chem. C*, 2013, **117**, 17940–17954.
93. M. J. Frisch, G. W. Trucks, H. B. Schlegel, G. E. Scuseria, M. A. Robb, J. R. Cheeseman, G. Scalmani, V. Barone, B. Mennucci, G. A. Petersson, H. Nakatsuji, M. Caricato, X. Li, H. P. Hratchian, A. F. Izmaylov, J. Bloino, G. Zheng, J. L. Sonnenberg, M. Hada, M. Ehara, K. Toyota, R. Fukuda, J. Hasegawa, M. Ishida, T. Nakajima, Y. Honda, O. Kitao, H. Nakai, T. Vreven, J. A. Montgomery, Jr., J. E. Peralta, F. Ogliaro, M. Bearpark, J. J. Heyd, E. Brothers, K. N. Kudin, V. N. Staroverov, T. Keith, R. Kobayashi, J. Normand, K. Raghavachari, A. Rendell, J. C. Burant, S. S. Iyengar, J. Tomasi, M. Cossi, N. Rega, J. M. Millam, M. Klene, J. E. Knox, J. B. Cross, V. Bakken, C. Adamo, J. Jaramillo, R. Gomperts, R. E. Stratmann, O. Yazyev, A. J. Austin, R. Cammi, C. Pomelli, J. W. Ochterski, R. L. Martin, K. Morokuma, V. G. Zakrzewski, G. A. Voth, P. Salvador, J. J. Dannenberg, S. Dapprich, A. D. Daniels, O. Farkas, J. B. Foresman, J. V. Ortiz, J. Cioslowski and D. J. Fox, *Gaussian 09 Revision B.01*, Gaussian, Inc., Wallingford, CT, 2010.
94. (a) A. D. Becke, *Phys. Rev. A*, 1988, **38**, 3098–3100; (b) A. D. Becke, *J. Chem. Phys.*, 1993, **98**, 5648–5652; (c) C. T. Lee, W. T. Yang and R. G. Parr, *Phys. Rev. B*, 1988, **37**, 785–789.
95. (a) W. J. Hehre, D. R. and J. A. Pople, *J. Chem. Phys.*, 1972, **56**, 2257–2261; (b) P. C. Harihara and J. A. Pople, *Theor. Chim. Acta*, 1973, **28**, 213–222.
96. (a) W. R. Wadt and P. J. Hay, *J. Chem. Phys.*, 1985, **82**, 284–298; (b) P. J. Hay and W. R. Wadt, *J. Chem. Phys.*, 1985, **82**, 299–310.
97. M. E. Casida, *J. Mol. Struct.: THEOCHEM*, 2009, **914**, 3–18.
98. J. Grafenstein, A. M. Hjerpe, E. Kraka and D. Cremer, *J. Phys. Chem. A*, 2000, **104**, 1748–1761.

## References

99. (a) B. Grimm, C. Risko, J. D. Azoulay, J.-L. Bredas and G. C. Bazan, *Chem. Sci.*, 2013, **4**, 1807–1819; (b) M. E. Köse, *J. Phys. Chem. A*, 2012, **116**, 12503–12509.
100. T. Yamamoto, B.-L. Lee, H. Kokubo, H. Kishida, K. Hirota, T. Wakabayashi and H. Okamoto, *Macromol. Rapid Commun.*, 2003, **24**, 440–443.
101. (a) T. Kanbara, Y. Miyazaki and T. Yamamoto, *J. Polym. Sci. Part A: Polym. Chem.*, 1995, **33**, 999–1003; (b) T. Yamamoto, Z.-H. Zhou, T. Kanbara, M. Shimura, K. Kizu, T. Maruyama, Y. Nakamura, T. Fukuda, B.-L. Lee, N. Ooba, S. Tomaru, T. Kurihara, T. Kaino, K. Kubota and S. Sasaki, *J. Am. Chem. Soc.*, 1996, **118**, 10389–10399.
102. (a) T. T. Larsen-Olsen, T. R. Andersen, B. Andreasen, A. P. L. Bottiger, E. Bundgaard, K. Norrman, J. W. Andreasen, M. Jorgensen and F. C. Krebs, *Sol. Energy Mater. Sol. Cells*, 2012, **97**, 43–49; (b) T. Tromholt, M. V. Madsen, J. E. Carle, M. Helgesen and F. C. Krebs, *J. Mater. Chem.*, 2012, **22**, 7592–7601.
103. (a) R. Kroon, R. Gehlhaar, T. T. Steckler, P. Henriksson, C. Müller, J. Bergqvist, A. Hadipour, P. Heremans and M. R. Andersson, *Sol. Energy Mater. Sol. Cells*, 2012, **105**, 280–286; (b) E. Wang, J. Bergqvist, K. Vandewal, Z. Ma, L. Hou, A. Lundin, S. Himmelberger, A. Salleo, C. Müller, O. Inganäs, F. Zhang and M. R. Andersson, *Adv. Energy Mater.*, 2013, **3**, 806–814; (c) R. Kroon, A. Lundin, C. Lindqvist, P. Henriksson, T. T. Steckler and M. R. Andersson, *Polymer*, 2013, **54**, 1285–1288.
104. (a) F. Babudri, G. M. Farinola, F. Naso and R. Ragni, *Chem. Commun.*, 2007, 1003–1022; (b) D. J. Crouch, P. J. Skabara, J. E. Lohr, J. J. W. McDouall, M. Heeney, I. McCulloch, D. Sparrowe, M. Shkunov, S. J. Coles, P. N. Horton and M. B. Hursthouse, *Chem. Mater.*, 2005, **17**, 6567–6578; (c) D. J. Crouch, P. J. Skabara, M. Heeney, I. McCulloch, D. Sparrowe, S. J. Coles and M. B. Hursthouse, *Macromol. Rapid Commun.*, 2008, **29**, 1839–1843.
105. (a) Y. Y. Liang, Z. Xu, J. B. Xia, S. T. Tsai, Y. Wu, G. Li, C. Ray and L. P. Yu, *Adv. Mater.*, 2010, **22**, E135–E138; (b) H. Y. Chen, J. H. Hou, S. Q. Zhang, Y. Y. Liang, G. W. Yang, Y. Yang, L. P. Yu, Y. Wu and G. Li, *Nature Photon.*, 2009, **3**, 649–653; (c) H. X. Zhou, L. Q. Yang, A. C. Stuart, S. C. Price, S. B. Liu and W. You, *Angew. Chem. Int. Ed.*, 2011, **50**, 2995–2998; (d) H. J. Son, W. Wang, T. Xu, Y. Liang, Y. Wu, G. Li and L. Yu, *J. Am. Chem. Soc.*, 2011, **133**, 1885–1894; (e) S. Albrecht, S. Janietz, W. Schindler, J. Frisch, J. Kurpiers, J. Kniepert, S. Inal, P. Pingel, K. Fostiropoulos, N. Koch and D. Neher, *J. Am. Chem. Soc.*, 2012, **134**, 14932–14944; (f) A. C. Stuart, J. R. Tumbleston, H. Zhou, W. Li, S. Liu, H. Ade and W. You, *J. Am. Chem. Soc.*, 2013, **135**, 1806–1815; (g) H. J. Son, L. Lu, W. Chen, T. Xu, T. Zheng, B. Carsten, J. Strzalka, S. B. Darling, L. X. Chen and L. Yu, *Adv. Mater.*, 2012, **25**, 838–843.
106. Y. Lu, Z. Xiao, Y. Yuan, H. Wu, Z. An, Y. Hou, C. Gao and J. Huang, *J. Mater. Chem. C*, 2013, **1**, 630–637.

## References

107. (a) L. Dou, W.-H. Chang, J. Gao, C.-C. Chen, J. You and Y. Yang, *Adv. Mater.*, 2012, **25**, 825–831; (b) H. Y. Chen, S. C. Yeh, C. T. Chen and C. T. Chen, *J. Mater. Chem.*, 2012, **22**, 21549–21559.
108. H. A. Saadeh, L. Lu, F. He, J. E. Bullock, W. Wang, B. Carsten and L. Yu, *ACS Macro Letters*, 2012, **1**, 361–365.
109. (a) E. Zhou, J. Cong, K. Hashimoto and K. Tajima, *Macromolecules*, 2013, **46**, 763–768; (b) P. Shen, H. Bin, Y. Zhang and Y. Li, *Polym. Chem.*, 2014, DOI: 10.1039/C3PY00968H.
110. E. Wang, L. Hou, Z. Wang, S. Hellström, W. Mammo, F. Zhang, O. Inganäs and M. R. Andersson, *Org. Lett.*, 2010, **12**, 4470–4473.
111. L. Hou, E. Wang, J. Bergqvist, B. V. Andersson, Z. Wang, C. Müller, M. Campoy-Quiles, M. R. Andersson, F. Zhang and O. Inganäs, *Adv. Funct. Mater.*, 2011, **21**, 3169–3175.
112. Y.-X. Xu, C.-C. Chueh, H.-L. Yip, F.-Z. Ding, Y.-X. Li, C.-Z. Li, X. Li, W.-C. Chen and A. K. Y. Jen, *Adv. Mater.*, 2012, **24**, 6356–6361.
113. A. J. Moule and K. Meerholz, *Adv. Funct. Mater.*, 2009, **19**, 3028–3036.
114. G. Brocks and A. Tol, *J. Phys. Chem.*, 1996, **100**, 1838–1846.
115. M. L. Tang and Z. N. Bao, *Chem. Mater.*, 2011, **23**, 446–455.
116. (a) Distefan.G, Pignatar.S, G. Innorta, Fringuel.F, G. Marino and A. Taticchi, *Chem. Phys. Lett.*, 1973, **22**, 132–136; (b) A. Modelli, M. Guerra, D. Jones, G. Distefano, K. J. Irgolic, K. French and G. C. Pappalardo, *Chem. Phys.*, 1984, **88**, 455–461; (c) M. Shahid, T. McCarthy-Ward, J. Labram, S. Rossbauer, E. B. Domingo, S. E. Watkins, N. Stingelin, T. D. Anthopoulos and M. Heeney, *Chem. Sci.*, 2012, **3**, 181–185.
117. X. Wang, P. Jiang, Y. Chen, H. Luo, Z. Zhang, H. Wang, X. Li, G. Yu and Y. Li, *Macromolecules*, 2013, **46**, 4805–4812.
118. I. Osaka, T. Kakara, N. Takemura, T. Koganezawa and K. Takimiya, *J. Am. Chem. Soc.*, 2013, **135**, 8834–8837.
119. J. Cao, Q. Liao, X. Du, J. Chen, Z. Xiao, Q. Zuo and L. Ding, *Energy Environ. Sci.*, 2013, **6**, 3224–3228.
120. Z. F. Ma, E. G. Wang, K. Vandewal, M. R. Andersson and F. L. Zhang, *Appl. Phys. Lett.*, 2011, **99**, 143302.
121. (a) B. Liu, Y. P. Zou, B. Peng, B. Zhao, K. L. Huang, Y. H. He and C. Y. Pan, *Polym. Chem.*, 2011, **2**, 1156–1162; (b) G. Zhang, Y. Fu, Z. Xie and Q. Zhang, *Macromolecules*, 2011, **44**, 1414–1420; (c) C. Hu, Y. Fu, S. Li, Z. Xie and Q. Zhang, *Polym. Chem.*, 2012, **3**, 2949–2955; (d) R. Stalder, C. Grand, J. Subbiah, F. So and J. R. Reynolds, *Polym. Chem.*, 2012, **3**, 89–92; (e) K. Vandewal, Z. F. Ma, J. Bergqvist, Z. Tang, E. G. Wang, P. Henriksson, K. Tvingstedt, M. R. Andersson, F. L. Zhang and O. Inganäs, *Adv. Funct. Mater.*, 2012, **22**, 3480–3490; (f) K. Cao, Z. Wu, S. Li, B. Sun, G. Zhang and Q. Zhang, *J. Polym. Sci. Part A: Polym. Chem.*, 2013,

## References

- 51**, 94–100; (g) X. F. Xu, P. Cai, Y. Lu, N. S. Choon, J. W. Chen, X. Hu and B. S. Ong, *J. Polym. Sci. Part A: Polym. Chem.*, 2013, **51**, 424–434.
122. S. Ko, E. T. Hoke, L. Pandey, S. Hong, R. Mondal, C. Risko, Y. Yi, R. Noriega, M. D. McGehee, J.-L. Brédas, A. Salleo and Z. Bao, *J. Am. Chem. Soc.*, 2012, **134**, 5222–5232.
123. C. Aleman and L. Julia, *J. Phys. Chem.*, 1996, **100**, 1524–1529.
124. (a) G. Barbarella, M. Zambianchi, A. Bongini and L. Antolini, *Adv. Mater.*, 1992, **4**, 282–285; (b) D. Fichou, *J. Mater. Chem.*, 2000, **10**, 571–588.
125. (a) Y. Huang, X. Guo, F. Liu, L. Huo, Y. Chen, T. P. Russell, C. C. Han, Y. Li and J. Hou, *Adv. Mater.*, 2012, **24**, 3383–3389; (b) C. Piliago, T. W. Holcombe, J. D. Douglas, C. H. Woo, P. M. Beaujuge and J. M. J. Frechet, *J. Am. Chem. Soc.*, 2010, **132**, 7595–7597.
126. (a) J. H. Hou, H. Y. Chen, S. Q. Zhang, R. I. Chen, Y. Yang, Y. Wu and G. Li, *J. Am. Chem. Soc.*, 2009, **131**, 15586–15587; (b) Z. Li, J. P. Lu, S. C. Tse, J. Y. Zhou, X. M. Du, Y. Tao and J. F. Ding, *J. Mater. Chem.*, 2011, **21**, 3226–3233; (c) C. J. Shi, Y. Yao, Y. Yang and Q. B. Pei, *J. Am. Chem. Soc.*, 2006, **128**, 8980–8986.
127. G. Wegner, *Thin Solid Films*, 1992, **216**, 105–116.
128. (a) I. Osaka, T. Abe, S. Shinamura and K. Takimiya, *J. Am. Chem. Soc.*, 2011, **133**, 6852–6860; (b) R. Rieger, D. Beckmann, A. Mavrinskiy, M. Kastler and K. Mullen, *Chem. Mater.*, 2010, **22**, 5314–5318; (c) T. Lei, Y. Cao, X. Zhou, Y. Peng, J. Bian and J. Pei, *Chem. Mater.*, 2012, **24**, 1762–1770.
129. Y. Wu, Z. Li, W. Ma, Y. Huang, L. Huo, X. Guo, M. Zhang, H. Ade and J. Hou, *Adv. Mater.*, 2013, **25**, 3449–3455.
130. (a) S. H. Park, A. Roy, S. Beaupre, S. Cho, N. Coates, J. S. Moon, D. Moses, M. Leclerc, K. Lee and A. J. Heeger, *Nature Photon.*, 2009, **3**, 297–303; (b) T. Y. Chu, S. Alem, P. G. Verly, S. Wakim, J. P. Lu, Y. Tao, S. Beaupre, M. Leclerc, F. Belanger, D. Desilets, S. Rodman, D. Waller and R. Gaudiana, *Appl. Phys. Lett.*, 2009, **95**, 063304; (c) N. Blouin, A. Michaud and M. Leclerc, *Adv. Mater.*, 2007, **19**, 2295–2300; (d) N. Blouin and M. Leclerc, *Acc. Chem. Res.*, 2008, **41**, 1110–1119; (e) R. P. Qin, W. W. Li, C. H. Li, C. Du, C. Veit, H. F. Schleiermacher, M. Andersson, Z. S. Bo, Z. P. Liu, O. Inganäs, U. Wuerfel and F. L. Zhang, *J. Am. Chem. Soc.*, 2009, **131**, 14612.
131. (a) A. P. Zoombelt, M. A. M. Leenen, M. Fonrodona, Y. Nicolas, M. M. Wienk and R. A. J. Janssen, *Polymer*, 2009, **50**, 4564–4570; (b) B. C. Thompson, B. J. Kim, D. F. Kavulak, K. Sivula, C. Mauldin and J. M. J. Frechet, *Macromolecules*, 2007, **40**, 7425–7428; (c) J. M. Szarko, J. C. Guo, Y. Y. Liang, B. Lee, B. S. Rolczynski, J. Strzalka, T. Xu, S. Loser, T. J. Marks, L. P. Yu and L. X. Chen, *Adv. Mater.*, 2010, **22**, 5468–5472; (d) L. Q. Yang, H. X. Zhou and W. You, *J. Phys. Chem. C*, 2010, **114**, 16793–16800; (e) L. Biniek, S. Fall, C. L. Chochos,

## References

- D. V. Anokhin, D. A. Ivanov, N. Leclerc, P. Leveque and T. Heiser, *Macromolecules*, 2010, **43**, 9779–9786.
132. J. C. Bijleveld, A. P. Zoombelt, S. G. J. Mathijssen, M. M. Wienk, M. Turbiez, D. M. de Leeuw and R. A. J. Janssen, *J. Am. Chem. Soc.*, 2009, **131**, 16616–16617.